

RADIATION-INDUCED PARTICULATES FROM
ORGANIC VAPORS

A THESIS

Presented to
The Faculty of the Graduate Division

by
Richard Ruonn-Ching Chu

In Partial Fulfillment
of the Requirements for the Degree
Doctor of Philosophy
in the School of Chemical Engineering

Georgia Institute of Technology

November, 1973

RADIATION-INDUCED PARTICULATES FROM

ORGANIC VAPORS

Approved:

Chairman

Date approved by Chairman: Nov 13, 1973

ACKNOWLEDGMENTS

The author is deeply grateful to Dr. Clyde Orr, Jr., his advisor for this study. His helpful suggestions and encouragement are sincerely appreciated. The laboratory supervision and advice, especially on x-ray experiment, of Dr. James A. Knight, Jr., who served as a member of the thesis committee, are gratefully acknowledged. The author is also indebted to Dr. Michael J. Matteson, who also served as a member of the thesis committee, for his comments and encouragement. The author, in addition, thanks Mr. Edward Y. H. Keng for his support and comments during the course of this work.

The author acknowledges the assistance of Mr. Eugene Weaver in the design and construction of the experimental equipment. Thanks are also due Mr. Donald Lillie and his excellent glass blowing work. Mr. James Hubbard, Mr. James Johnson, and Mr. Larry Glassman deserve considerable credit for obtaining the scanning electron micrographs and electron microprobe analyses of products. Thanks are extended to Mr. George Turner of the School of Chemistry for his helpful work in mass spectrometry. The cooperation of Mr. William Tedder and Mr. William Huang relating to the experimental investigation and gas analyses are also appreciated. The assistance given on figure preparation by Mr. Leigh Chu, the author's brother, and Miss Martha Shoemaker of the Photo Lab is gratefully acknowledged. Sincere appreciation is also extended to Miss Eva Ju for the typing of this manuscript.

The author appreciates the research assistantships he received

through the Engineering Experiment Station for studies supported by the U. S. Public Health Service under Grant EC-00338. The author also is grateful for the research and teaching assistantships arranged by Dr. G. L. Bridger.

Two senior faculty members of the School of Chemical Engineering, particularly Dr. Waldemar T. Ziegler and Dr. Herbert C. Lewis, who always offer valuable guidance and advice, and a young faculty member, Dr. John D. Muzzy, who made helpful comments and gave assistance on calorimetric work, are also sincerely acknowledged.

The following support of friends is also unforgettable: Mr. Fu-Chu Wen, who offered suggestions on nucleation phenomena; Mr. T. I. Chao, who performed the NMR analyses; Mr. Kenneth Chan, Mr. Ju-Fu Shiau, and Mr. James Nabors, all of whom helped in various ways during the course of this study.

Finally, the author wishes to thank his parents, Mr. and Mrs. Yao-Tsu Chu, and his brothers, Mr. Leigh Chu and Mr. Nelson Chu, without whose love and encouragement this study would not have become a reality.

TABLE OF CONTENTS

	Page
ACKNOWLEDGMENTS	ii
TABLE OF CONTENTS	iv
LIST OF ILLUSTRATIONS	vi
SUMMARY	x
Chapter	
I. INTRODUCTION	1
Background	
Pffeferkorn's Investigation	
Condensed Phase Produced by Ionizing Radiation	
Photochemical Reactions and Aerosols	
Purpose of the Research Effort	
II. EXPERIMENTAL	10
X-ray Irradiation Systems	
Ultraviolet Irradiation Systems	
III. SPECTROMETRIC ANALYSES AND CHEMICAL NATURE OF PARTICULATES. .	26
Infrared Spectrophotometric Analysis of Particulates	
Mass Spectrometric Analysis of Particulates	
IV. RADIOCHEMICAL OXIDATION AND THE FORMATION OF PARTICULATES .	46
The Ionizing Effects of X-rays on Air	
X-ray Induced Formation of Ozone and Nitrogen Dioxide	
Radiochemical Oxidation of Hydrocarbons in Air	
Formation of Particulates as Functions of Hydrocarbon Concentration, Irradiation Time, X-ray Intensity, and Humidity	
V. PHOTOCHEMICAL OXIDATION AND THE FORMATION OF PARTICULATES .	65
Formation of Atomic Oxygen and Ozone	
Cyclohexene-Air System	
Photodissociation and Photo-oxidation of Aromatics	
Benzene-Air Systems	

TABLE OF CONTENTS (Continued)

	Page
V. (Continued)	
Photo-oxidation and Particulate Formation with the Addition of NO, NO ₂ and H ₂ O	
VI. MICROPHYSICAL PHENOMENA AND GROWTH OF PARTICULATES . . .	90
Sample Collection and Measurement of Size Distribution	
Electron Microscopic Examination of Particulates	
Physical Properties of Particulates	
Growth of Particulates	
Nucleation Phenomena	
VII. CONCLUSIONS AND RECOMMENDATIONS	130
Conclusions	
Recommendations	
APPENDICES	
A. Gas Analytical Methods	135
Gas Chromatography and Hydrocarbon Analyzer	
Analysis of Aliphatic Aldehydes	
Analysis of Nitrogen Dioxide	
Analysis of Ozone and Oxidants	
B. Materials and Chemicals	138
C. Nomenclature	141
BIBLIOGRAPHY	143
VITA	154

LIST OF ILLUSTRATIONS

Figure	Page
1. Electron Micrograph of Iron Oxide Whiskers	3
2. Electron Micrograph of Particulates Attached to Whiskers after 1.5 hr. X-ray Irradiation in Air Containing Traces of Benzene and Moisture	4
3. The X-ray Tube, the Irradiation Chamber, and an Inside View of the Lead Vault	11
4. The Colorimeter, the Lead Vault, the Particle Mass Monitor, and the X-ray Master Control Panel	15
5. Schematic Drawing of Ultraviolet Irradiation Chamber and Mercury Lamp	18
6. Ultraviolet Irradiation Chamber and Analyzing Equipment	19
7. Equipment of Photochemical Reaction System	20
8. Infrared Spectrum of Particulate Products from the X-ray Irradiation of Benzene-Air Mixture	29
9. Infrared Spectrum of Particulate Products from the X-ray Irradiation of Cyclohexene-Air Mixture	29
10. Infrared Spectrum of Particulate Products from the X-ray Irradiation of Acetylene-Oxygen Mixture	31
11. Infrared Spectrum of Particulate Products from the X-ray Irradiation of Acetylene-Oxygen Mixture	31
12. Infrared Spectrum of Particulate Products from the Photochemical Reaction of Benzene-Nitric Oxide-Air Mixture	34
13. Infrared Spectrum of Particulate Products from the Photochemical Reaction of Benzene-Air Mixture	34
14. Infrared Spectrum of Particulate Products from the Photochemical Reaction of Toluene-Air Mixture	36
15. Infrared Spectrum of Particulate Products from the Photochemical Reaction of o-Xylene-Air Mixture	36

LIST OF ILLUSTRATIONS (Continued)

Figure		Page
16.	Mass Spectrum of Particulate Products from the X-ray Irradiation of Acetylene-Air Mixture	40
17.	Mass Spectrum of Particulate Products from the Photochemical Reaction of Benzene-Air Mixture	42
18.	Mass Spectrum of Particulate Products from the Photochemical Reaction of o-Xylene-Air Mixture	43
19.	Mass Spectrum of Particulate Products from the Photochemical Reaction of Benzene-Nitric oxide-Air Mixture	45
20.	Yield of Particulates as a Function of Hydrocarbon Concentration	59
21.	Yield of Particulates as a Function of Irradiation Time	61
22.	yield of Particulates as a Function of X-ray Intensity	62
23.	Yield of Particulates as a Function of Relative Humidity	63
24.	Concentration Change of Reactants and Products during Ultraviolet Irradiation of Cyclohexene-Air Mixture	67
25.	Disappearance Rate of Benzene, Toluene, and o-Xylene in Dry Air During Ultraviolet Irradiation	71
26.	Concentration Change of Reactants and Products during Ultraviolet Irradiation of Benzene Vapor in Previously Irradiated Dry Air	74
27.	Concentration Change of Reactants and Products during Ultraviolet Irradiation of Benzene-Air Mixture	76
28.	Concentration Change of Reactants and Products during Ultraviolet Irradiation of Benzene-Nitric Oxide-Air Mixture	81
29.	Yield of Particulate as a Function of Initial Nitric Oxide Concentration	85
30.	Disappearance Rate of Benzene as a Function of Initial Humidity	87
31.	Yield of Particulates as a Function of Initial Humidity	88

LIST OF ILLUSTRATIONS (Continued)

Figure	Page
32. Electron Micrograph of Particulates Formed from X-ray Irradiation of Benzene-Saturated Air	93
33. Electron Micrograph of Particulates Formed from X-ray Irradiation of Benzene-Saturated Air	94
34. Electron Micrograph of Particulates Formed from Ultraviolet Light Irradiation of 10 ppm Benzene in Air	96
35. Electron Micrograph of Particulates Formed from Ultraviolet Light Irradiation of 10 ppm Benzene and 10 ppm Nitric Oxide in Air	97
36. Scanning Electron Micrograph of Whiskers and the Attached Particulates Formed from X-ray Irradiation of Benzene-Saturated Air	98
37. Scanning Electron Micrograph of Particulates Formed from X-ray Irradiation of Air Containing Partially Saturated Benzene and Water Vapor	100
38. Scanning Electron Micrograph of Particulates Formed from X-ray Irradiation of Acetylene-Air Mixture	101
39. Scanning Electron Micrograph of Particulates Formed from Ultraviolet Irradiation of Air Containing 10 ppm Benzene	102
40. Scanning Electron Micrograph of Nuclepore Filter and the Attached Particulates Formed from Ultraviolet Irradiation of Air Containing Both Benzene and Nitric Oxide at 10 ppm	103
41. Scanning Electron Micrograph of Nuclepore Filter and Particulates Formed from Ultraviolet Irradiation of Air Containing 10 ppm Toluene	104
42. Scanning Electron Micrograph of Nuclepore Filter and Particulates Formed from Ultraviolet Irradiation of Air Containing 10 ppm Xylene	105
43. Electron Micrograph of Whiskers and Particulates Formed from X-ray Irradiation of Benzene-Air Mixture before Exposure to Vacuum	107

LIST OF ILLUSTRATIONS (Continued)

Figure	Page
44. Electron Micrograph of Whiskers and Particulates Formed from X-ray Irradiation of Benzene-Air Mixture After Exposure to Vacuum for Two Days	108
45. Particulates Formed from X-ray Irradiation of Benzene-Air Mixture Before (Upper Photo), after 4 Hours (Middle Photo), and after 30 Hours (Bottom Photo) at 250°C	109
46. Reduction in Weight of Particulates as a Function of Heating Time and Oven Temperature	111
47. Size Distributions of X-ray Induced Particulates as Functions of Aging Time	113
48. Median Diameters of X-ray Induced Particulates as Functions of Aging Time	114
49. Size Distributions of X-ray Induced Particulates as Functions of Acetylene Concentrations	115
50. Comparison Between Size Distributions of X-ray Induced Particulates Formed in Dry and Humidified Air Containing 10 per cent Acetylene	116
51. Size Distributions of Nonvolatile Photochemical Particulates Sampled During Different Irradiation Periods from Air Containing 10 ppm Benzene	118
52. Size Distributions of Nonvolatile Photochemical Particulates with Addition of Nitric Oxide Sampled during Different Irradiation Periods	120
53. The Onset of Formation of Photochemical Particulates	122
54. Concentration Profile of Condensation Nuclei and Aerosols during Ultraviolet Irradiation of Trans-2-Butene-Nitric Oxide-Air, Toluene-Nitric Oxide-Air, and 1,3,5-Trimethylbenzene-Nitric Oxide-Air Mixtures	124
55. Characteristics of Nucleation	125

SUMMARY

An effort has been made to study aerocolloids formed by the interaction of vapors and radiation as reported by Pfefferkorn and other investigators. Ultrafine particulates were produced by x-ray or UV irradiation from trace hydrocarbons in air. Infrared, mass spectrometric, and other analytic methods consistently indicated that carbonyl and hydroxyl groups were predominant and characteristic components of these highly oxygenated products.

A typical product from x-ray irradiation was found to contain approximately seven oxygen atoms for each reacted benzene molecule. The existence of aldehydes, ketones, esters, and carboxylic acids, both of aliphatic and aromatic types, were also detected. Products generally appear to be a mixture containing many different functional groups, each in low yield. Therefore, no overall trend was discernible. For photochemical systems, apparent first-order rate constants of 1, 1.5, 1.9, and $2.0 \times 10^{-3} \text{ sec}^{-1}$, respectively, were observed for 10 ppm each benzene, toluene, cyclohexene, and o-xylene in air. Many tests indicated that part of the particulate product was always a polymeric substance having a molecular weight over 200 and a carbon chain length of more than 10 atoms.

Deformation of the particulates, the presence of agglomerates, and their mode of attachment to one another were examined by both transmission and scanning electron microscopy. The size and mass of all types of particulates were found to increase in proportion to the irradiation time, aging time, hydrocarbon concentration, nitrogen oxide concentration, and

relative humidity when under 5 per cent. Two mechanisms, namely, condensation of supersaturated vapors and chemical combination of reactive species, are proposed to describe the nucleation and growth of particulates.

CHAPTER I

INTRODUCTION

Background

The conversion of gaseous substances into particulate matter has attracted the attention of many scientists since John Tyndall published his famous "Tyndall beam" experiments.⁽¹²⁹⁾ This work represented the first observation of ultrafine particle formation as a result of photochemical processes. It is now known that Tyndall observed the photolytic decomposition of substances such as butyl nitrite, allyl iodide, etc. In addition to photolysis, radiolysis induced by high energy radioactive particles or rays also leads to the formation of particulate matter.

In general, the basic processes of formation of particulates from gases and vapors may be classified as follows:⁽⁹¹⁾⁽¹³¹⁾ (1) condensation and crystallization, (2) radiation chemistry and photochemistry, (3) non-photochemical reaction in the gas phase, (4) combustion, and (5) electric discharge chemistry. There is not always a distinct boundary between the different processes. Also, two or more processes may be responsible for one formation. Any of the latter four processes, for example, may produce nuclei or critical embryo on which particles may grow from supersaturated vapor by processes of condensation or crystallization. In this study, attention is focused on particulate formation by both radiation chemistry and photochemistry.

Pffeferkorn's Investigation

Pffeferkorn reported⁽¹⁰¹⁾⁽¹⁰²⁾ the formation of non-volatile particulates on various crystals when exposed to a mixture of air and organic vapors irradiated with x-rays or ultraviolet light. Low concentrations, or traces, of organic vapors were sufficient to form droplets under these radiations. This work implied that the existence of crystals and their surface conditions were important factors in the formation of droplets. Actually, the droplets were formed in the gas phase and only collected on the crystals; this was established early in this investigation of the phenomenon. In other words, the surfaces of crystals serve as collectors of droplets or as heterogeneous nucleation sites and do not appear to be vital to the formation and growth of droplets. Some observations were made by Pffeferkorn on the solubility of these droplets in organic solvents, the variation of organic vapors, the effect of humidity, and the addition of NO_2 on the production of droplets. Droplets became larger and more numerous with intense and prolonged radiation, with high humidity, and with the addition of NO_2 . However, little study was devoted to the formation and properties of the particulate matter, and, because of the extremely small size of the droplets, no chemical analyses were undertaken.

In preliminary experiments of this investigation, some of Pffeferkorn's work was repeated; iron oxide whiskers and air-benzene mixtures were prepared and irradiated simultaneously by x-rays. Figure 1 is an electron micrograph showing tiny iron oxide whiskers prior to the x-ray radiation. Figure 2 indicates the same spot of the iron grid after it and the benzene-air mixture had been subjected to irradiation.

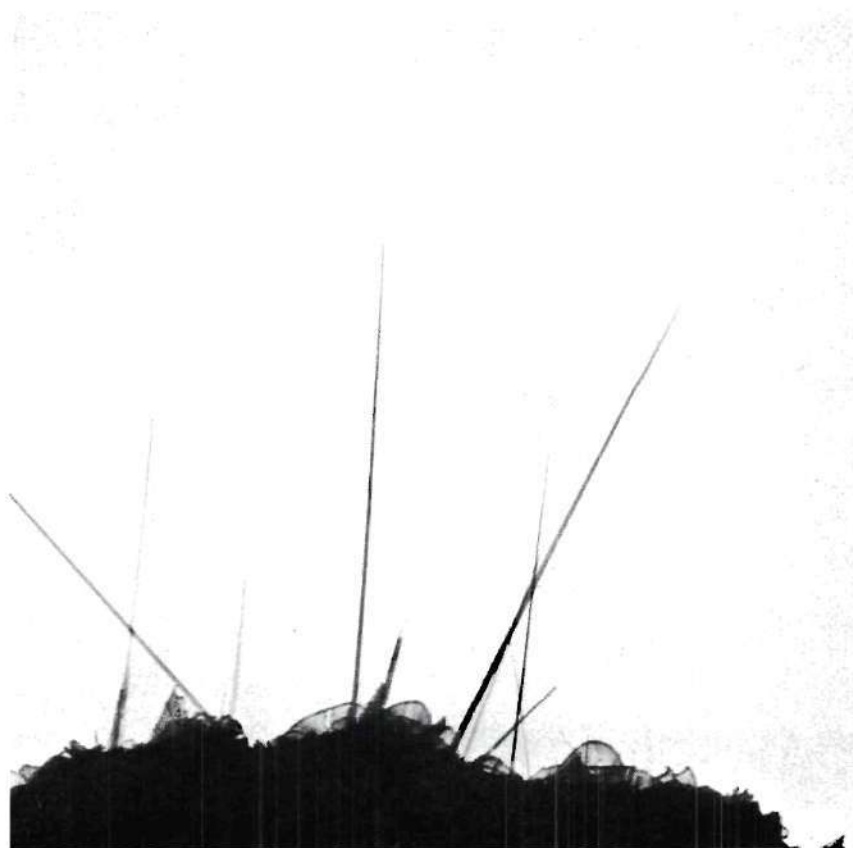


Figure 1. Electron Micrograph of Iron Oxide Whiskers. X10,600

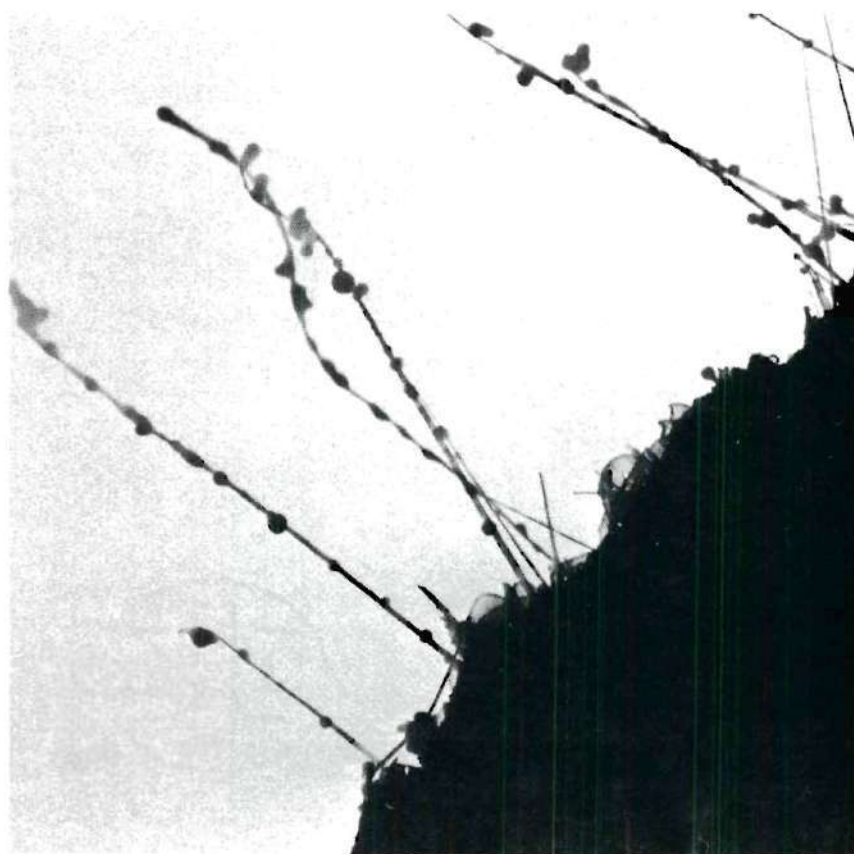


Figure 2. Electron Micrograph of Particulates Attached to Whiskers after 1.5 hr. X-ray Irradiation in Air Containing Traces of Benzene and Moisture. X10,600

Condensed Phase Produced by Ionizing Radiation

An organic vapor, especially a vapor from an unsaturated organic compound, under the influence of ionizing radiations has long been known to produce polymeric, non-volatile, liquid or solid, particles. Chemical reactions induced by the absorption of ionizing radiations are of numerous types, such as polymerization, dissociation, oxidation, hydrogenation, and reduction. For instance, polymerization occurs when acetylene gas is bombarded by α -ray from radon to form spherical cuprene particles, a light yellow powder being produced at ordinary temperature and pressure.⁽⁸³⁾ In this work a yellow precipitate settled on the bottom of the irradiation vessel indicating the formation of particulates in the gas phase. Electron microscopic examinations by Watson and Kaufman⁽¹³³⁾ in the same type of study showed round particles joined by short necks and appearing to be liquid in nature were formed. Radiolysis⁽⁶⁰⁾⁽⁶⁷⁾ of benzene, n-hexane, cyclohexane, and cyclohexene in the vapor state produces oily non-volatile liquids in addition to hydrogen and other light hydrocarbons under α -ray irradiation. The average molecular weight of these liquid products ranged from 330 to 360. The material was clear to slightly yellow in color. The product from benzene was the most colored and the most viscous of the four. Ethylene was reported to form a liquid polymer under the irradiation of α -ray.⁽⁸³⁾ Propane, a mixture of CH_4 and CO_2 , and a mixture of C_2H_2 and O_2 also produced polymeric substances under similar conditions.⁽⁸²⁾ Ambient air produces ultrafine particles or condensation nuclei under the influence of ionizing radiation.⁽²²⁾⁽²³⁾ The generation of ultrafine particles from ambient air was examined by Belyaeva⁽⁹¹⁾ who found the concentration of particles and condensation nuclei to increase by factors of 4 to 10, re-

spectively, when α -rays were present. The production of condensation nuclei by mixing filtered air with thoron, a radio-isotope of radon, has also been investigated by Megaw.⁽⁹¹⁾ Nuclei concentration increased from 10^2 to about 10^5 per cubic centimeter when the dosage was increased from 2 to 15 rads. Since traces of various hydrocarbons and moisture are characteristic components of polluted atmospheres and cosmic and x-rays enter the atmosphere from space, the formation of ultrafine particles most likely occurs naturally.⁽³⁰⁾⁽⁶⁹⁾

Photochemical Reactions and Aerosols

Irradiation of trace concentrations of reactive species by sunlight or artificial ultraviolet light, in some cases, produces aerocolloids ranging from 0.1 to 1.0 micrometer in diameter. Because they scatter light, these particles probably influence visibility in the atmosphere. So-called photochemical smog is formed by reactions involving airborne hydrocarbons and nitric oxides which are introduced into the atmosphere by automobile and industrial emissions.⁽⁴³⁾⁽⁵⁵⁾⁽⁵⁶⁾⁽¹⁰⁹⁾ The smog formation process is characterized by the oxidation of nitric oxide to nitrogen dioxide; the oxidation of olefinic and aromatic hydrocarbons to aldehydes and ketones; and the formation of oxidant, peroxyacyl nitrate, and other peroxides and nitrates.⁽⁷⁸⁾

In general, olefinic hydrocarbons of six carbons and higher and aromatic hydrocarbons at parts-per-million concentrations in the presence of similar concentrations of nitric oxides⁽⁷⁶⁾⁽¹⁰⁶⁾ produce aerosols when irradiated. Two-to-five carbon olefins produce large amounts of aerosols in the presence of both nitrogen dioxide and sulfur dioxide. With nitric oxide there is an induction period for some photochemical reactions and

the formation of aerosol; significant aerosol production starts only after nitric oxide is converted into nitrogen dioxide. For olefin-nitrogen dioxide systems, the production of aerosol increases with increasing concentration of each reactant. Chemical analysis of atmospheric and synthetic aerosols shows the presence of carbonyl, hydroxyl, and nitrate ester-type compounds; other compounds such as organic acids and peroxides are also characteristic components. In other words, particulate matter generally appears to be highly oxygenated. Degradation, evaporation, and oxidation of such organic aerosols have also been observed during the course of irradiation.⁽⁵¹⁾

Aromatic hydrocarbons and olefinic hydrocarbons as well are major participants in atmospheric photo-oxidation reactions. Boocock and Cvetanovic⁽²¹⁾ have reported reactions between oxygen atoms and benzene, and Jones and Cvetanovic⁽⁶⁸⁾ have reported reactions between atomic oxygen and toluene. Altshuller, et al.,⁽¹⁰⁾ and Altshuller and Cohen⁽⁸⁾ have compared the reactivities of aromatic hydrocarbons with olefins, paraffins, and other organic compounds. Altshuller and Leach⁽¹²⁾ found that alkyl benzenes disappeared at a significant rate in dilute irradiated auto exhaust. Most of the aromatic hydrocarbons investigated except benzene are subject to significant photo-oxidation; benzene shows very low reactivity on the basis of most laboratory data. Toluene was reported less photochemically reactive than ethylene and the xylenes were more reactive. Irradiated aromatic hydrocarbon-nitric oxide mixtures form oxidant concentrations equal to or greater than those produced in olefin-nitric oxide mixtures, but olefin-nitric oxide systems produce lower yields of formaldehyde and other aliphatic aldehydes. These irradiated mixtures were

also reported by Altshuller, et al.,⁽¹³⁾ to form photochemical aerosols, cause reduction in visibility, and to result in eye irritation and plant damage. Formation of condensation nuclei and aerosols was also investigated by irradiating toluene-nitric oxide and 1,3,5-trimethylbenzene-nitric oxide mixtures in the parts-per-million concentration range. Condensed-phase or aerosol products were reported to contain as much as 50 per cent of the reacted carbon atoms from the irradiation of some alkyl benzene-nitric oxide systems in the parts-per-million concentration range. Kopczynski⁽⁷⁶⁾ reported that the chemical nature of condensed-phase products appears to be polymeric and generally to contain hydroxyl, carbonyl, nitrate, and nitro groups.

The photochemical oxidation of organic compounds is extremely complex.⁽⁶⁶⁾ Chemists have discovered the build-up of a variety of free-radical intermediates. The problem in a photochemical system involving three or more free-radical intermediates is that it is not possible to derive the mechanism by methods that only analyze for final products and reactants. Since irradiated mixtures simulating actual atmospheric concentrations contain merely traces of reactants and products, more sensitive instrumentation is required.

While the details of hydrocarbon photo-oxidation are not known, relatively well-defined laboratory systems involving photochemical reaction chambers in which reactive species are confined and conditions are maintained, make possible the analysis of gaseous products and particulates.⁽¹²¹⁾ Theoretically also, development of a diffusion model⁽⁴⁷⁾⁽⁸⁴⁾ is possible by application of modern particle collection and analytical chemical methods. The chemical reaction scheme and the physical process

will be resolved successfully only after the identification of the aerosol components.

Purpose of the Research Effort

The general objective of the work presented here was to investigate the formation of non-volatile particulates when a mixture of air and organic vapors was irradiated with x-rays or ultraviolet light. Olefinic and aromatic organic compounds were to be investigated since these apparently produce the most significant amounts of aerosol for such a study. Soft x-ray and ultraviolet light with short wavelength, i.e., in the region between 2894 and 2224 Å, ^{o(32)} were to be employed.

The first effort of this task was to establish the physical conditions of particulate formation. In other words, it required the design and operation of chemical reaction chambers. Afterwards, microphysical properties such as the size distribution and mass concentration of the particulates could be determined as functions of irradiation time, humidity, and the concentration of foreign gases. Radiochemical and photochemical mechanisms were to be considered along with the chemical analysis of the particulates. An attempt was to be made to determine if the particulates were polymers. Finally, an effort was to be made to describe the path to aerosol formation, i.e., to study the nucleation and growth of the particulates.

CHAPTER II

EXPERIMENTAL

X-Ray Irradiation SystemsX-Ray Irradiation Chambers

Most experiments were performed under dynamic conditions; however, some benzene-air systems were irradiated under static conditions. Iron electron microscope grids which carried iron oxide, needle-like crystals, or whiskers, were mounted within the containers on a specially made holder for the collection of particulates at different positions. These iron grids were oxidized in an air stream at about 500°C for various time periods until the whiskers appeared and grew on their surface. After exposure to the irradiated gases for a short time, many spherical particulates could be detected on the whiskers. Typical electron micrographs showing the same spot before and after the irradiation have already been presented as Figures 1 and 2.

Under dynamic conditions, x-ray irradiations were mainly carried out in three chambers of different sizes. The first one having a volume of 170 cubic centimeters was a piece of 3.2 cm O.D. and 21 cm long Pyrex tube with a sealed bottom. It was attached to the x-ray tube by a groove and an O-ring. A laboratory jack was used to push the chamber against the x-ray tube. The assembled unit which was most frequently used is shown in Figure 3. The second cell, having a volume of 710 cubic centimeters, was a piece of 6.5 cm O.D. and 20 cm long Pyrex tube with a sealed

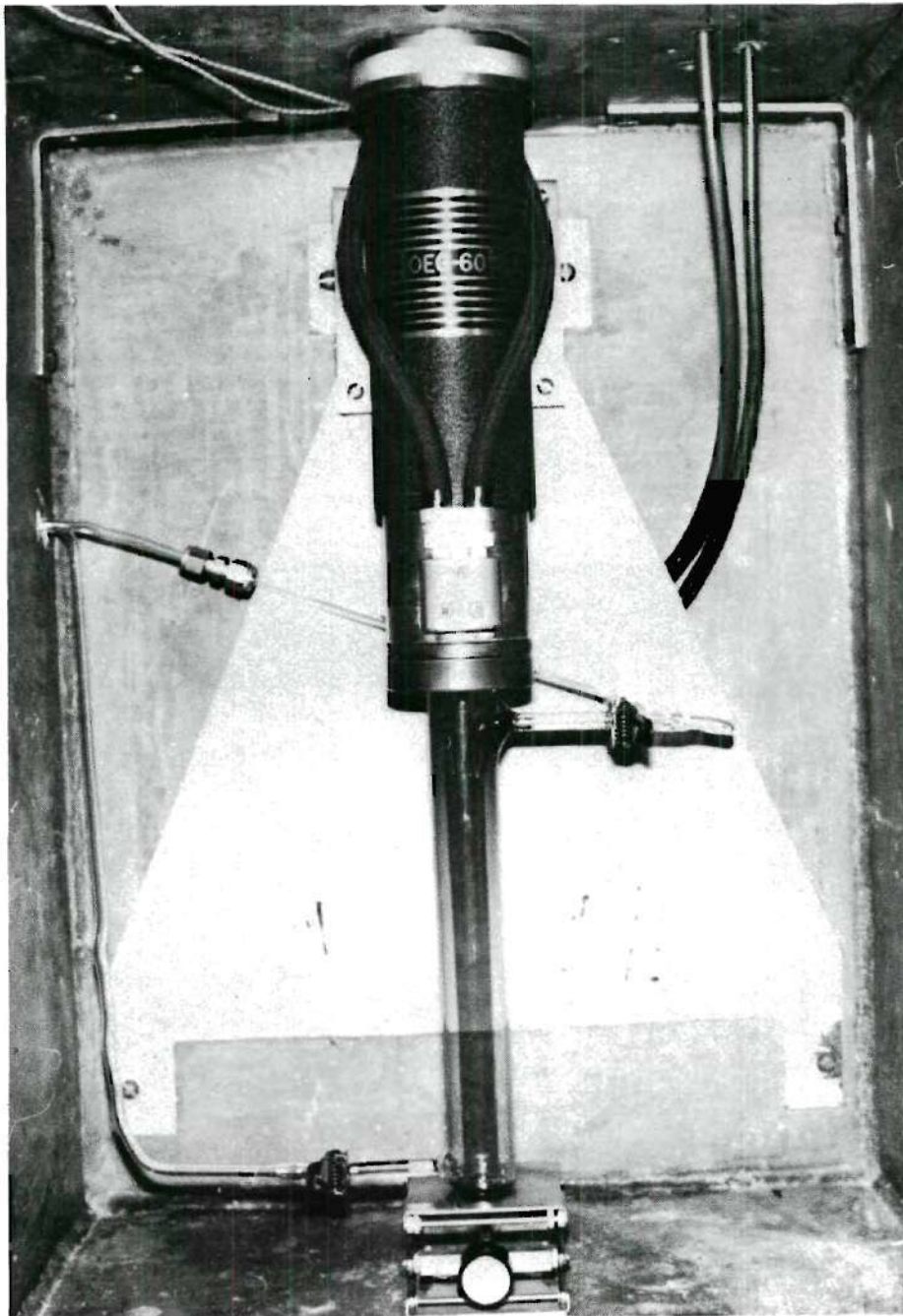


Figure 3. The X-ray Tube, the Irradiation Chamber, and an Inside View of the Lead Vault.

bottom. The other end was fused to a piece of 3.2 cm O.D. and 5 cm long Pyrex tube to accommodate the x-ray tube. The third irradiation cell was a modified 3000 cc flask also with a 3.2 cm O.D. neck. The air or gaseous stream with hydrocarbon additives and moisture entered at the bottom inlet, passed through the chamber, and left at the upper outlet. The flow rate was regulated at 100 cc/min. in most cases. An average irradiation time was obtained by division of cell volume by flow rate.

Component Introduction Mechanism

Reactants were added to the entering air stream by one of three different methods. The first method employed a low-flow rotameter which was mounted in each gas stream to control the desired amount of gaseous reactant such as acetylene. When low concentration was required, the mixing process proceeded in consecutive stages. Part of the mixed stream from the first stage was subsequently introduced into the second stage through a fine needle valve, while the remainder was exhausted to the outside. The second method involved a motor-driven syringe which introduced the gaseous reactant into the chamber at a uniform rate.⁽⁶¹⁾ The disadvantage of this method was that the syringe had to be restored and reloaded every 10 to 15 minutes. Thus, it was primarily employed for preliminary tests and not for the continuous ones.

The third method made use of diffusion cells for the introduction of low concentrations of liquid reactants.⁽⁶¹⁾⁽⁸⁰⁾ One diffusion cell was constructed by connecting a cold trap and a test tube by means of a capillary tube. Another consisted of a 140 cc reactant container and a 250 cc flask connected also by a capillary tube. The inlet and outlet lines

of the flask were designed to promote mixing and to minimize exit effects. By changing the level of the liquid component in the reactant container the level of reactant in the capillary tube was achieved. In this manner a constant distance was maintained from the surface of volatile liquid to the cell space. The air stream passed through the cell at a constant flow rate. The vapor emitted from the liquid in the capillary tube reached the air stream largely by molecular diffusion. The mass transfer rate by volume, W , may be expressed by the relationship⁽⁸⁰⁾

$$W = D_A \frac{A}{L} \ln \frac{P}{P-p_A} \quad (2.1)$$

where D_A is the diffusivity of component A in air, A the cross-section of the capillary tube, L the length of diffusion path, P the total pressure, and p_A the vapor pressure of component A. When P is much larger than p_A , the term $\ln \frac{P}{P-p_A}$ may be replaced by $\frac{p_A}{P}$.

Since this apparatus was not thermostated, variations of room temperature would affect the vapor pressure and diffusivity of the liquid additive and therefore change the mass transfer rate and the concentration of reactant. Gas chromatography and a hygrometer were employed to monitor the hydrocarbon concentration and the gas humidity; adjustments of mass transfer rate were made when necessary.

For some experiments at high hydrocarbon concentration and with moisture, impingers were used which allowed the air or gas to bubble through the liquid additive. Thus the air stream was partly saturated with the additives.

Experimental Procedures

The irradiation chamber and the tubing were cleaned by thorough

washing and heating in an oven overnight. Next, the air lines, the diffusion cell or impingers, and the irradiation tube or chamber were assembled. The system required about 20 minutes to achieve a steady state after introduction and adjustment of the air stream rate and the rate of liquid additive. Gas chromatography and a hygrometer were used to check the hydrocarbon concentration and gas humidity. In most cases, the gaseous products in the gas stream were sampled and analyzed by gas chromatography and with the hygrometer. The particles were collected by Millipore or Nucleopore filters, thermal precipitators, and a particle mass monitor; they were examined by electron microscopy.

When the desired concentration levels of reactants attained a steady state, the x-ray generator was turned on. Sampling and related measurements were started after about 10 minutes which allowed the irradiated system to reach another steady state. During the irradiation period, the inlet air stream was often sampled and analyzed so that a constant additive concentration could be maintained. The x-rays were turned off after an adequate irradiation time period.

The X-ray Source and Dosimetry

The source of x-radiation was provided by a Machlett, Model OEG-60, x-ray tube (Figure 3) operating at 50 pkv and 50 ma. X-rays, arising from the bombardment of a tungsten target by the electron beam, emerged from the tube through a beryllium window.⁽⁷⁴⁾ The window provided a wide-angle (60°) cone of radiation. The spectrum of the OEG-60 x-ray tube at the maximum settings was investigated by Raridon.⁽⁹⁸⁾ The median wavelength of the spectrum was about 0.4 Å. The master control panel from which the voltage and the current were controlled is shown in Figure 4. The photograph also

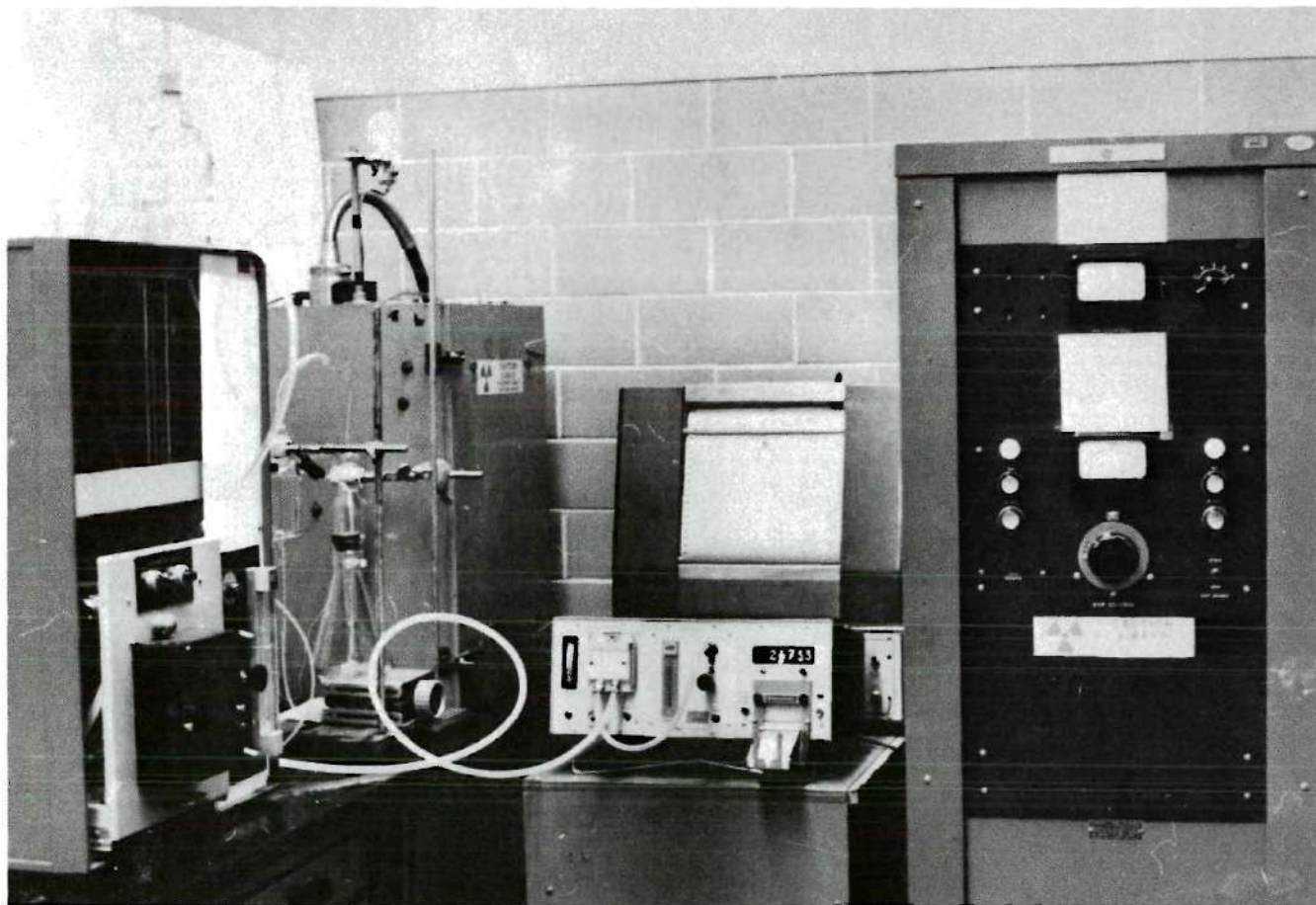


Figure 4. The Colorimeter, the Lead Vault, the Particle Mass Monitor, and the X-ray Master Control Panel.

shows the lead vault which housed the x-ray tube and the irradiation cell.

When the unit was operated at the maximum settings of 50 pkv and 50 ma, the intensity of the x-ray was about 10^{20} ev/min. or two million roentgens per minute. The total beam intensity was 6.4×10^{21} ev/hr at a distance of 2 cm from the window.⁽⁹⁸⁾ Chemical dosimetry using ferrous sulfate solutions gave dose rates of 3.17×10^{18} , 0.88×10^{18} , and 0.0132×10^{18} ev/gm/min. at distances of 1-1/2 in., 2 in. and 2-3/4 in., respectively, from the beryllium window.⁽⁷⁵⁾

Ultraviolet Irradiation Systems

The generation of photochemical smog from parts per million concentrations of hydrocarbons and nitric oxide in humidified air using reaction chambers and UV light has been investigated in a number of laboratories.⁽³⁹⁾⁽⁵³⁾⁽¹³⁶⁾ More experimental work at concentrations approximating those of the atmosphere is still needed. In this study, the concentrations of aromatic and olefinic compounds and nitrogen oxides were employed at somewhat more than ordinary atmospheric levels -- about 10 ppm -- so as to produce adequate amounts of particulates for microphysical and microchemical analysis.

The Mercury Vapor Lamp and Immersion Well

The source of ultraviolet light in the photochemical reaction chamber of this study was a 450 watt Hanovia, type 679A-36, medium-pressure, quartz, mercury-vapor lamp which produced 175.8 watts of radiant energy with wavelengths primarily between 2224 and 13673 Å.⁽³²⁾ The spectral distribution was centered at about 3660 Å. A quartz double-walled well assembly was employed to permit transmission of wavelengths down to 1849 Å and to provide a passageway for coolant to remove heat from the mercury

lamp. A schematic diagram of the immersion well and the lamp are shown in Figure 5.

Light Intensity Measurement

Both the reaction chamber and the lamp (see Figures 5, 6, and 7) were not of simple shape; thus the radiation was not uniformly distributed within the reaction region. In order to account for this and to include factors for light distribution and effective path length, intensities were established by the rate of photolysis of NO_2 at low concentration in nitrogen.⁽²⁷⁾⁽¹²⁴⁾ These results were expressed by a first-order rate constant for NO_2 photolysis, K_d , the equation⁽¹²⁷⁾ being

$$\frac{d(\text{NO}_2)}{dt} = -K_d (\text{NO}_2) \quad (2.2)$$

where K_d is considered equal to ϕK_a with ϕ being a primary quantum yield which was taken as unity⁽⁶⁴⁾ and K_a the rate of light absorption. For this 45-liter chamber and the 450-watt mercury lamp, NO_2 at 1.0 ppm in Matheson zero-grade nitrogen gas had a half life of 3 minutes. This gives a value of K_d of 0.23 min.^{-1} and is a measure of the light intensity in one series of experiments. Another value for K_d of 0.17 min.^{-1} was obtained when a Pyrex glass sleeve was placed between the lamp and the immersion well to prohibit the transmission of light with wavelength below about 2800 \AA . These two values are close to typical noonday sunlight intensities which range from 0.15 to 0.3 min.^{-1} ,⁽⁷⁷⁾ these measurements being made in San Francisco between 11 a.m. to 3 p.m. on several sunny clear days in September.

The Ultraviolet Light Irradiation Chambers⁽⁴²⁾⁽¹¹⁰⁾

Two glass reaction chambers were constructed. One, an annular

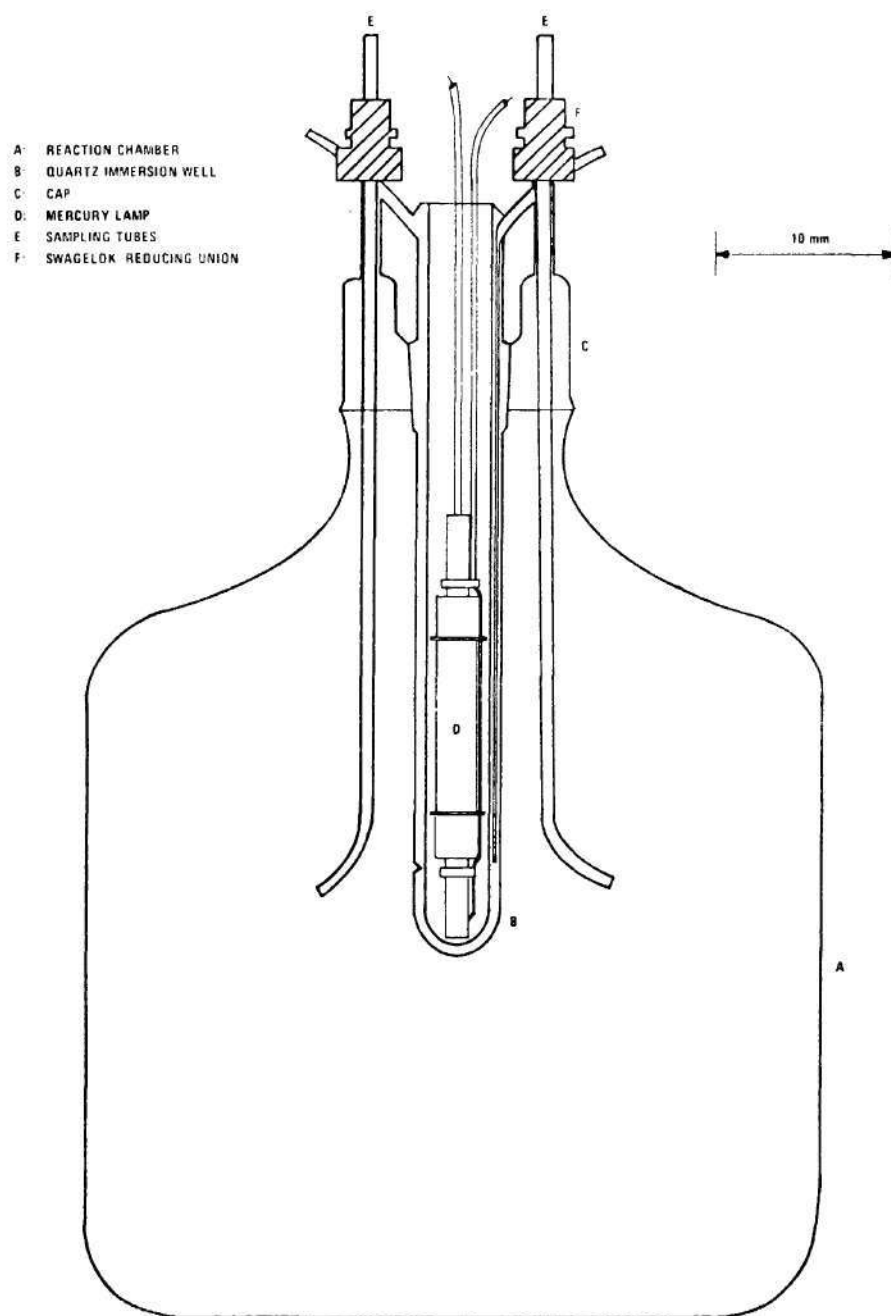


Figure 5. Schematic Drawing of Ultraviolet Irradiation Chamber and Mercury Lamp.

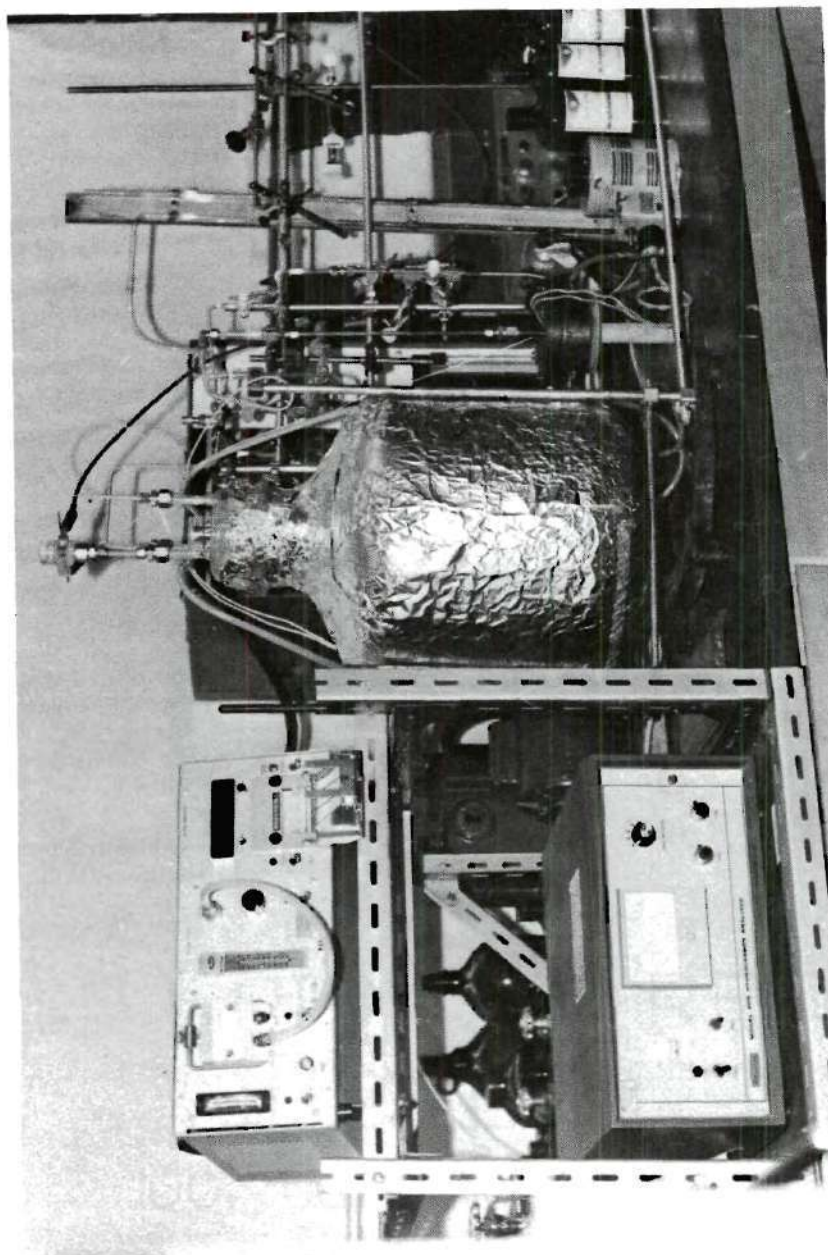


figure 6. Ultraviolet Irradiation Chamber and Analyzing Equipment.

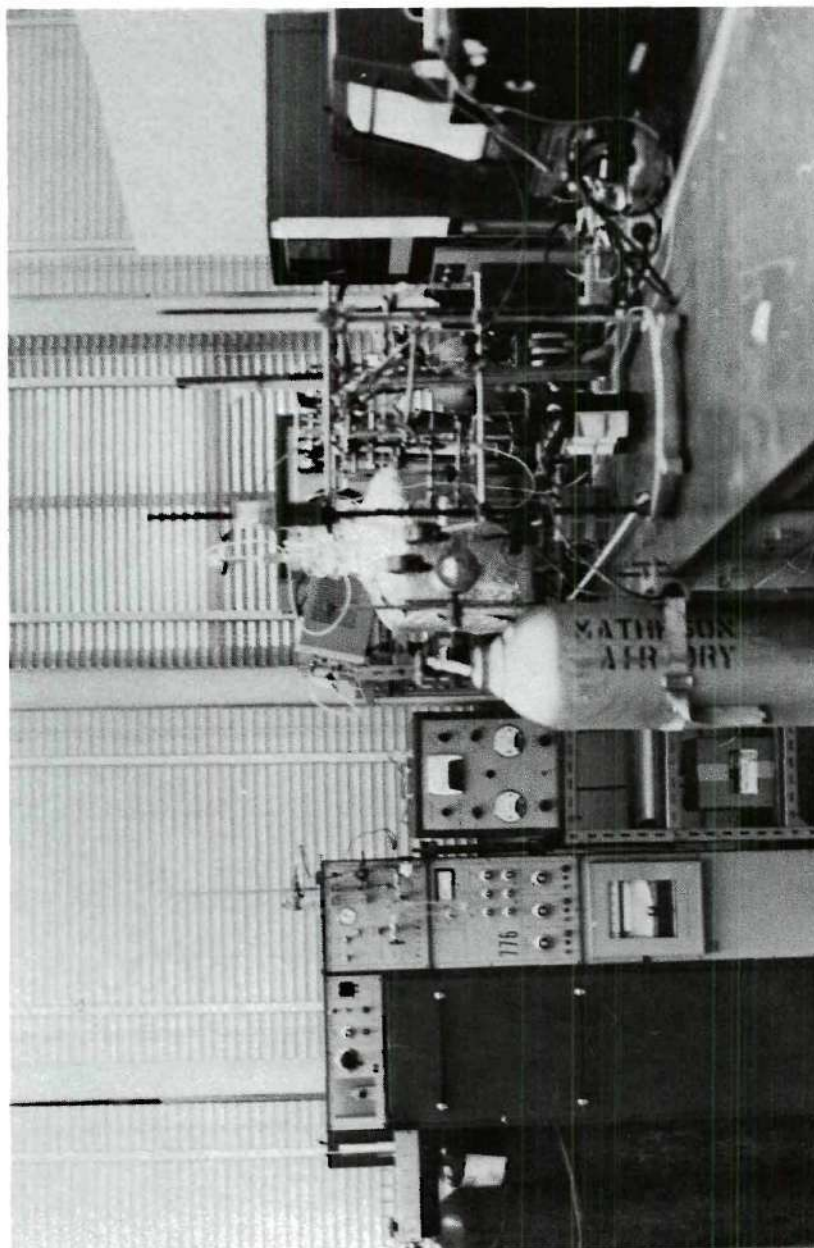


Figure 7. Equipment of the Photochemical Reaction System.

type, was mainly employed for preliminary studies. The outermost part was a piece of 10 cm O.D. Pyrex glass tube 30 cm long; it was connected to the quartz immersion well by a female 60/50 standard tapered ground joint. Most experimental work was performed in a modified 12-gallon Pyrex glass bottle (Figure 6). The mouth of the bottle was enlarged and ground smooth. A special glass connector (Figure 5) was made to accommodate the quartz immersion well with a female 60/50 standard tapered ground glass joint. The glass joint was fitted to the bottle with the connector. The connector incorporated sampling ports and one input port. Each port was connected to glass tubing by Swagelok fittings. The two sampling ports extended to the end of the quartz immersion well, keeping 3 cm from its wall. The input port had no extension, so the input reactants were injected near the top of the chamber and the products were withdrawn from the middle portion of the chamber (see Figure 5). All-glass or -quartz construction provided an essentially inert reaction system.

No stirrer or other agitating device was employed. Concentration measurements as a function of time showed that hydrocarbon vapor and other gaseous constituents became homogeneous in a short time after introduction. Dilution tests, for example, showed that this followed an exponential decay pattern. Furthermore, radiation to the walls of the chamber during an actual test generated convection currents in the chamber which produced further mixing and prevented gas stratification. The outer walls of the reaction chamber were covered with aluminum foil both to increase the radiation intensity and to serve as a safety feature. The wall temperature was found to be 32°C after 20 minutes of operation, or slightly higher than the ambient temperature of 28°C inside the chamber.⁽²⁾⁽²⁸⁾ The pressure in

the chamber was measured by a mercury manometer at 2 to 3 mm of mercury above atmospheric pressure. The total volume of the reaction chamber was 45.5 liter.

Dilution tests and concentration measurements indicated that there was no significant loss in total hydrocarbon content when the chamber was filled with benzene and other hydrocarbon compounds at 10 ppm concentration and allowed to stand for two hours. Concentration measurements of propionaldehyde on the other hand showed a 3 to 5 per cent loss after two hours of standing. This indicates there was some adsorption of propionaldehyde by the Pyrex glass which may account for part of the decrease of aliphatic aldehydes after the maximum concentration was attained during the ultraviolet irradiation process as described subsequently. Also humidity studies showed some significant water vapor condensation and adsorption onto chamber walls. For example, when the chamber was dosed with an amount of water sufficient to produce a relative humidity of 18.9 per cent at 28°C, the measured humidity value was actually 14.3 per cent.

The effect of the Pyrex wall and the possible existence of wall reactions were also considered. The chamber was sometimes pre-conditioned by being exposed to a reaction mixture prior to an actual test to minimize further adsorption. When a series of experiments with one particular reactant mixture was performed, data were taken from the second or later tests. This precaution was taken because rates of wall reactions have been shown to be considerably reduced by allowing reaction products to form an extremely "thin layer" on the surfaces of walls.⁽⁹⁴⁾

The simultaneous analysis, sampling, or monitoring of two or more products required that samples be drawn from the chamber at flow rates

from 300 to 500 cc/min. To compensate for the volume of gas removed, purified air was added at the same flow rate. Concentration measurements proved that the dilution followed an exponential decay, i.e., that the concentration of the organic reactant was described by the expression

$$C = C_0 e^{-\frac{Qt}{45500}} \quad (2.3)$$

where C and C_0 are the time dependent and original concentrations respectively, t the time in minutes, and Q the flow rate in cubic centimeters per minute. Heterogeneous decomposition of ozone on walls has also been noted.⁽³⁹⁾ Increases in the rates of NO_2 and ozone formation and hydrocarbon disappearance were found after the walls of the chamber were cleaned by both heating and evacuation and upon conditioning by NO_2 .⁽⁵³⁾

Controllable Reactant Introduction Mechanism

Reactants were added to the chamber through an injection system consisting of a greaseless needle valve, stainless steel and glass tubing, and a glass injection port with rubber septum. A weighed quantity of water was injected through the septum into the injection port. The desired amount of hydrocarbon was injected as a liquid with a 5 microliter syringe. Both the water and the hydrocarbon were vaporized by heating the injection port. A measured volume of one of the nitrogen oxides was also injected with a gas-tight syringe. Purified air was then used to purge the injection port and sweep the reactants into the reaction chamber. Steady and homogeneous distribution of reactants was attained in a few minutes. In some tests, a diffusion cell was also used to provide a continuous addition of hydrocarbon to the reaction chamber. Details of the diffusion cell are described in the preceding section of this chapter.

Reactant concentration was made slightly excessive during the introduction period, but irradiation was started just as the dilution reduced concentrations to the desired values. Purified dilution air passed through a calibrated rotameter, a by-pass line, and a fine needle valve on its way to the chamber. The flow rate was adjusted to equal the sampling flow rate and was checked by pressure readings from the chamber.

Experimental Procedures

The reaction chamber was cleaned between different tests by washing with diluted hydrofluoric and hydrochloric acid solutions followed by several distilled water rinses. The chamber was dried by blowing air through it. For a series of identical chemical tests, the cleaning procedure between runs involved only evacuating and purging in order to maintain the chemical passivity of the chamber walls. The chamber was purged by dry air just before starting each run, and a total hydrocarbon analyzer was employed to measure the concentration of hydrocarbon in the exhaust. Always the hydrocarbon content was brought below 2.0 ppm CH_4 . When zero air was used in the purging, the hydrocarbon content was usually carried below 1.0 ppm CH_4 .

At this time other analytical instruments were turned on to begin equilibrating. These included the gas chromatograph, hygrometer, and the NO_2 colorimetric analyzer. The ozone scrubbing sampler and aldehyde scrubbing sampler were readied. Also, sampling and monitoring devices for particulate products were started and checked. These included Millipore or Nuclepore filters, thermal precipitator, electrostatic precipitator, particle mass monitor, and electron microscope. The details of each device and its function will be discussed in subsequent sections.

Next, the calculated amount of hydrocarbon was measured and injected with the microliter syringe. For a test involving humidity, the desired quantity of water was introduced before the injection of the hydrocarbon. When the flow of the entering air steam was adjusted equal to the sampling rate and the hydrocarbon concentration reached the desired value, the mercury lamp was turned on and cooling water was allowed to run through the jacket of the immersion well. Thereafter readings from the particle mass monitor, the NO_2 indicator, and the colorimetric analyzer were taken as nearly simultaneously as possible. Particulate samples were taken also by filtration, thermal and electrostatic precipitation, and gas samples were collected for gas chromatography, for the flame ionization detector of hydrocarbons, and for ozone and aldehyde analysis.

After 100 minutes or other desired reaction period, the mercury lamp and all other instruments were turned off, and the reaction chamber was immediately purged to avoid accumulation of reaction products. Samples for ozone and aldehyde analysis and the collected particulate samples were carefully stored for later evaluation.

CHAPTER III

SPECTROMETRIC ANALYSES AND CHEMICAL NATURE OF PARTICULATES

Investigation of the chemical nature of radiation-induced aerosols is subject to many difficulties. First, the yield of particulate products from the irradiation of hydrocarbons in the parts per million range is extremely low, often fractions of a milligram. Second, collection must be carefully accomplished to avoid contamination. Third, the particles are often insoluble in the common solvents employed in infrared spectral methods. And, finally, the KBr pressed disc⁽⁸¹⁾ and other techniques⁽¹⁰⁸⁾ are both difficult and inconvenient. Pfefferkorn⁽¹⁰²⁾ has phrased the situation as follows: "Nothing can yet be said of the chemical composition of these reaction products, since the weight of droplets -- which can only be seen under the electron microscope -- is so small that they cannot be analyzed with available chemical method."

Most x-ray induced particulates and photochemical aerosols are insoluble in common organic solvents, although particulates produced from photochemical reactions involving benzene-nitric oxide-air mixtures are partially soluble in ethanol and acetone. Thus, the separation of particulate components by thin layer or liquid chromatography followed by mass spectral analysis of the isolated substances was seriously restricted due to the absence of suitable solvents. Nuclear magnetic resonance (NMR) spectrometry was also confronted by the same obstacle, although some analysis work was attempted on the products from benzene-nitric oxide-air

mixtures. Four different solvents were used -- CH_3OH , CCl_4 , $\text{C}_2\text{H}_5\text{OD}$, and CH_3COCH_3 -- but the effort was fruitless, primarily because of the low amount of dissolved components. Again, a proper solvent not being available rendered ultraviolet spectrometric analysis out of the question. Electron microprobe method was used for the non-destructive analyses of some x-ray induced particulates. An Electron Probe X-ray Microanalyzer, Model MS-64, manufactured by Acton Laboratories of Massachusetts was employed, and four different samples, each produced from the x-ray irradiation of benzene or acetylene in air with and without the addition of water vapor, were examined. The ratio of carbon, nitrogen, and oxygen in these samples was found to be remarkably similar, an average ratio of C:N:O of 12: 5: 10 by number of atoms being obtained. The surprising constituent is the high amount of nitrogen. Some of the nitrogen in products from the C_2H_2 -air system may be in the form of nitrites, since the mass spectra showed ion fragments at 30 (NO) and 60(CH_2ONO) which are indicative of alkyl nitrites.⁽¹⁷⁾ However, the high ratios of nitrogen atoms in the samples produced from either benzene or cyclohexene in air still remain a mystery.

Infrared Spectrophotometric Analysis of Particulates

Mader and coworkers⁽⁶⁾ carried out infrared analyses of atmospheric and synthetic aerosols which indicated the presence of carbonyl and hydroxyl groups as well as compounds of nitrates and esters. Renzetti and Doyle,⁽¹⁰⁸⁾ using ether extraction on aerosol samples which were produced from the ultraviolet irradiation of automobile exhaust, also showed the presence of carbonyl and hydroxyl groups. Sawicki and Hauser⁽¹¹⁴⁾ employed infrared

spectral methods to detect carboxylic acids and aldehydes in airborne particulates by the reactions of various types of carbonyl compounds with phosphorus pentachloride and with diethylamine. Sloane,⁽¹¹⁸⁾ however, established that specially made thin cellulose nitrate-acetate membrane filters, of the types manufactured by the Millipore Corporation, could be used in a differential technique involving an infrared analysis. Thomas and Dwyer⁽¹²⁶⁾ applied this technique to the analysis of gas-chromatographic effluents. Hannah and Dwyer⁽⁵⁷⁾ also made infrared analyses of suspended particulates with Millipore filters, although attenuated reflection was measured instead of absorption or transmission.

Infrared Spectrophotometer and Sampling Method

Particulates were collected at the outlet of the x-ray or ultraviolet irradiation chamber by a ultrafine Millipore TH filter of 25 μm thickness held by a standard Swinny Filter Holder. Afterwards, the filter was placed in a specially made sample cell of a double beam infrared spectrophotometer. Another matched TH filter was placed in the reference beam of the instrument to negate the spectrum of the sample beam filter. Paired filters were checked by running them in the sample and reference beams and making the required compensation before collecting the sample. Thus, particulates were examined spectroscopically as a thin layer collected on a filter.⁽¹¹⁸⁾ Their spectra were recorded between wavelength of 2 and 15 μm using a Perkin-Elmer, Model 211, Infrared Spectrophotometer equipped with automatic slit control and NaCl prism.

Chemical Structure of X-ray Irradiation Products

The infrared spectrum (Figure 8) of samples produced by the x-ray irradiation of air and benzene systems are similar to those of phenolic

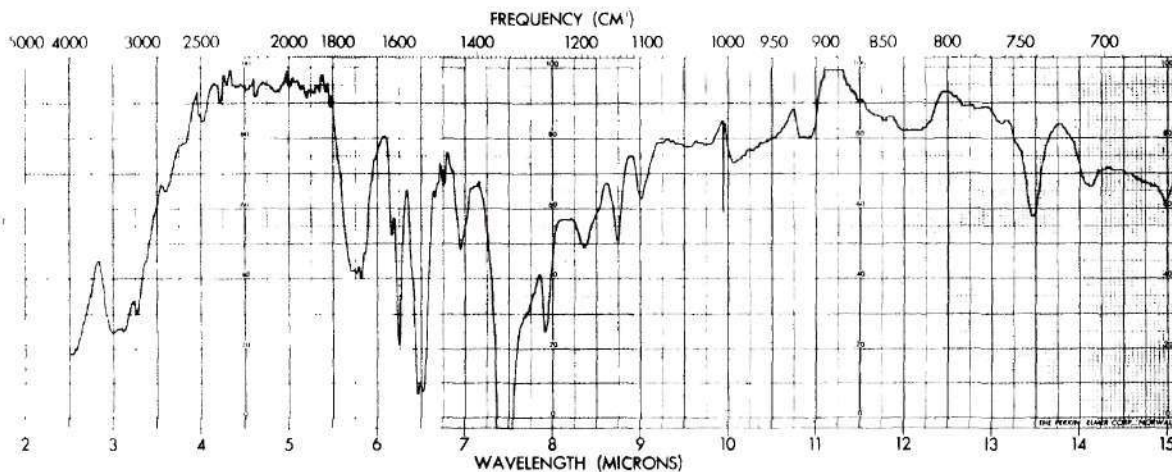


Figure 8. Infrared Spectrum of Particulate Products from the X-ray Irradiation of Benzene-Air Mixture.

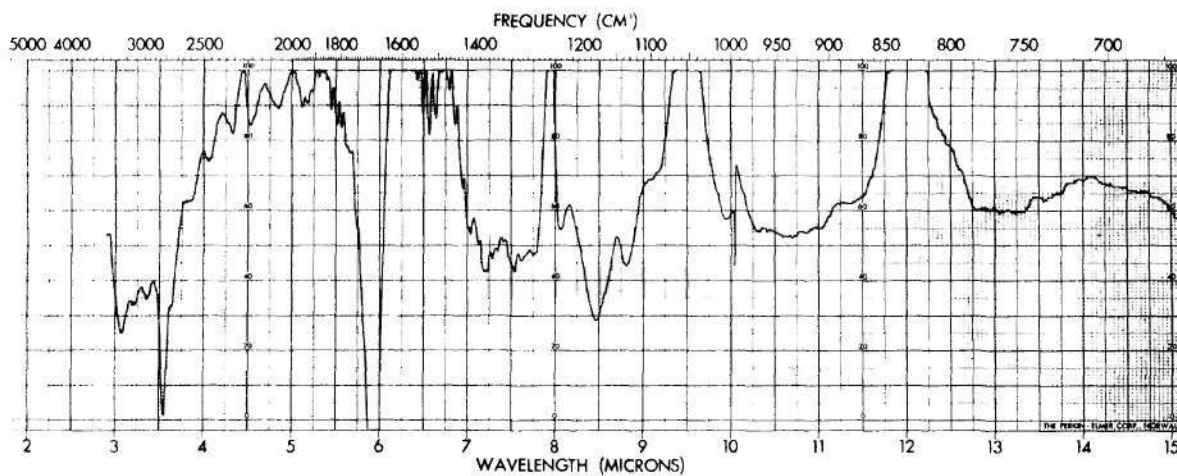


Figure 9. Infrared Spectrum of Particulate Products from the X-ray Irradiation of Cyclohexene-Air Mixture.

resins except for a strong band at 1720 cm^{-1} which likely results from the C=O stretching vibration and a strong band at 1340 cm^{-1} which probably results from O-H bending vibration.⁽¹¹⁷⁾ Evident aromatic characteristics are revealed. An absorption band occurring at 3200 cm^{-1} indicates benzene ring C-H stretching vibration. The peak at 1765 cm^{-1} results from the possible existence of phenyl acetate. Weaker combination and overtone bands at 1600, 1530, and 1480 cm^{-1} are highly characteristic of the benzene ring substitution pattern. The bands at 708 and 742 cm^{-1} probably arise from monosubstitution or 1,2 substitution in the benzene ring. Those bands at 920, 1200, 1270, and 1440 cm^{-1} most likely result from aromatic C-C stretching and C-H bending vibrations. The band at 3400 cm^{-1} likely results from O-H stretching vibrations; the band at 1340 cm^{-1} indicates O-H bending vibration; and the band at 1145 cm^{-1} results from a C-OH or C-O-C stretching vibration.

The aromatic vibration modes and the strong band at 1720 cm^{-1} , which shows a C=O stretching vibration, indicate the presence of aromatic aldehydes. The bands at 1720, 1270, and 1110 cm^{-1} also indicate the characteristic vibration modes of benzoates and phthalates. When purified air is replaced by dry nitrogen, the absorptions at 1765, 1720, 1340, and 1145 cm^{-1} in the product spectra diminish while all other aromatic characteristic bands remain. This suggests an attack of oxygen on aromatic bonds to form oxygenated compounds.

The spectra of products from the x-ray irradiation of acetylene-air and acetylene-oxygen systems are shown in Figures 10 and 11. The band at 3320 cm^{-1} is thought to result from an O-H stretching vibration. The peak at 2950 cm^{-1} indicates an aliphatic C-H stretching vibration. The band at

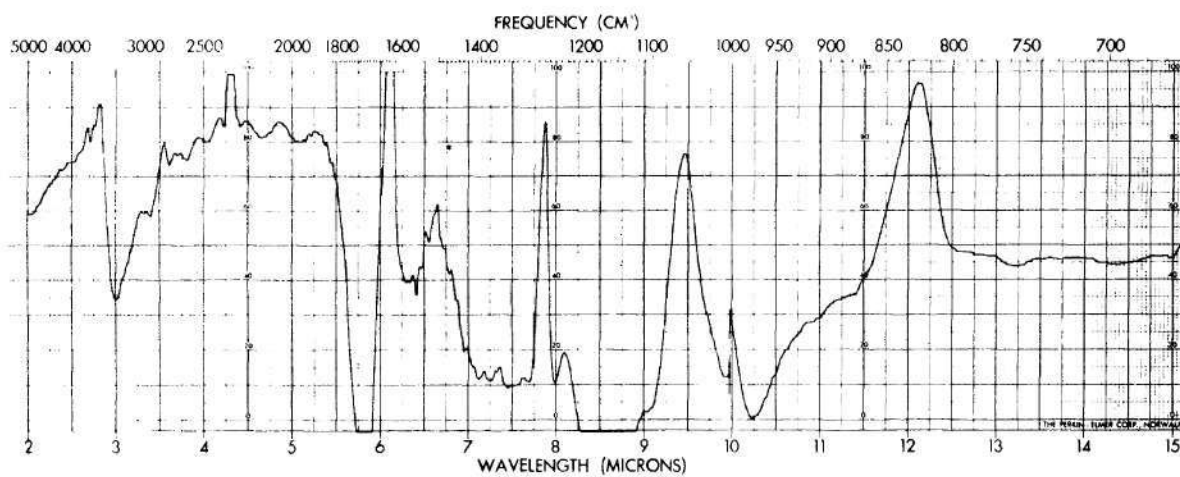


Figure 10. Infrared Spectrum of Particulate Products from the X-ray Irradiation of Acetylene-Air Mixture.

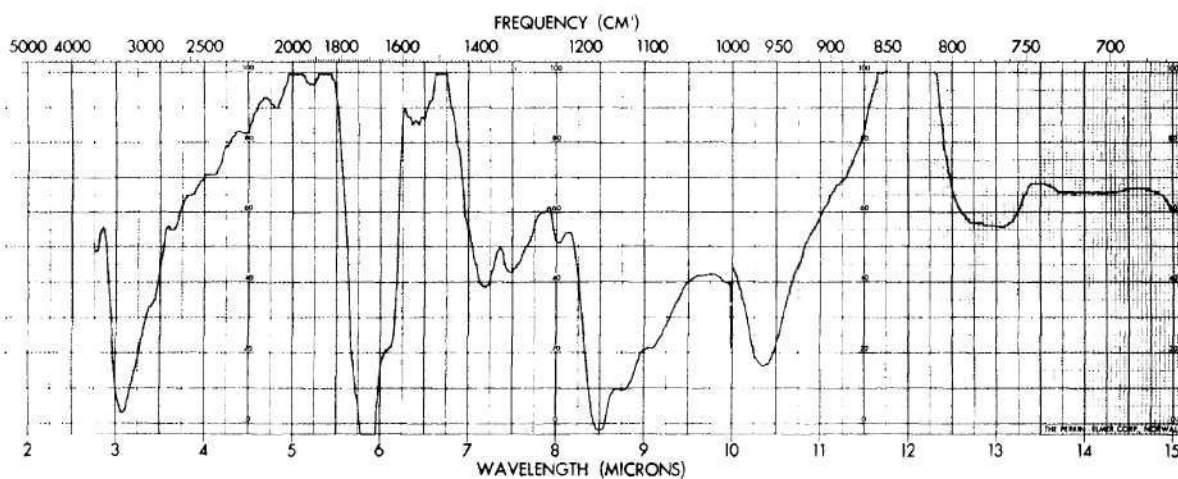


Figure 11 Infrared Spectrum of Particulate Products from the X-ray Irradiation of Acetylene-Oxygen Mixture.

1170 cm^{-1} probably either results from a C-OH or a C-O-C stretching vibration, and, combined with the existence of a broad band between 1300 and 1400 cm^{-1} , it indicates the existence of tertiary aliphatic alcohols. The bands at 980 and 1400 cm^{-1} probably show the existence of a vinyl group. The strong band at 1720 cm^{-1} may again result from a C=O group.

In the spectrum of samples produced from the x-ray irradiation of a cyclohexene-air mixture (Figure 9), the bands at 2820 and 3000 cm^{-1} are thought to result from aliphatic C-H stretching and the band at 1400 cm^{-1} from C-H bending. Also an absorption band exists at 1710 cm^{-1} which suggests the presence of a carbonyl group. Part of the shoulder at the 1600 cm^{-1} side of the C=O peak disappeared within an hour, probably showing the evaporation of one carbonyl component in the mixture. The band at 1185 cm^{-1} indicates a C-OH bending or a C-O-C stretching vibration. According to one study of the infrared spectra of carboxylic acids,⁽¹¹⁴⁾ the peak at 1710 cm^{-1} , the shoulder at 2550 cm^{-1} , and broad bands from 1300 to 1400 cm^{-1} and from 870 to 1000 cm^{-1} , offer evidence that carboxylic acids are important constituents. The sample shows strong carbonyl absorption and is also highly aldehydic. The shoulders at 2700 and 2800 cm^{-1} are characteristic of aldehydic C-H stretching vibrations.⁽¹⁰³⁾

Sears and Parkinson⁽¹¹⁵⁾ noticed oxidation products to form in nuclear irradiated polystyrene. The O-H band at 3400 cm^{-1} and the C=O band at 1700 cm^{-1} increased greatly in intensity during an exposure following irradiation in vacuum. This result is very similar to the highly oxidized products found here which also contain hydroxyl and carbonyl groups. McAndrews⁽⁸⁷⁾ reported radical yields in electron irradiated aromatics, phenyl ($\text{C}_6\text{H}_5\cdot$) and cyclohexadienyl ($\text{C}_6\text{H}_7\cdot$) radicals being the principal

products. These and other radicals appear to be characteristic intermediates during x-ray irradiation. Such a radiation-induced oxidation mechanism could derive from an attack of molecular oxygen on the benzene ring, on unsaturated compounds, or through combination with these free radicals. Therefore, irradiation of gas mixtures form many new compounds such as phenols, aromatic aldehydes, alcohols, peroxides, and other oxygenated organic compounds. The spectra of these compounds overlap each other and tend to obscure the band characteristic of individual molecules.

Chemical Structure of Photochemical Products

The infrared spectrum of fresh aerosol produced from the photochemical reaction of 10 ppm benzene in purified air in the presence of 10 ppm NO is shown in Figure 12. The band close to 3300 cm^{-1} is thought to result from an O-H stretching vibration; the shoulder at about 3000 cm^{-1} indicates an aromatic C-H stretching vibration; while the strong band at approximately 1720 cm^{-1} probably results from a C=O stretching vibration. An overlapping of bands is evident, especially between 900 and 1400 cm^{-1} . The bands at 1200 , 1260 , and 1310 cm^{-1} probably indicate O-H bending, and the band at 1400 cm^{-1} could result from C-O stretching vibrations. N-containing groups are not evident in significant amounts according to the interpretation of this infrared spectrum.

In the spectrum (Figure 13) of particulate material produced from the photochemical reaction of 10 ppm benzene in purified air, again, the band at 3300 cm^{-1} indicates O-H stretching, and the peak at 2860 cm^{-1} results from aliphatic C-H stretching vibration. The strong band at 1720 cm^{-1} , which results from a C=O stretching vibration, indicates the exist-

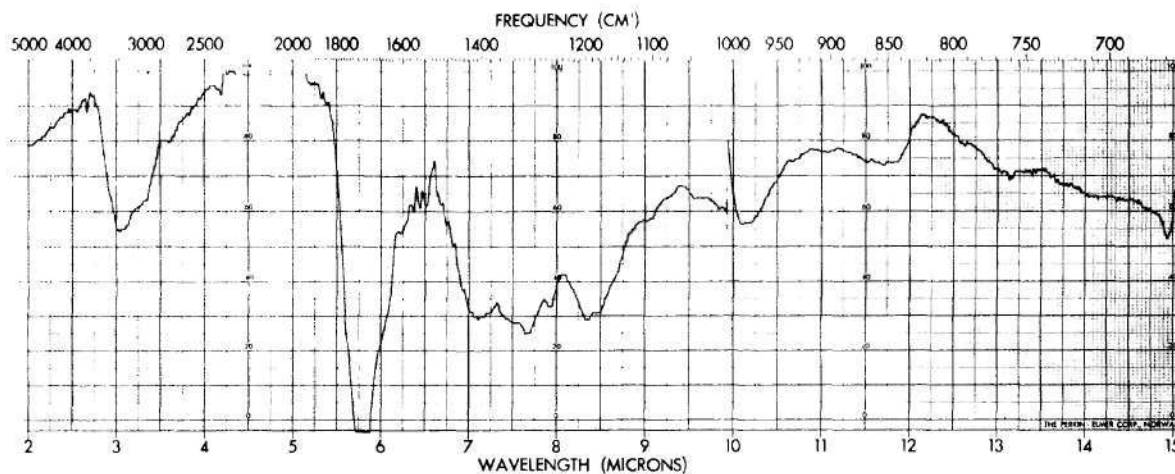


Figure 12. Infrared Spectrum of Particulate Products from the Photochemical Reaction of Benzene-Nitric Oxide-Air Mixture.

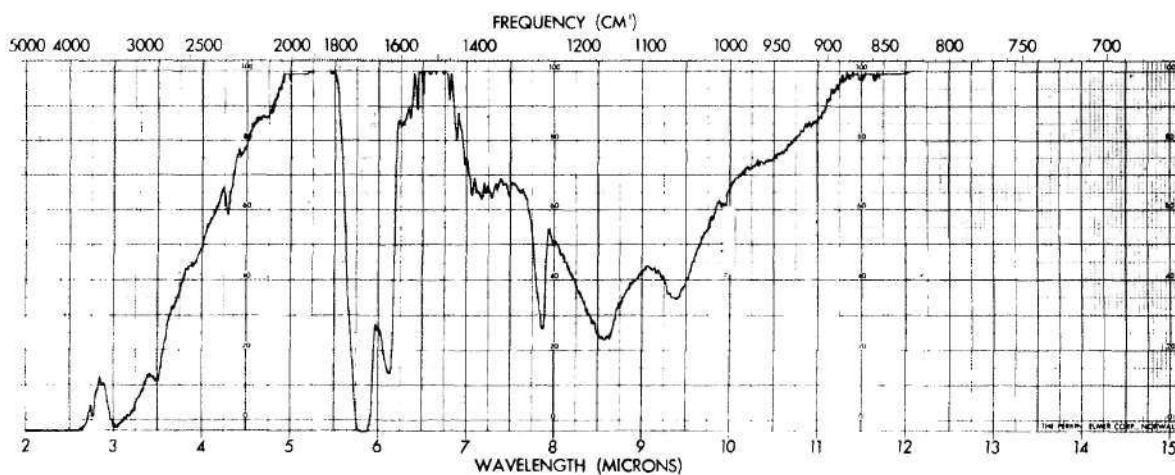


Figure 13. Infrared Spectrum of Particulate Products from the Photochemical Reaction of Benzene-Air Mixture.

ence of esters. A similar spectrum was obtained when water vapor was added to the air.

Strong similarity exists between the infrared spectra of products from the ultraviolet irradiation of 10 ppm toluene and 10 ppm o-xylene in purified air. With toluene (Figure 14) there is a strong band at 1710 cm^{-1} . The overlapping of bands elsewhere makes further interpretation difficult. For the o-xylene (Figure 15) the peak at 3350 cm^{-1} indicates the O-H stretching vibration, and the shoulder at 2950 cm^{-1} likely results from aliphatic C-H stretching. The strong band at 1730 cm^{-1} shows C=O stretching and, because of the bands at 1275 and 1060 cm^{-1} , also indicates the presence of aromatic esters. The weak band at 1375 cm^{-1} probably results from an aromatic C-C stretching vibration. Bands at 1220 and 1165 cm^{-1} indicate, possibly, C-OH stretching vibration. Peaks at 840 and 750 suggest unsymmetrical aromatic substitutions. The band at 1165 cm^{-1} might indicate the structure C-O-C, i.e., ethers.⁽¹¹⁷⁾ The spectrum of the irradiation products from o-xylene-air mixtures bears a strong similarity to that of diethylphthalate.⁽¹²⁰⁾

Mass Spectrometric Analysis of Particulates

A pure organic compound produces a certain fragment pattern or spectrum in a mass spectrometer, and the identification of certain compounds can be achieved by comparison with a reference spectrum.⁽²⁶⁾⁽¹¹⁷⁾ Since the products from either the x-ray or ultraviolet irradiation system are obviously mixtures of highly oxygenated organic compounds, only some of the components can be identified qualitatively by comparison of their mass spectrum peaks with those commonly encountered in the mass spectra of

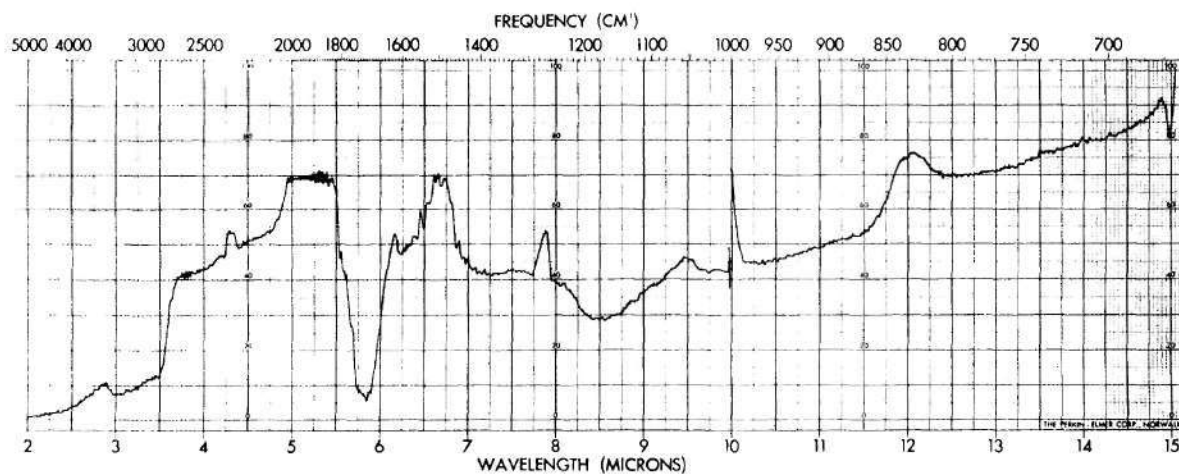


Figure 14. Infrared Spectrum of Particulate Products from the Photochemical Reaction of Toluene-Air Mixture.

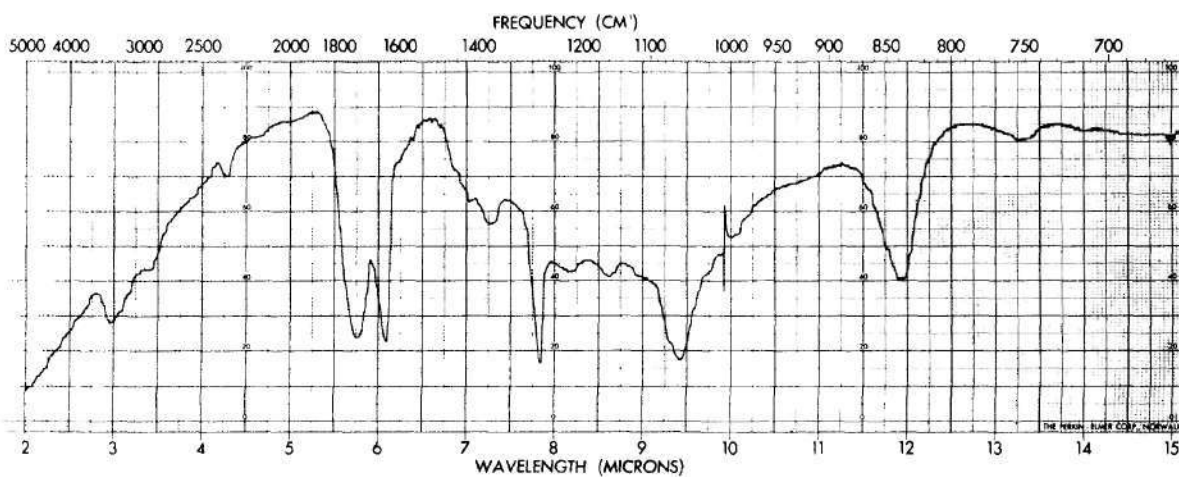


Figure 15. Infrared Spectrum of Particulate Products from the Photochemical Reaction of o-Xylene-Air Mixture.

organic compounds. This method should, however, be used with caution. It is probably of most value when used in conjunction with the analytical results of the preceding section, i.e., the infrared spectral studies.⁽¹⁷⁾

A mass spectrum results from dissociation under electron impact. A mass spectrometer must be operated with an extremely high vacuum. Under this condition collisions and combinations are negligible, which means the measured masses are probably those of the primary ions.⁽⁸¹⁾ In the x-ray irradiation reactions of this work, the involvement of energetic intermediates, such as those appearing according to mass spectra, could be completely obscured in the final particulate product. Meyerson⁽⁹⁰⁾ has discussed the similarity of patterns from radiolysis, photolysis, and mass spectroscopy for phenyl alkyl ketone. It was concluded that mass spectra are most useful as a guide in studying radiolytic systems. And, in the investigation of energetic intermediates and reaction mechanisms of radiolytic and photolytic systems, it must be recognized that some of the intermediates may have resulted from fragmentation in the mass spectrometer.

Mass Spectrometer and Sampling Method

The mass spectrometer used for the analysis of particulate samples was a Varian Analytical Instrument Division product, Model M66. This particular mass spectrometer was capable of resolving mass numbers m/e , i.e., the ratio of mass to charge, up to 2000. Mass spectra were obtained at a beam energy of 70 electron volts, under a vacuum of 1×10^{-5} to 5×10^{-7} torr, while samples were "baked" at a probe temperature from 100 to 330°C depending on the volatility of the samples. Under these conditions many fragment ions were formed. The resulting spectrum is a presentation

of the masses of the fragment ions versus their relative intensities.

The sampling method employed for x-ray irradiation had to be adjusted to the requirements of the analysis. Since the x-ray irradiation process involved steady-state, continuous flow, the reaction was allowed to proceed for approximately 30 minutes before sampling for mass spectrometric analysis was begun. The sample was then collected from the outlet of the irradiation system by thermal precipitation at a flow rate of approximately 100 cc/min. for a period of from 30 min. to one hour. Finally, the sample was transferred from the precipitator to a capillary tube and sealed before it was taken to the mass spectrometer.

For photochemical reaction systems,⁽¹¹⁶⁾ the chamber was first flushed with purified air, then the hydrocarbon or nitric oxide at 10 ppm was injected into the chamber through a septum using a microliter gas-tight syringe. As soon as a homogeneous concentration in the chamber was attained, the irradiation lamp was turned on. Aerosol sampling at a flow rate of 1600 cc/min. was started at the same time. Thus these experiments were dynamic in nature and allowed on the average a 30-minute residence time in the chamber undergoing irradiation. At the end of each 30-minute period, another 10 ppm of hydrocarbon or nitric oxide was added to the chamber. The particulate product was again collected by thermal precipitator, transferred to a capillary tube, and sealed for later mass spectrometric analysis.

Mass Spectra of X-ray Irradiation Products

Investigations were made using acetylene at different concentrations in purified air or oxygen. In all product spectra here, homologous series peaks were found at low mass numbers up to 100, terminating in a series of

much smaller peaks without the appearance of any parent or molecular ion peaks. A typical example is shown in Figure 16. This mass spectrum was given by the particulate product from the x-ray irradiation of 5.0 per cent acetylene in purified air, and was obtained at an electron beam energy of 70 eV, a probe temperature of 250°C, and a vacuum of 2×10^{-6} torr.

An examination of Figure 16 shows the complexity of the sample: there are paraffinic characteristics, i.e., the major peaks are 14 units (CH_2) apart and the peaks at 43 (C_3H_7) and at 57 (C_4H_9) are large. There exist olefinic and aromatic peaks such as 39 (C_3H_3), 41 (C_3H_5), 55 (C_4H_7), 77 (C_6H_5), and 79 (C_6H_7). Therefore, it is concluded that this sample is a mixture of hydrocarbon compounds with saturated and unsaturated components. The peaks at 18 (H_2O), 28 (CO), 29 (CHO), and 44 (CH_3CHO or CO_2) indicate highly oxygenated compounds. Since most oxygenated compounds break with loss of H_2O , the complementary losses of mass 28 and 44 indicate the presence of aldehydic and acidic compounds. The sample would thus appear to consist of aldehydes and carboxylic acids with their polymers as important constituents. Significant peaks were found in the mass spectrum of the aerosol products at mass numbers much greater than the molecular weight of the reactant, e.g., acetylene. This would indicate that acetylene, when irradiated in air, reacted with itself or with oxygen and radiation induced radicals to form compounds of high molecular weight. Compound carbon chain length could be of the order of 10 or higher for the vaporized sample, i.e., the resolved part of the sample in the mass spectrometer. Turner⁽¹²⁸⁾ in performing mass spectrometric analyses noted the existence of a black non-volatile residue under high vacuum and temperature.

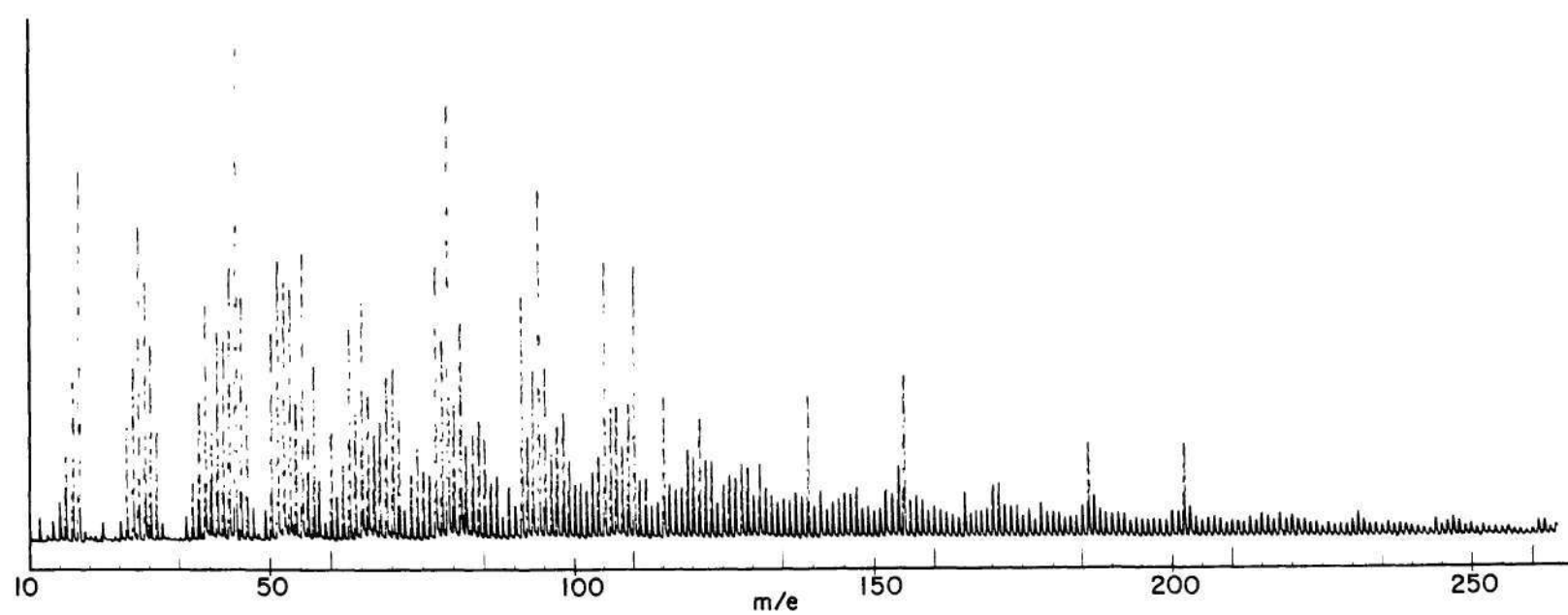


Figure 16. Mass Spectrum of Particulate Products from the X-ray Irradiation of Acetylene-Air Mixture.

Mass Spectra of Photochemical Aerosols from Traces of Benzene in Air

The mass spectrum shown in Figure 17 was obtained for particulate products from the photochemical reaction of 10 ppm benzene in purified air. It was obtained at 70 eV, 10^{-5} torr, and 250°C. The finding of most interest from this spectrum is that it indicates the possible presence of an aromatic ketone, perhaps fluorenone, and low molecular weight compounds containing hydroxyl and carbonyl groups. The peak at 180 indicates the parent ion of fluorenone and the peak at 152 probably is an aromatic fragment after loss of CO.⁽¹⁸⁾ The existence of other quinonic compounds such as xanthone and fluorenone-ol is suggested by the small "parent peak" at 196. The peak at 168 could show the existence of diphenylene oxide.

Another spectrum obtained from what was supposed to be an identical sample tested similarly at 70 eV, 250°C, and a vacuum of 5×10^{-7} torr showed no parent peaks at high mass number. Instead distinct peaks at 18 (H_2O), 29 (CHO), and 44 (CH_3CHO) showed characteristics of compounds containing carbonyl groups. Other ion fragments such as 77 (C_6H_5), 93 (C_6H_5O), and 105 (C_6H_5CO) offer evidence for the possible presence of aromatic aldehydes and ketones or quinonic compounds.

Figure 18 shows the mass spectrum obtained from a photochemical aerosol sample obtained from 10 ppm o-xylene in purified air at a probe temperature of 100°C, a pressure of 10^{-5} torr, and with an electron energy of 70 eV. Again, a prominent peak at 105 and others at 91, 77, and 60 were obtained. These mass numbers would suggest the presence of the fragment ions C_6H_5CO , $C_6H_5CH_2$, C_6H_5 , and CH_3COOH , and indicate the original presence of aromatic ketones and organic acidic and aldehydic compounds as main components of the resolved and vaporized part of the sample.

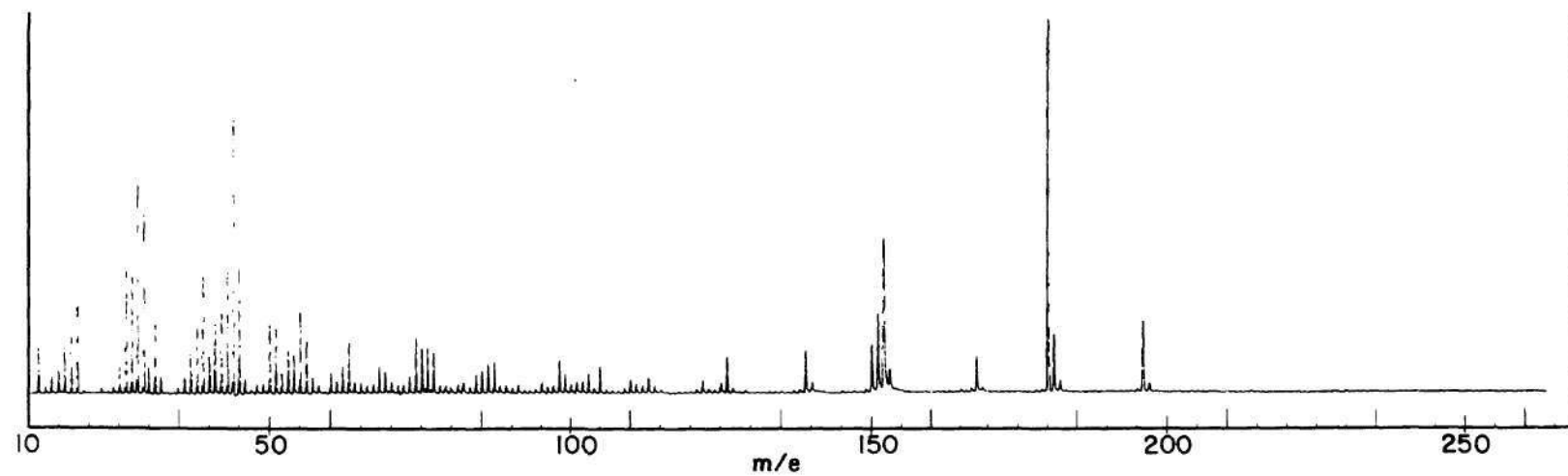


Figure 17. Mass Spectrum of Particulate Products from the Photochemical Reaction of Benzene-Air Mixture.

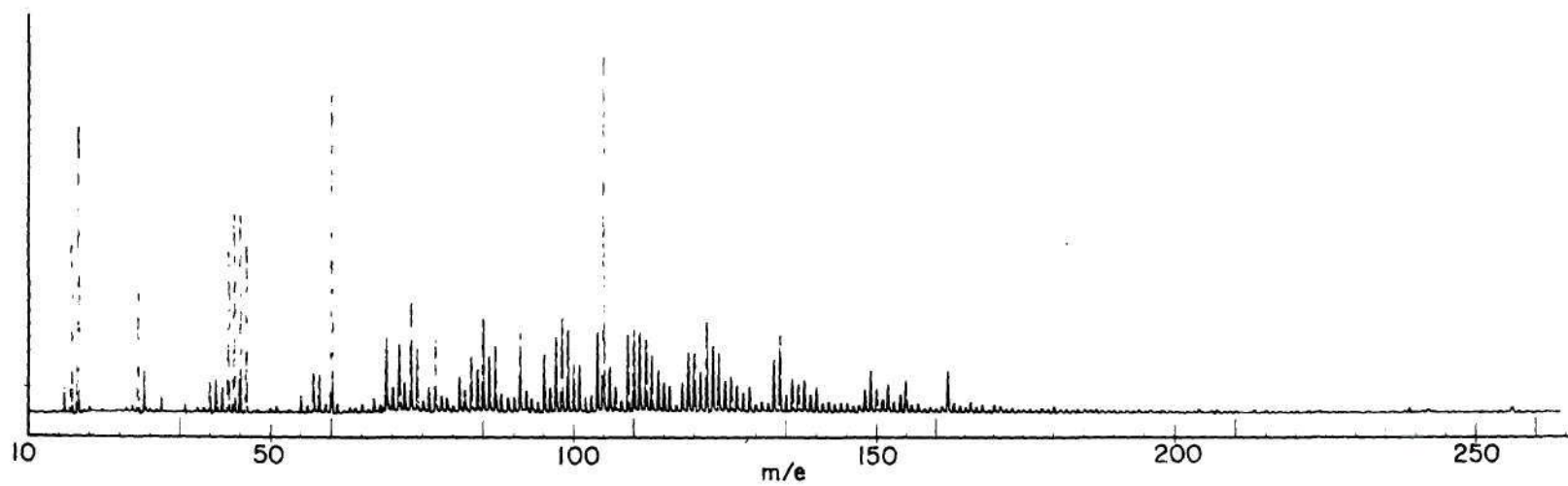


Figure 18. Mass Spectrum of Particulate Products from the Photochemical Reaction of o-Xylene-Air Mixture

Mass Spectra of Photochemical Aerosols from Traces of Benzene and Nitric Oxide in Air

The mass spectrum of particulate products from the photochemical reaction of 10 ppm benzene and 10 ppm nitric oxide in purified air was obtained at an electron energy of 70 eV, probe temperature of 150°C, and a pressure of 10^{-6} torr (Figure 19). This spectrum shows paraffinic and olefinic characteristics as indicated by large peaks at 43 and 57, and peaks at 41, 55, 69, 83, and 97. Strong peaks at 18 (H_2O), 28 (CO), and 44 (CH_3CHO) probably result from hydroxyl and carbonyl groups in the mixture. No peaks at 39, 51, 53, 63, 65, 77, and 91 indicate the absence of aromaticity in this sample. This differs considerably from the spectra of products from other benzene-air systems without nitric oxide. No significant peak at a mass number of 45 shows the doubtful presence of nitrosomethane which is the primary product of the reaction between methyl radicals and NO .⁽³²⁾ Fragment ions detected at masses 17, 28, and 41 are unlikely to be the N-containing species NH_3 , N_2 , and CH_3CN , respectively. Infrared spectra of this sample also indicated little absorption in the ranges for nitrate, nitro, and nitroso compounds.

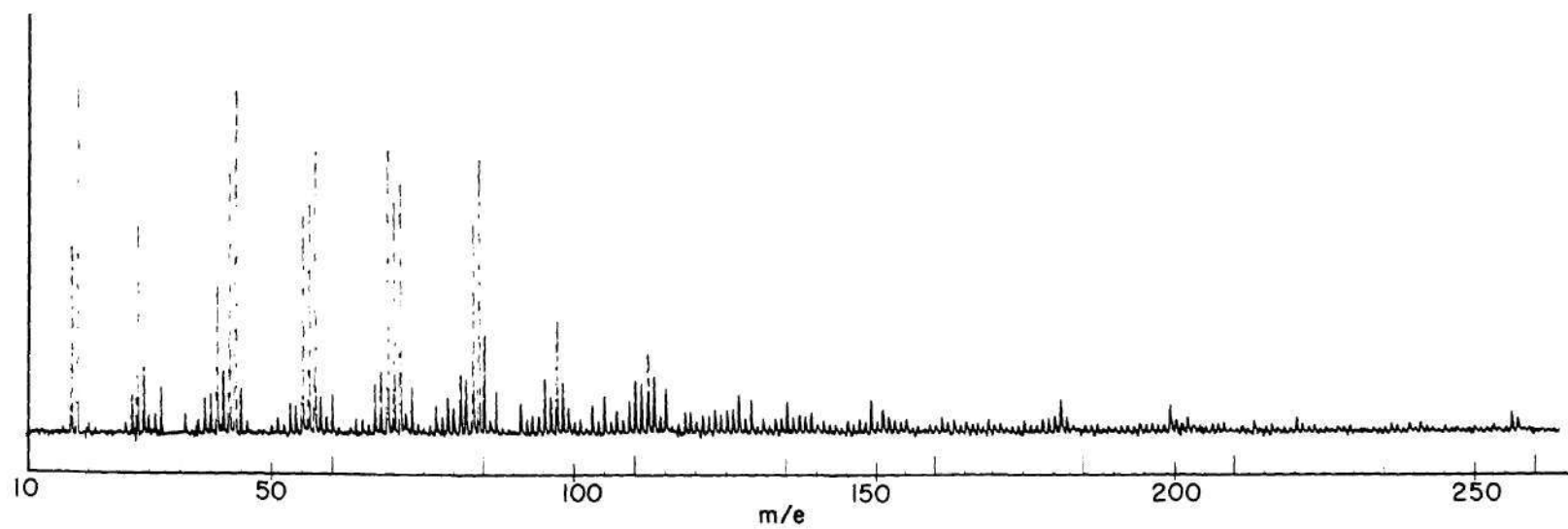


Figure 19. Mass Spectrum of Particulate Products from the Photochemical Reaction of Benzene-Nitric oxide-Air Mixture

CHAPTER IV

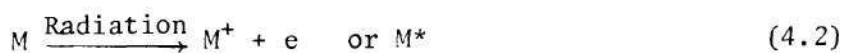
RADIOCHEMICAL OXIDATION AND THE FORMATION OF PARTICULATES

The Ionizing Effects of X-rays on Air

The energy of a quantum of radiation is related to wavelength by

$$E = \frac{hc}{\lambda} = \frac{12395}{\lambda} \quad (4.1)$$

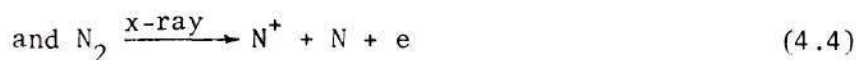
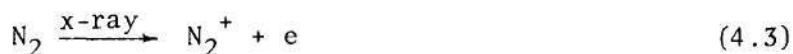
where E is the energy in eV and λ the wavelength in Å. A median wavelength at about 0.4 Å was determined from the continuous spectrum of the x-ray source of this study.⁽⁹⁸⁾ Hence the x-ray beam possessed an average energy of about 31 KeV. The formation of a photoelectron by a process of photon absorption predominates when an x-ray interacts with a molecule. According to the data of C.E. Lea,⁽⁸¹⁾ about 86 per cent of electrons are photoelectrons when water molecules undergo x-irradiation. The other result is the ejection of an electron by the Compton effect, i.e., a collision process between a photon and an electron in which the electron is driven from a molecule. This process produces about 14 per cent "fast" electrons having an average energy of 1600 eV. A 1600-eV electron ionizes and excites many molecules as it passes near them. One ion pair is produced from air by each 32.5 eV on average. Thus a 1600-eV electron produces numerous ion pairs and excited molecules, the initial chemical activation in radiation chemistry with gaseous molecules is generally written



where e is a free electron and M* is an excited molecule. The extent of

chemical reaction in many cases is proportional to the number of ion pairs and excited molecules produced in the reaction medium by the x-ray radiation.

When air is irradiated with x-rays, chemically active species, i.e., ions, excited molecules, and atoms are formed. These are highly reactive and have a very short lifetime. No attempt was made to measure the actual ionization of the x-irradiated air with or without hydrocarbon additives. Calculations have shown, however, that Compton electrons have an average energy much higher than the ionization potential of air. Therefore, the primary constituents of air, i.e., nitrogen and oxygen, are thought to undergo the following ionization processes as proposed by Dmitriev⁽⁴¹⁾:



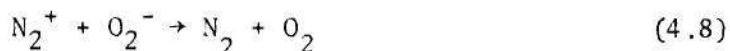
Equation (4.3) shows the molecular ionization of nitrogen with an electron energy equal to or greater than 15.6 eV, while equation (4.4) indicates dissociative ionization of nitrogen beginning at 24.3 eV. Because of the higher energy barrier, process (4.4) is much less probable than process (4.3). Similarly, equations (4.5) and (4.6)



show the formation of oxygen ions starting at 12.2 eV and the dissociative ionization of oxygen starting at 19.2 eV. All of the "slow" electrons released as a result of reactions (4.3) to (4.6) are subject to capture by oxygen molecules as indicated by equation (4.7).



All air ion species disappear rapidly as a result of neutralization processes such as the following :



X-ray Induced Formation of Ozone and Nitrogen Dioxide

When ultrapurified air with a trace of benzene was exposed to x-rays at the highest intensity for an average irradiation time of 3 minutes, a concentration of 6.0 ppm ozone was attained and detected by the iodide solution method. Steady state was attained within 10 minutes. The concentration would then decrease to zero in about 20 minutes following cut-off of the radiation. With dry-grade oxygen and all conditions the same as the preceding except that irradiation was terminated after two minutes, a constant ozone concentration of 11.4 ppm was reached. A final test was made with air containing 450 ppm acetylene. After a period of 10 to 15 minutes, the measured ozone concentration of 13.3 ppm was higher than those of the other two systems.

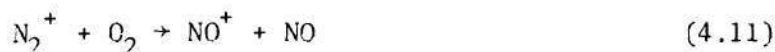
Equation (4.6) has already shown the dissociative ionization of oxygen molecules to form oxygen atoms and ions. The only possible chemical reactions of these elementary oxygen species lead to the formation and decomposition of ozone. The following two equations indicate mechanisms for the formation of ozone :





where M is the third molecule, either nitrogen or oxygen. Ozone molecules can also be formed by the mutual neutralization of the O_3^+ ion by a negatively charged ion or an electron.

A spectrophotometric method using the Saltzman reagent⁽¹¹¹⁾ indicated a low concentrations of NO_2 in the x-ray irradiated air. A steady concentration of NO_2 at approximately 1.0 ppm was established after 5 minutes of irradiation. The average irradiation time for a test was about 2 minutes. The reactions that account for the formation of nitrogen oxides must be secondary reactions involving ionized nitrogen molecules, e.g., the reactions (4.3) and (4.4) which show the production of N_2^+ , N^+ , and N. Dmitriev⁽⁴¹⁾ proposed the following reaction mechanism for the formation of nitrogen oxides:



Again, the ions NO^+ and NO_2^+ would form neutral molecules upon collision with negative ions or electrons. Although NO was not detected, equations (4.11), (4.13), and (4.14) indicate an abundant production of it; the NO probably converted into NO_2 in the presence of molecular and atomic oxygen. Therefore part of the NO_2 spectrometric response must have been due to the converted NO. Usually ozone is the main product in air under

weak ionizing radiation, while oxides of nitrogen are the dominant products in air under strong radiation. The fact that the yield of oxides of nitrogen was lower than of ozone is consistent with the general observation that low energy radiation produces less oxides of nitrogen than it does of ozone. The energy of the x-ray radiation as employed here was quite weak compared to nuclear radiation sources.

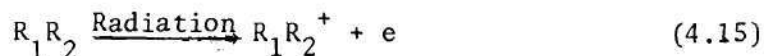
The productions of oxygen ions and excited oxygen molecules, in many cases, are proportional to the oxygen concentrations under equal amounts of radiation. According to this assumption, the production of ozone from pure oxygen is expected to be nearly 4.75 times that from air since air consists of about 21 per cent oxygen and 78 per cent nitrogen. Calculations from the above results indicate a ratio near 3 to 1 on the assumption that the production of ozone was proportional to the irradiation time. Equations (4.13) and (4.14) account for the formation of oxygen atoms.⁽²⁵⁾ Since oxygen atoms combine readily with oxygen molecules to form ozone, this may well be a reasonable explanation for the formation of ozone.

Radiochemical Oxidation of Hydrocarbons in Air

When a hydrocarbon compound is exposed to a radiation source, it is dissociated or polymerized. However, in the presence of air or oxygen, oxidation reactions seem to suppress those reactions which the oxidized component alone would undergo.⁽³³⁾ The prevalence of the oxidation reaction is due to the abundance and reactivity of oxidizing agents such as the oxygen atom, ozone, oxygen ion, and excited molecular oxygen.

From the IR spectra of irradiation products, it is apparent that both aromatic and aliphatic reactants are ruptured or dissociated by x-ray

radiation. The first products appearing when such organic substances are exposed to high energy radiation are positively charged ion-radicals with the simultaneous release of an electron from the molecule, according to the reaction⁽¹⁰⁴⁾



where R_1 and R_2 can be either aryl and alkyl radicals or a hydrogen atom. Since the parent ion-radicals possess a high energy, they tend to undergo processes such as collisions and dissociations in order to reduce the high energy. The secondary products then include carbonium ions, excited molecules, excited free radicals, and normal free radicals. Electron capture by both molecules and ions may also occur. The highly reactive hydrocarbon ions or radicals will spontaneously react with each other and activated oxygen-containing species. Dimerization of the intermediate radicals and addition to the dimers of a second reactive radical may occur also.

The oxidation mechanisms in these x-ray irradiation systems are very complicated ones. The kinetics cannot be solved in detail without complete analyses of samples taken at different intervals in a batch process. This investigation shows that the principal final products are oxygenated compounds consisting of aromatic and aliphatic units. It is believed that the initial hydrocarbon radical intermediates are able to react with those highly reactive oxygen-containing intermediates to give many different final products, each in so small a yield that no overall trend is recognizable.

Radiochemical Formation of Gas-Phase Aldehydes

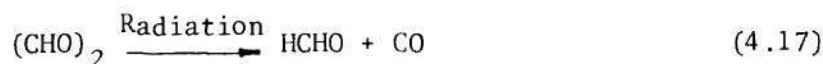
Low molecular weight aldehydes, probably including glyoxal, were

among the major products of the radiochemical oxidation of acetylene in air. These aldehydes form rapidly in the initial stages of the reaction and gain a steady state concentration after 3 to 5 minutes. When air containing 450 ppm C_2H_2 was irradiated with x-rays, a constant aliphatic aldehyde concentration of 9.5 ppm in the gas phase was indicated by the spectrophotometric method. However, the x-ray irradiation of air systems containing either a trace of benzene (19 ppm) or a trace of cyclohexene (35 ppm) failed to produce any significant aldehyde response in the spectrophotometer.

Reactive species, such as atomic oxygen produced from radiation ionization, are effective against both olefinic and acetylenic compounds, although they react much more slowly with alkynes than with alkenes due to the π electrons of the triple bond being more firmly held between the carbon nuclei.⁽¹⁰⁷⁾ When a C_2H_2 molecule reacts with oxygen atoms, one of the reactions produces a dialdehyde, glyoxal, $(CHO)_2$



Under the influence of radiation, glyoxal could be dissociated and form formaldehyde and carbon monoxide.⁽³⁷⁾



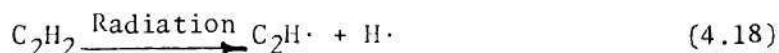
Meanwhile, other oxygenated compounds such as carboxylic acids, ketones, or dicarbonyl compounds are also formed. But glyoxal and formaldehyde are probably the predominant ones.

Formation of Particulates from C₂H₂-Air Systems

As described in the preceding chapter, the IR spectrum of particulates produced from C₂H₂ in O₂ or in air (Figures 10 and 11) indicates the existence of abundant -OH, C=O, C-OH, and aliphatic groups. The product is a yellow solid which is very much like cuprene, although cuprene is produced in the absence of oxygen. Comparison of the IR spectrum of the particulates with that of cuprene clearly shows the difference, i.e., there is no OH absorption at 3300 cm⁻¹ and no C=O absorption at 1700 cm⁻¹ in the spectrum of cuprene. The mass spectrum of the particulate product reveals the following ion fragments in the order of abundance: CH₃CHO, C₆H₅, H₂O, C₄H₇, CO, and CHO. These species could also come from the hydrocarbon ions and free radicals which were present during x-ray irradiation. The H₂O ion fragment indicates the existence of -OH groups or alcoholic characteristics.⁽¹⁷⁾ The C₄H₇ fragment and the peak at a mass number of 79 probably signifies aliphatic properties, especially those of polycycloalkanes. And the CH₃CHO, CO, and CHO ion fragments undoubtedly are evidence of carbonyl groups. For pure compounds, molecular weights can be obtained from the mass number of the parent ions. Apparently the particulates are not pure compounds but are a mixture of different hydrocarbon units containing hydroxyl and carbonyl groups. Since significant peaks appear up to a mass number of 202 and higher, this could mean the presence of particulates that contain polycycloalkanes and many different oxygenated hydrocarbon compounds of up to units of 10 or more carbon atoms.

Palmer, et al.,⁽⁹⁹⁾ studied the effect of soft x-ray on the polymerization of acetylene by using basically identical x-ray equipment to that employed in this study. The infrared spectrum of the fresh polymer

cuprene resulting from irradiation with 1-MeV electrons was examined by Jones.⁽⁶⁷⁾ As a result, it is generally agreed that cuprene is an insoluble, infusible, and non-volatile polymeric material. Oxygen can be picked up subsequently by cuprene to almost 30 per cent by weight, the affinity of cuprene for oxygen being explained by the existence of aliphatic double bonds in the cuprene structure. Since the mass spectrum given herein indicated the existence of high molecular weight oxygenated hydrocarbons of up to 10-carbon units, there may be di- or trimerization of acetylene during the irradiation. Further chain reactions to produce large "polymers" were definitely inhibited by the presence of oxygen and water. Again, the abundance of -OH and C=O groups probably was the result of oxidation of triple bonds or double bonds when attacked by oxygen-containing oxidizing agents, or of reactions between oxygen molecule and radicals, or of reactions with other excited hydrocarbon molecules. Radicals such as $C_2H\cdot$ and $C_2H_3\cdot$ were reported to be present during α -irradiation⁽⁸³⁾ according to the reactions:



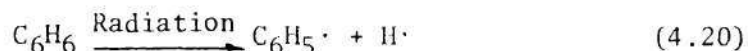
Since dissociation of the H- C_2H bond requires less than 5.25 eV, the existence of C_2H and C_2H_3 radicals is very possible in this x-ray irradiation. When radon was mixed with oxygen and acetylene, Lind and Bardwell⁽⁸¹⁾ reported an entirely different reaction than with pure acetylene. Instead of a yellow solid, a colorless liquid was produced which contained very small amounts of oxygen with an empirical formula of $C_{36}H_{53.4}O$. In view of the

highly oxygenated characteristics of products found here and the fact that they were yellow solids, the latter substances obviously do not fall into this category.

Formation of Particulates from C₆H₆-Air Systems

Particulates were produced by the x-ray irradiation of about 100 ppm benzene in dry air. The infrared spectrum (Figure 8) of these particulates indicates an abundance of carbonyl and hydroxyl groups, and it also shows the characteristic vibration modes of both aromatic and aliphatic compounds. The mass spectrum was obtained at an electron beam energy of 70 eV, probe temperature of 100°C, and under a vacuum of 4×10^{-6} torr. The spectrum shows alkyl characteristics; the major peaks are 14 units apart, and the peaks at 43 (C₃H₇), 57 (C₄H₉), and 69 (C₅H₉) are large. Some aromatic and cycloalkene properties are indicated by mass peaks at 65 (C₅H₅), 39 (C₃H₃), 69 (C₅H₉), and 81 (C₆H₉). Aromaticity was not as intense as indicated by the infrared spectrum. Again, predominant mass numbers at 17 (OH), 18 (H₂O), 29 (CHO), 44 (CH₃CHO or CO₂), and 57 (C₂H₅CO) suggest a highly oxygenated compound.

Henri, et al.,⁽⁶⁰⁾ studied the α -irradiation of benzene along with four other C₆-hydrocarbons in the vapor state. They found that 99 weight per cent of the product was accounted for by a liquid substance with an average molecular weight of 330, and the remainder was mostly gaseous products consisting mainly of 40 per cent H₂ and 55 percent C₂H₂. The production of C₂H₂ probably comes from a dissociation of benzene. The presence of H \cdot as a product indicates that H \cdot is an intermediate during the reaction; it is probably formed by many reactions, the following one being typical:



Radicals $\text{C}_6\text{H}_5\cdot$ and $\text{C}_6\text{H}_7\cdot$ were reported by McAndrews, *et al.*⁽⁸⁷⁾ in a 2-MeV electron irradiation of benzene. Futrell⁽⁸¹⁾ investigated the radiolysis of n-hexane both in the vapor and liquid states. An attempt was made to determine the participation of free radical reactions for each product by considering three types of reactions: initial fragmentation, ion-molecule reactions, and radical interaction. This is already a complicated case and the one here becomes much more complicated since the energetic oxidizing species have also to be taken into consideration. Since $\text{C}_6\text{H}_5\cdot$ is an intermediate during irradiation, polyphenyls are possibly the final products formed by the interactions of the radicals. As in the case of γ -irradiation of the biphenyl, polyphenyls and their hydrogenated derivatives were the major products.⁽⁸¹⁾ This could explain the high molecular weight of the product as revealed by its mass spectrum. In the spectrum of samples produced in the absence of oxygen, the characteristic bands for carbonyl, hydroxyl, and other oxygen-containing groups diminished, showing an attack by oxygen on aromatic bonds to form oxygenated compounds. The infrared spectrum showed that the O-H band at 3400 cm^{-1} and the C=O band at 1700 cm^{-1} increased greatly in intensity during exposure to oxygen in the atmosphere. Similar chemical changes in the post-irradiation oxidation of polystyrene were noticed by Sears and Parkinson.⁽¹¹⁵⁾

Formation of Particulates from Cyclohexene-Air Systems

The preceding chapter describes some of the chemical structure of the particulate product resulting from the x-ray irradiation of an air-cyclohexene mixture (Figure 9). Strong characteristics of aliphatic hydro-

carbon bonds, hydroxyl, and carbonyl group are indicated by corresponding absorption bands. Carboxylic acids and aliphatic aldehydes would be predicated to be major components from the mixture. This mass spectrum was also obtained at an electron beam energy of 70 eV, probe temperature 100°C, and under a vacuum of 5×10^{-6} torr. Again, alcoholic or hydroxyl groups are shown by mass numbers at 18 (H_2O), 17 (OH), and 45 (CH_3CHOH). Carbonyl groups are indicated by mass peaks at 43 (CH_3CO), 44 (CH_3COH or CO_2), 45 (COOH), and 57 ($\text{C}_2\text{H}_5\text{CO}$). Cycloalkyl properties are predicated by ion fragments such as 55 (C_4H_7), 69 (C_5H_9), 71 (C_5H_{11}), and 83 (C_6H_{11}). Other aliphatic hydrocarbon characteristics are given by masses at 28 (C_2H_4), 41 (C_3H_5), 57 (C_4H_9), and 99 (C_7H_{15}). Ion fragments at 41, 45, 70, 73, 97, 98, 121, and 139 offer evidence that a number of carboxylic acids are also important components. The mass number at 83 (C_6H_{11}) probably indicates the existence of the cyclohexene structure. It is also interesting to note significant mass peaks at high mass numbers, viz., 121, 135, 139, 159, and 163, indicating the possible dimerization or trimerization of excited cyclohexene molecules, their derivatives, and intermediates.

Henri, et al.,⁽⁶⁰⁾ also investigated the α -irradiation of cyclohexene in the gaseous state and found that 95 per cent of the product was a liquid substance with an average molecular weight of 360 with the remainder gaseous products, including 33 per cent H_2 , 31 per cent C_2H_2 and C_2H_4 , 18.5 per cent C_6H_{12} , and some C_3H_4 , CH_4 , and C_6H_6 . This result indicates that radicals such as $\text{H}\cdot$, $\text{C}_2\text{H}\cdot$, $\text{CH}_2\cdot$, $\text{CH}_3\cdot$, $\text{C}_6\text{H}_{11}\cdot$ and many others were probable intermediates during the radiolysis of cyclohexene. Eastman and Silverstein⁽⁴⁴⁾ reported the vapor phase ozonolysis of cyclohexene to yield formic acid and trans-1,2-cyclohexandiol in small amounts with adipic acid

as the major product. Before separation and identification, the ozonide showed strong infrared absorption at 3390, 2940, and 1620 cm^{-1} which was attributed to O-H, aliphatic C-H, and C=O vibrations, respectively. Apparently, the x-ray induced product bears a strong resemblance to their ozonolysis product. Since ozone, and probably atomic oxygen, oxygen ions, and excited oxygen molecules are important components, they may play a role as oxidizing agent during the irradiation process. Adipic acid, formic acid, and trans-1,2-cyclohexandiol may account for a portion of the oxygenated products.

Formation of Particulates as Functions of Hydrocarbon Concentration,
Irradiation Time, X-ray Intensity, and Humidity

Two reaction mixtures were examined in this phase of the study. Mixtures of benzene and acetylene at various concentrations in air were irradiated to determine the concentration dependence of particulate production. Particulate production by x-irradiation was found to increase as the concentration of the two hydrocarbon compounds in air increased. These results are shown in Figure 20. Small changes in the mass concentration of particulates were detected for benzene-air mixtures after irradiations of 2 minutes duration, but much greater increases were found with benzene vapor concentration increase after an irradiation time of 7 minutes. This same pattern was found with air-acetylene mixtures although particulate formation was lower by more than one order of magnitude.

Radiolytic fragmentation would be expected to increase with longer irradiation, resulting in a higher concentration of reactive intermediates which in turn would form larger amounts of particulate. The observed

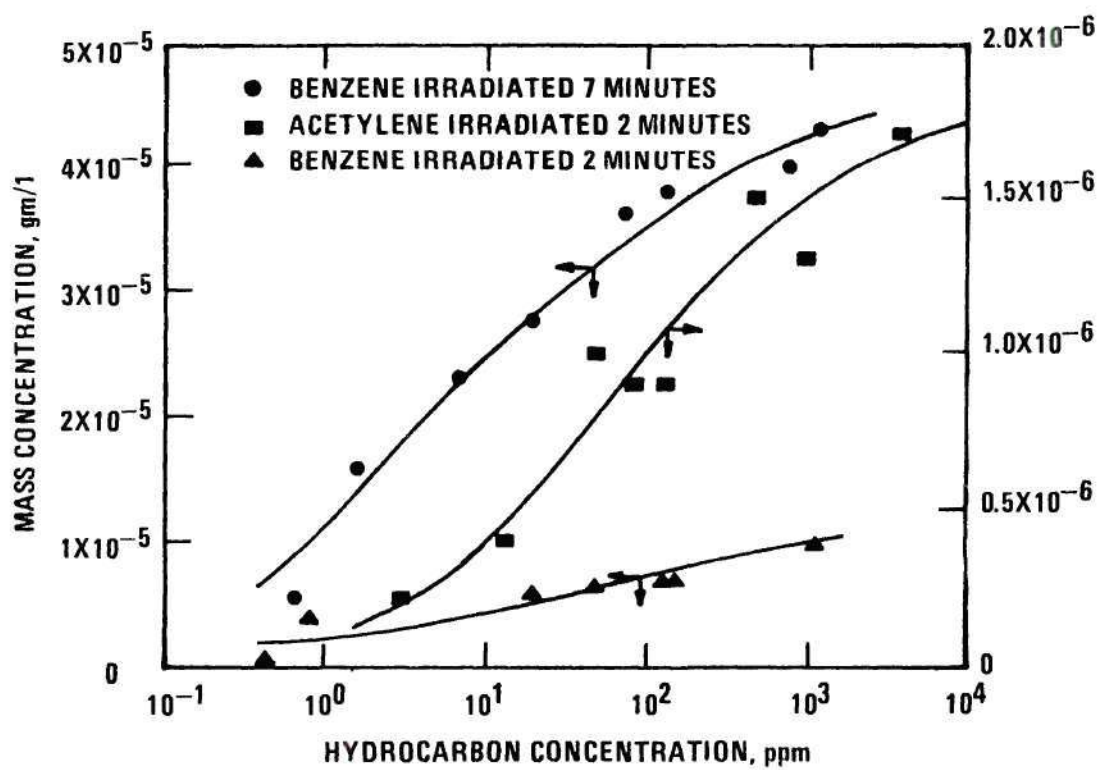


Figure 20. Yield of Particulates as a Function of Hydrocarbon Concentration. (See Reference 72, p. 96, Figure 3)

trend toward greater particulate production with hydrocarbon concentration increase is also predictable, since the extent of a chemical reaction is proportional to the number of ion-radicals and ion pairs produced in the reaction medium by radiation. When all the other factors, such as x-ray intensity and irradiation time, were fixed, higher concentration of hydrocarbon in a homogeneous medium means more ion-radicals which in turn yields more reactive intermediates; the latter combine, or polymerize, to form the high molecular weight products.

For the same reason, particulate concentration appears to be proportional to irradiation time. These experimental results are presented in Figure 21 for benzene-air and acetylene-air mixtures at constant concentration irradiated for different times but with all other parameters and conditions held constant. Figure 22 shows the production of particulates as a function of x-ray intensity. The reaction mixture here was air containing 1.0 per cent acetylene. Intensity levels were adjusted by choosing various combinations of voltage and rectified tube current. No dosimetric measurement was made to indicate the precise dose rate, so these results give the qualitative response and not a quantitative measurement.

The experimental work described in the preceding section was accomplished using hydrocarbons in dry air. Thus, the presence of water vapor is not necessary for the generation of particulates. Other tests were made in the tubular x-ray irradiation chamber using benzene and acetylene in humidified air. Humidity was measured with either the Model 880 or 990 Dew Point Hygrometer of Cambridge Systems, Inc., Mass. Data are presented in Figure 23 demonstrating that the aerosol producing

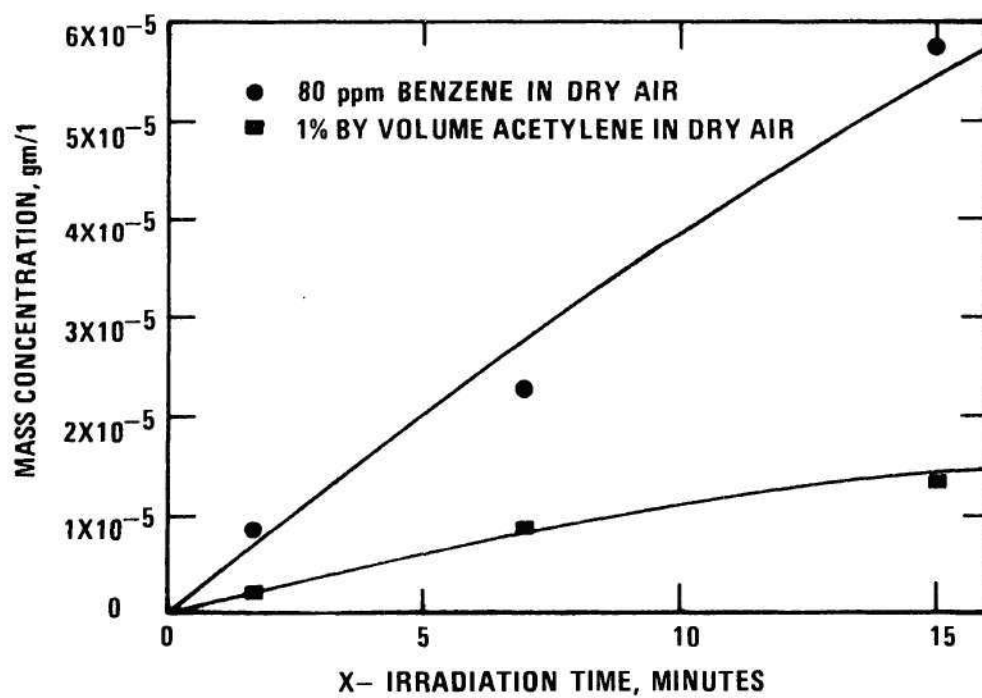


Figure 21. Yield of Particulates as a Function of Irradiation Time.
(See Reference 72, p. 97, Figure 6)

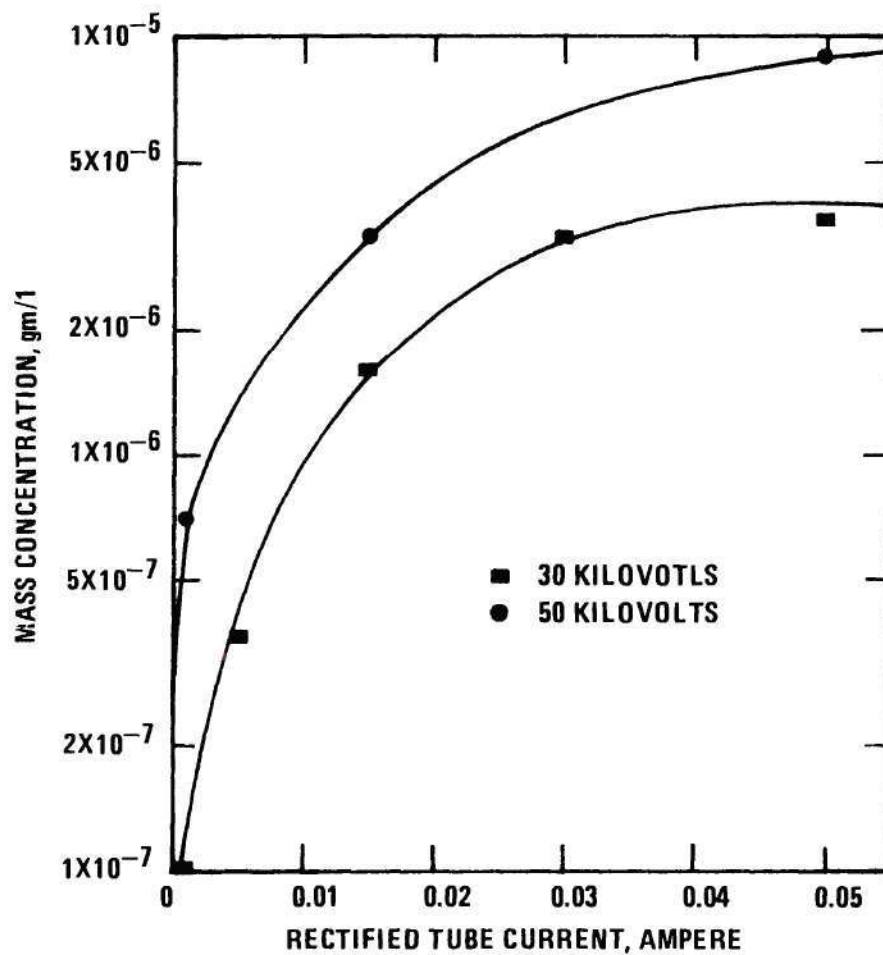


Figure 22. Yield of Particulates as a Function of X-ray Intensity.
(From air containing 1 per cent acetylene, see Reference
72, p. 97, Figure 5)

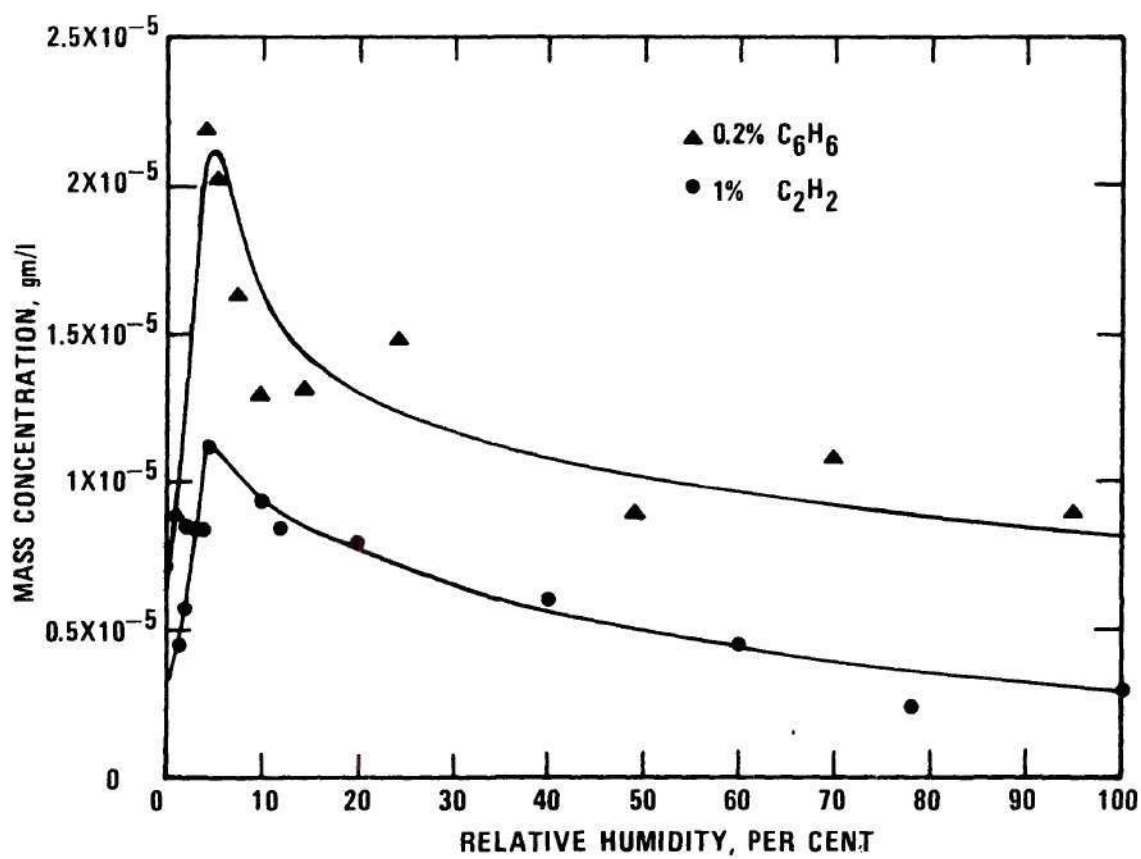


Figure 23. Yield of Particulates as a Function of Relative Humidity.
(See Reference 72, p. 98, Figure 9)

reactions of benzene and acetylene were enhanced by the presence of water vapor, especially at low humidities. Humidity is thus of importance in x-ray induced reactions. A sharp increase in the formation of particulates is evident with the maximum rate of mass generation occurring at approximately 5 per cent relative humidity. Even though mass accumulation above 5 per cent relative humidity decreased, larger particulate sizes were formed at higher humidities. This result for air containing 10 per cent acetylene is discussed further in Chapter VI. These findings differ somewhat from those of Pfefferkorn ⁽¹⁰²⁾ as there it is reported that both the formation rate and the size of the particulates increase with higher humidities.

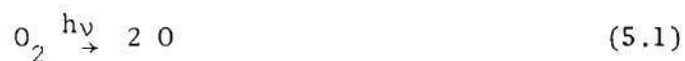
Water molecules apparently promote oxidation reactions as has been seen in gas phase ozonolysis ⁽⁴⁴⁾ in which carbonyl compounds are produced as the ozonide is treated with water vapor. Since ozone is found to play an important role in the oxidation, ozonide and epoxides are products of the oxidation, the addition of water to these compounds certainly would add oxygen and hydrogen to the molecular structure and therefore cause the weight increase of particulates through hydroxylation and hydrolysis. ⁽¹⁰⁷⁾ However, the reason for the inhibition of aerosol formation at high humidity is not well understood.

CHAPTER V

PHOTOCHEMICAL OXIDATION AND THE FORMATION OF PARTICULATES

Formation of Atomic Oxygen and Ozone

When purified dry air was the only component in the irradiation chamber, steady-state concentrations of ozone between 13 and 18 ppm, depending on the dilution rate, were generated after the mercury lamp was turned on. A similar production of ozone was also found during other tests in which cyclohexene or benzene was added to the air. Since this study used ultraviolet light with wavelengths down to 2224 \AA , it appears that a ground-state oxygen molecule could absorb ultraviolet radiation at 2424 \AA to form normal oxygen atoms at the ground state $3p^{(32)}(132)$ according to



The dissociation energy is 5.115 eV or 118.0 kcal./mole, corresponding to a wavelength of 2424 \AA . Therefore the ozone formation is probably explained by the combination of an oxygen atom and a molecule by⁽⁸⁹⁾⁽¹¹³⁾



The ozone molecule then undergoes photolysis to produce an oxygen atom in the excited state ^1D by absorption of radiation between wavelengths of 2200 \AA and 2800 \AA as follows :



In view of the fast rate of reaction (5.2), the equilibrium concentration of ozone is much higher than that of atomic oxygen. The rate constants for atomic oxygen-hydrocarbon reactions are generally higher than those for ozone-hydrocarbon reactions by a factor 10^4 to 10^5 . Hence the reaction of atomic oxygen and a hydrocarbon molecule is of importance in these photochemical reactions, especially in the early stage as the atomic oxygen acts as initiator for the further photo-oxidation of the hydrocarbon. (70) (123)

Cyclohexene-Air System

The object of this study was to determine the nature and extent of the photochemical oxidation of cyclohexene in dry air. Cyclohexene was chosen because it has been reported⁽⁷⁹⁾ to produce very high concentrations of aerosol when irradiated with traces of nitric oxide. Experiments were conducted using purified air containing 10 ppm cyclohexene in the 45-liter photochemical reaction chamber described above. The aerosol profile and the rates of formation and depletion of the principal species were measured as functions of time; the results are presented in Figure 24. As soon as the mercury lamp was turned on and during the first 1000 seconds, a rapid disappearance of cyclohexene and the formation of ozone, aldehyde and particulates were observed. A rate constant of $1.9 \times 10^{-3} \text{ sec}^{-1}$ was calculated by the method of half times for the apparent first-order reaction of this period. The consumption of cyclohexene slowed and its concentration reached a low steady value after about 2000 seconds.

Cyclohexene was depleted very rapidly in comparison with the slow disappearance and short "induction period" for the reaction of benzene. This is probably due to the high reactivity between cyclohexene and ozone.

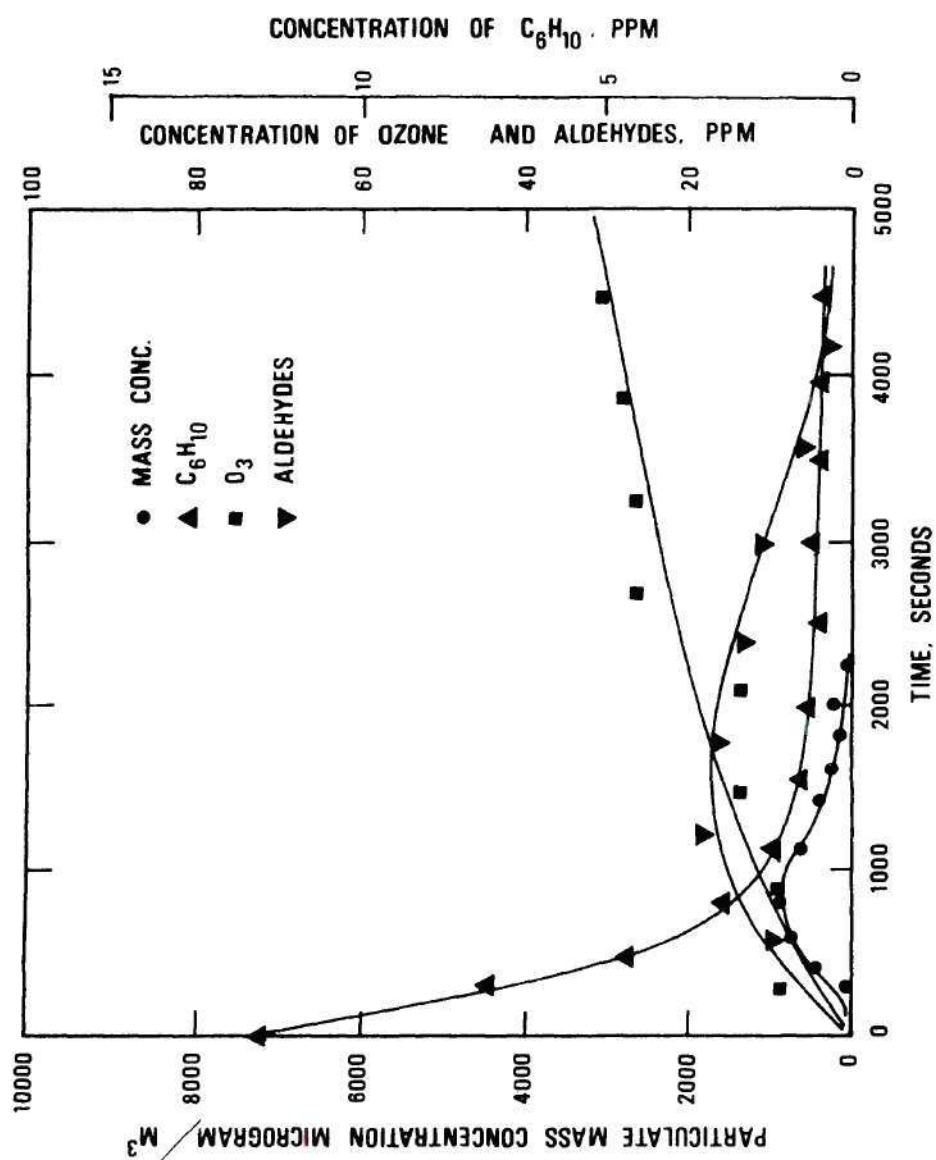


Figure 24. Concentration Change of Reactants and Products during Ultraviolet Irradiation of Cyclohexene-Air Mixture.

Cadle and Schade⁽³¹⁾ obtained a value of $3.5 \times 10^4 \text{ l mol}^{-1} \text{ sec}^{-1}$ as the rate constant for the ozone-cyclohexene reaction, which is at least 3000 times that for ozone-xylene. Since benzene is generally less photochemically reactive than xylene by a ratio of 1 to 3, the rate constant of the ozone-cyclohexene reaction probably is higher than that of the ozone-benzene reaction by a factor of approximately 10^4 .

Figure 24 also shows the aldehyde profile, the aldehyde gradually increasing from time zero. The formation of aldehydes at the beginning is probably due to the reaction of cyclohexene with ozone and atomic oxygen. Other investigators⁽⁴⁴⁾ have also reported the formation of epoxides and aldehydes such as acetaldehyde and cyclopentenealdehyde as main products. The aldehyde concentration decreased after reaching a maximum value at about 1200 seconds, the reason probably being due to its further photo-oxidation. The aerosol profile too is shown in Figure 24; in this case very small amounts of aerosol, amounting to only about 3 per cent of the total weight of the reactant, were detected. Due to the volatility of the particulates, no attempt was made to analyze them chemically. Just like the aldehydic products, the particulate concentration decreased after attaining a maximum at about 900 seconds.

Photo-dissociation and Photo-oxidation of Aromatics

Using both natural and artificial sunlight which contained ultraviolet wavelengths greater than 2900 \AA , Chien⁽³⁴⁾ reported that cyclohexene and simple aromatic compounds such as benzene and toluene did not absorb light with wavelengths above 2900 \AA by studying the ultraviolet absorption spectra of the compounds.⁽¹⁰⁵⁾ Hence the photolysis of unsaturated hydrocarbons is not of importance in photochemical smog studies.

The ultraviolet light used in this study had wavelengths down to approximately 1900 Å. Generally speaking, benzene and toluene vapors show no chemical changes at 2537 Å. Only o-xylene undergoes a 1, 2-shift of the methyl group with low yield to form an isomer such as m-xylene and a photo-induced fragmentation to form free radicals such as H·, CH₃·, C₆H₄C₂H₅·, and C₆H₄CH₂· at 1849-2000 Å. Irradiation of benzene vapor produces an unidentified high energy isomer which decomposed to a cuprene-like polymer, C₂H₂, H₂, CH₄, C₂H₆, and C₆H₅CH₃.⁽⁴⁶⁾⁽¹¹⁶⁾⁽¹³⁵⁾ Toluene undergoes much the same decomposition. In both cases, the quantum yields are near unity.⁽³²⁾

The ultraviolet light source in this study was a medium-pressure mercury lamp which emitted low energy radiation at 1849-2000 Å. Due to the poor transmission of ultraviolet light through the combination of the quartz double walls and the cooling water in the immersion well, the radiation at 1849-2000 Å was especially weak. Therefore, it would be expected to cause only a low yield from these photo-dissociation processes at these wavelengths. In other words, only a small part of the aromatic reactants would undergo the photolytic change, i.e., the rupture of H-C or C-C bond at 1849 Å to form free radicals. One of the possible reactions of these free radicals is a rapid combination with molecular oxygen to form peroxyalkyl radical according to



The peroxyalkyl radicals would react again with oxygen to form alkoxyl radicals which, in turn, decompose or react with oxygen, peroxyalkyl, and another alkoxyl radical to produce aldehydes, alcohols, and other oxygen

containing compounds. Alkoxyl radicals would also add to unsaturated hydrocarbons to form polymeric substances. For instance, several unsaturated hydrocarbons with terminal $=CH_2$ groups could combine with alkoxyl radicals to produce polyperoxides.⁽⁸⁶⁾ This may explain in part why there are highly oxygenated polymer products.⁽⁷⁹⁾

Figure 25 gives a semilog plot of concentration versus time curves for benzene-air, toluene-air, and o-xylene-air mixtures following ultraviolet radiation.⁽⁴⁾⁽⁵⁰⁾ The hydrocarbon concentration in the chamber effluent during 4000 seconds of reaction was monitored with a flame ionization hydrocarbon analyzer. The curves are arbitrarily divided into three sections or phases which seem to represent three apparent first order reactions due to the formation of straight lines. For each of the mid-section reactions the apparent rate constants, having, respectively, values of 1×10^{-3} , 1.5×10^{-3} , $2.0 \times 10^{-3} \text{ sec}^{-1}$ for benzene-air, toluene-air, and o-xylene-air systems,⁽¹⁰⁾ were calculated by the method of half times by division of $\ln 2$ by time needed for consuming half of the reactant. The effects of dilution were taken into consideration in the calculation. Since dilution causes an exponential change in hydrocarbon concentration as shown by Equation (2.3), this does not alter first-order reaction characteristics. The slow initial disappearance of these simple aromatic compounds may be attributed to the time required for the warming-up of the mercury lamp and the build-up of ozone and atomic oxygen. Major portions of the aromatics were probably consumed in second-phase reactions once large quantities of aliphatic aldehydes and highly oxygenated particulates were produced. The formation of pyruvaldehyde (CH_3COCHO),

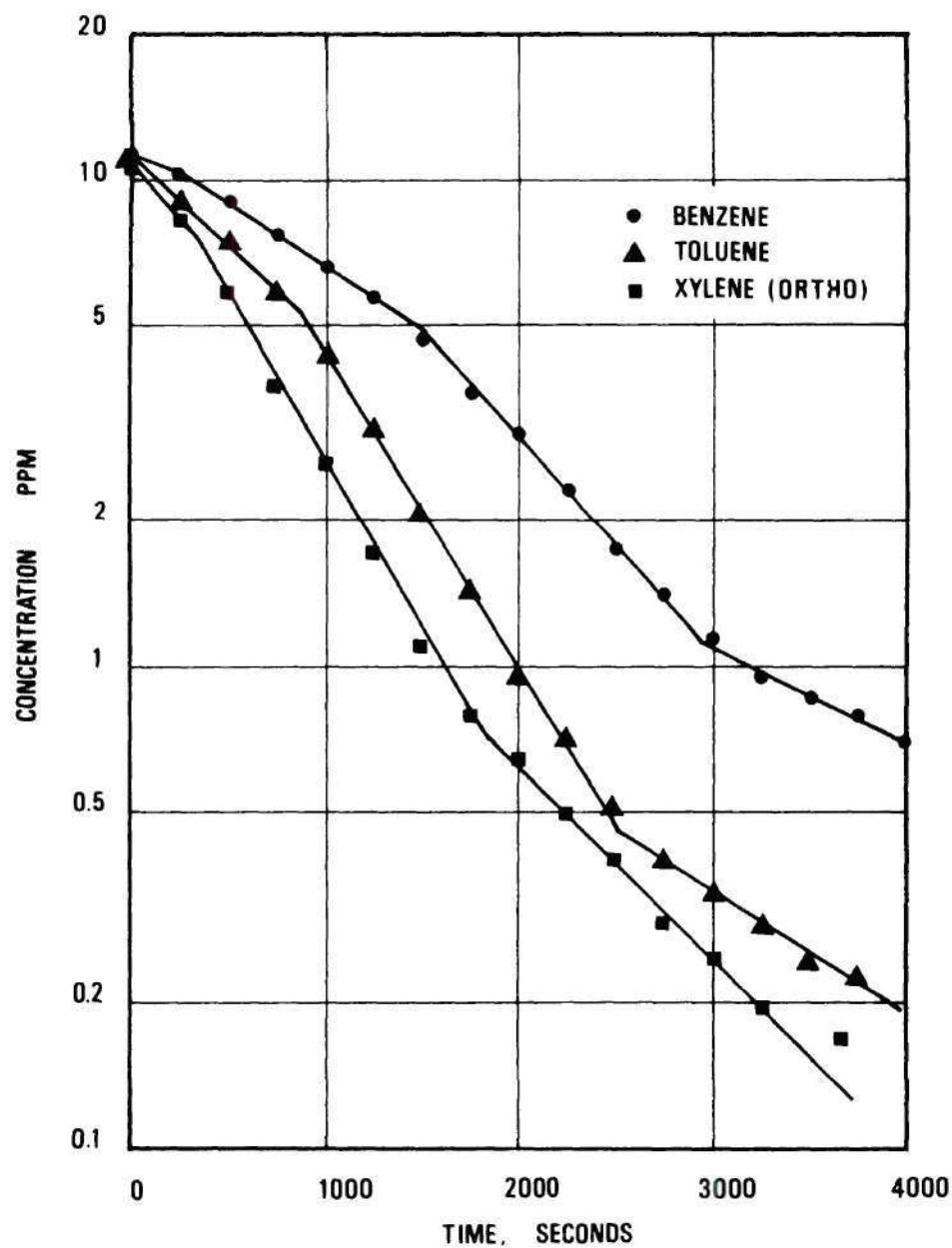


Figure 25. Disappearance Rate of Benzene, Toluene, and o-Xylene in Dry Air During Ultraviolet Irradiation.

glyoxal, and its derivatives from the ozonolysis of toluene or o-xylene could be a source of the aldehydes. The fact that methyl groups attached to a benzene ring can be oxidized -- mostly to carboxyl, and aldehyde or ketone groups -- would explain the strong absorptions at 3350 and 1730 cm^{-1} , which were attributed to O-H and C=O stretching vibration modes in the infrared spectra of the particulates (see Figures 14 and 15). Similarly three-phase reactions were reported by Alley, *et al.*,⁽³⁾ for reactions of butene, pentene, and hexene with the addition of NO_2 under the irradiation of artificial sunlight. Reaction rate constants of the order of 10^{-3} to 10^{-4} sec^{-1} were also calculated. The similarity is probably due to the fact that reactions in both cases are initiated by the attack of atomic oxygen on unsaturated hydrocarbons.⁽²¹⁾⁽⁶⁸⁾ The sources of atomic oxygen, of course, are different; the production of atomic oxygen in this study was shown to be induced by photo-dissociation of molecular oxygen at 2000-2424 Å, but the production of atomic oxygen in the study of Alley, *et al.*, was a result of the photo-dissociation of NO_2 at 3130-4047 Å.

Benzene-Air Systems

The photo-oxidation of benzene in the presence of ozone and of molecular and atomic oxygen has been investigated both in the liquid and in the gas phase. Boocock and Cvetanovic⁽²¹⁾ reported that the main product formed in the reaction of benzene with atomic oxygen was a nonvolatile material having aldehydic character. Avramenka, *et al.*,⁽¹⁵⁾ measured a reaction rate constant of $2.9 \times 10^{-11} \exp \left(-\frac{4700}{R_{\text{Gas}} T} \right) \frac{\text{cc}}{\text{mol} \cdot \text{sec}}$ with respect to benzene in the gaseous phase, and also reported the presence of a reactive radical and phenol, HCHO, and CO, indicating reaction mechanisms both

with and without the cleavage of the benzene ring. Grigriyan, et al.,⁽⁵⁴⁾ studied the gas phase photochemical reaction at room temperature, phenol and organic peroxides being detected as products. After a time the rate of phenol formation was inhibited due to competition between photochemical formation and decomposition. Wei, et al.,⁽¹³⁴⁾ investigated the formation of two polyenic dialdehydes, phenol, and other products from the irradiation of liquid benzene through which oxygen was bubbled at room temperature. The interesting part is that Wei, et. al., used an identical Hanovia mercury lamp to that employed in this study. A reaction mechanism was suggested that required the photo-initiated attack of oxygen on benzene leading to ring opening, formation of carbonyl group, and addition to another benzene ring.

Apparently the low yield and efficiency of the photo-dissociation of benzene and other aromatic compounds with subsequent photo-oxidation cannot explain the fast disappearance rates of the aromatic reactants. In view of the high concentration of ozone and atomic oxygen, the rapid consumption of aromatic reactants is probably due to the attack by these oxidizing agents to form oxygenated compounds. In order to understand the ozone-benzene reaction mechanism in the absence of ultraviolet light, a steady concentration of ozone was built up first by irradiating the air in the chamber. Meanwhile a constant dilution rate was maintained in the chamber. The ozone concentration as a function of irradiation time is shown in Figure 26. After the mercury lamp was turned off an amount of benzene which would produce a concentration of 10 ppm was injected. The benzene concentration was constantly measured with the hydrocarbon analyzer during the course of the reaction. The hydrocarbon concentration

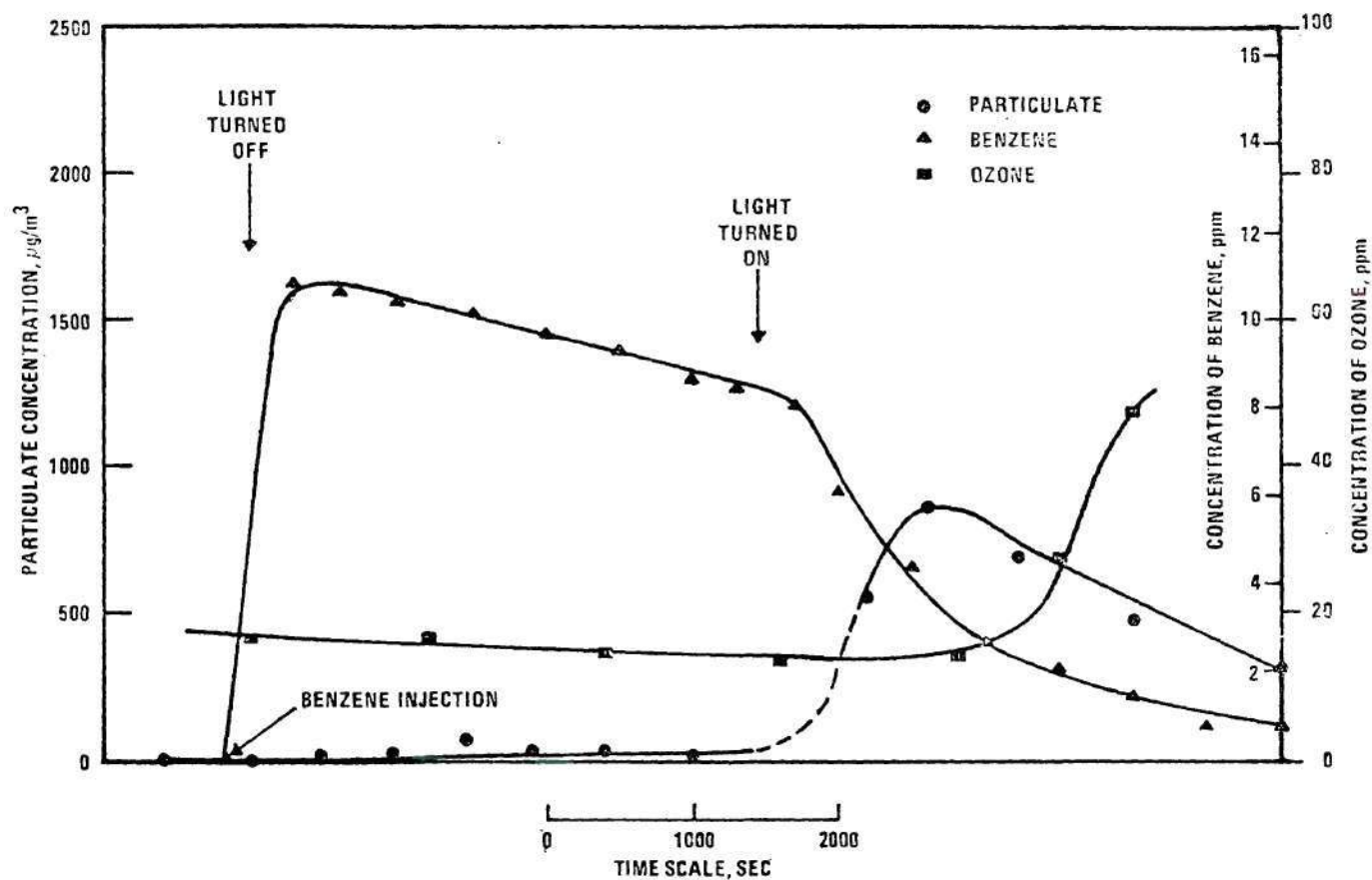


Figure 26. Concentration Change of Reactants and Products during Ultraviolet Irradiation of Benzene Vapor in Previously Irradiated Dry Air. (See Reference 71, P.20, Figure 6)

readings show a very low benzene disappearance rate, since the benzene concentration decreased almost as the rate of dilution. But a rapid disappearance rate was observed after the light was turned on at 2900 seconds. As mentioned in the preceding sections, atomic oxygen was produced under the influence of radiation, and the rate constants for the atomic oxygen-benzene reaction can be higher than that for the ozone-benzene reaction by a factor of 10^2 to 10^4 .⁽⁶⁾ Hence, the fast reaction between benzene and atomic oxygen explains in part why there is a rapid disappearance of benzene. From Figure 26, the ozone concentration will be seen to increase sharply after more than 80 per cent of the benzene has been exhausted.

Another test was made to study the photo-oxidation of benzene in the absence of ozone initially. After 10 ppm benzene was injected in the chamber, the ultraviolet light was turned on and the analysis and measurements of benzene, ozone, aldehydes, and particulates started. The results are shown in Figure 27. Again, the benzene depletion rate became rapid after 200 to 300 seconds when the mercury lamp warmed up and emitted radiation at its full strength. By comparison, the disappearance rate in this test was less than that in the previously mentioned test with ozone present. There could be two possible explanations. The first one depends directly on the reaction between benzene and ozone. The second requires ozone to absorb radiation at 2200 to 2800 Å and dissociate into atomic and molecular oxygen, thus causing an increase in the concentration of atomic oxygen which would, in turn, accelerate the atomic oxygen-benzene reaction. As may be seen, the ozone concentration is very low during the first 2000 seconds which probably indicates the fast addition of atomic oxygen to the benzene molecule. The ozone concentration increased significantly only

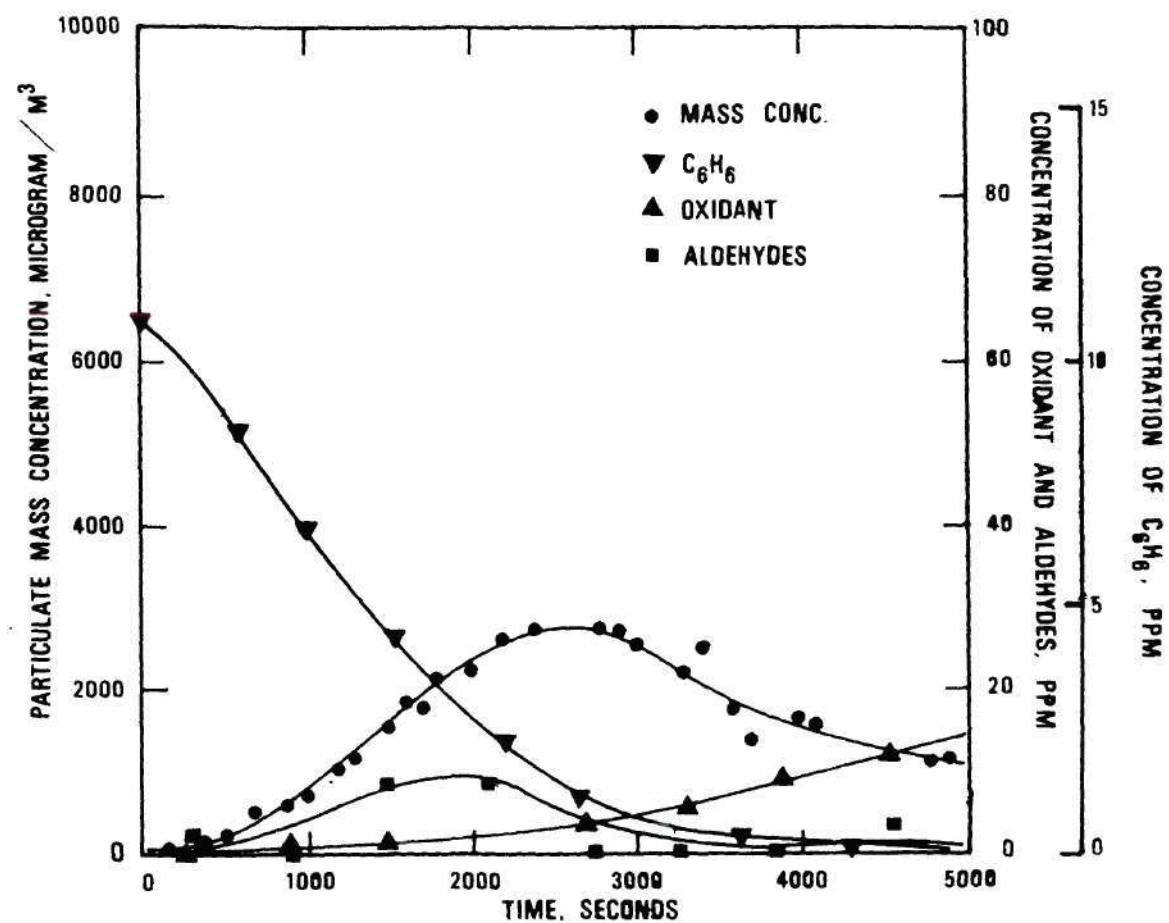
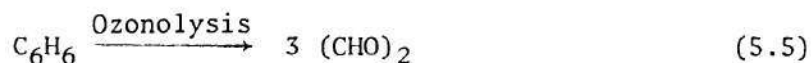


Figure 27. Concentration Change of Reactants and Products during Ultraviolet Irradiation of Benzene-Air Mixture.

after more than 80 per cent of the benzene had been depleted and its disappearance rate had been greatly reduced.

An aliphatic aldehyde concentration which reached a maximum value of about 8.5 ppm was observed during the interval from 1000 to 2500 seconds. The formation of aliphatic aldehydes was probably due to photo-oxidation reactions in which the benzene ring was attacked by oxidizing species such as atomic oxygen and ozone. For instance, the addition of ozone to the benzene nucleus would ultimately produce one kind of dialdehyde, glyoxal, according to the reaction



Then, glyoxal would absorb radiation in the range 2300 to 3200 Å⁽³²⁾ to form formaldehyde and carbon monoxide and, possibly, some hydrogen, the predominant reaction probably being



Formaldehyde, and some low carbon number aldehydes would again absorb ultraviolet light at 2500 to 3300 Å to produce some free radicals according to



R represents a hydrogen atom or alkyl or aryl organic groups. This photo-dissociation may account in part for the disappearance of aldehydes^{(9) (37)} after lengthy ultraviolet irradiation. The photo-oxidation of formaldehyde was investigated by Carruthers and Norrish.⁽⁶³⁾ It was reported that 45 per cent of the initial aldehyde formed formic acid, 20 per cent formed water and carbon monoxide, and 32 per cent was polymerized. The

carbon chain length was of the order of 10. This would provide another route for the production of high molecular weight and aldehydic particulates.

The mass concentration of airborne particulates produced by the ultraviolet irradiation of 10 ppm benzene in dry air was measured with a Thermo-Systems Particle Mass Monitor, Model 3205 A.⁽⁸⁵⁾⁽⁹⁵⁾ The aerosol profile is included in Figures 25 and 26. Significant particulate formation did not occur until the fast depletion of benzene started. The maximum concentration of particulates was between 800 and 3000 $\mu\text{g}/\text{m}^3$, depending on the initial concentration of oxygen and ozone when the benzene concentration was held constant at 10 ppm. Aerosol production from a benzene-air system in the presence of approximately 14 ppm ozone reached a maximum of about 800 $\mu\text{g}/\text{m}^3$ at 1200 seconds, while in systems initially without ozone production attained about 2600 $\mu\text{g}/\text{m}^3$ at 2400 seconds. The presence of ozone thus seems to enhance the initiation of particulate formation but inhibit the production quantitatively. The "downhill" concentration of particulates declined faster than expected because of dilution in both the two texts. The reason is probably due to an attack of atomic oxygen and ozone on particulates, presumably those of low molecular weight and vaporizable compounds being formed and evaporating from the condensed aerosol phase. To test whether or not particulates were a direct mixture of products from the photo-oxidation of benzene, a series of tests was made involving aerosol formation from benzene-dry nitrogen mixtures to which small quantities of oxygen were added. These results showed a distinct trend toward greater aerosol concentration profiles when higher concentrations of molecular oxygen were added.⁽⁴⁵⁾ Since a condensed

product is the major result, it appears that the rate of this photo-induced reaction is proportional to the concentration of oxygen in addition to the benzene concentration, especially at concentrations in the range of 10 to 100 ppm.

Infrared spectrophotometric analysis showed the presence of hydroxyl and carbonyl groups and both aromatic and aliphatic characteristics. It is also worthy of note that the mass spectrometric analysis of the particulates suggested the existence of aromatic ketones and quinonic compounds such as fluorenone, fluorenone-ol, xanthone, and diphenyl oxides. From the partial analysis of the gas and condensed phase products, 8.5 ppm aliphatic aldehyde was detected after about 2000 seconds. Assuming the aldehyde to be formaldehyde, which would be a logical choice as indicated by some of the reaction mechanisms in preceding sections, it would contain 14 per cent of the reacted carbon atoms. Infrared and mass spectrometric methods showed the presence of oxygen-containing compounds. If the condensed phase had consisted solely of a compound, or "monomer", with the formula of fluorenone, approximately 81 per cent of the reacted carbon atoms would be contained in the condensed phase. On the other hand, should the condensed phase have consisted only of quinone or mucondialdehyde $[\text{OHC}(\text{CH}_2)_4\text{CHO}]$ about 63 per cent of the carbon atoms would be in the condensed phase. All of the remaining compounds, to which the molecular formula is applied, would account for between 63 and 81 per cent of the consumed carbon atoms. Therefore it seems that as much as 63 to 81 per cent of the reacted carbon atoms may be contained in the condensed phase. One of the possible products containing reacted carbon atoms would be carbon monoxide; no attempt was made to measure its concentration during the course of the reaction.

Photo-oxidation and Particulate Formation with the
Addition of NO, NO₂, and H₂O

Although the photo-oxidation of alkylbenzene-nitrogen oxide mixtures, in general, proceeds as fast as those of olefin-nitrogen oxide mixtures and results in the production of significant ozone concentration levels,⁽⁵⁾ (7) (13) (27) (45) (49) benzene-nitrogen oxide mixtures have rather low reactivity like most paraffins. Yamate⁽¹³⁷⁾ reported the formation of aldehydes from benzene-nitrogen dioxide mixtures under the radiation of xenon light. Kopczynski⁽⁷⁶⁾ investigated the photo-oxidation of benzene and alkylbenzene with nitrogen dioxide present, and found that the percentages reacted during the first hour of reaction were 2, 4, and 7, respectively, for benzene, toluene, and o-xylene. These results also showed that as much as 50 per cent of the reacted carbon could be contained in the condensed phase. Grasley and collaborators⁽⁵³⁾ studied the photochemical reactions of toluene-nitrogen dioxide mixtures with the addition of water vapor; they found that reactions which produce condensed products were accelerated by water vapor. The onset of ultraviolet absorption by water vapor is at about 1850 Å,⁽³²⁾ but the mercury lamp of this study emitted radiation containing wavelength mostly above 1900 Å. Consequently, little or no absorption by water vapor would be expected, and photolysis of water molecules to form reactive species is unlikely.

Effects of NO and NO₂⁽⁵⁸⁾

In conducting tests with 10 ppm NO and 10 ppm benzene in air (Figure 28), the concentration of benzene was first adjusted, then nitric oxide was injected into the reaction chamber just as the lamp was turned on. As may be seen in the figure, nitric oxide is converted slowly at the

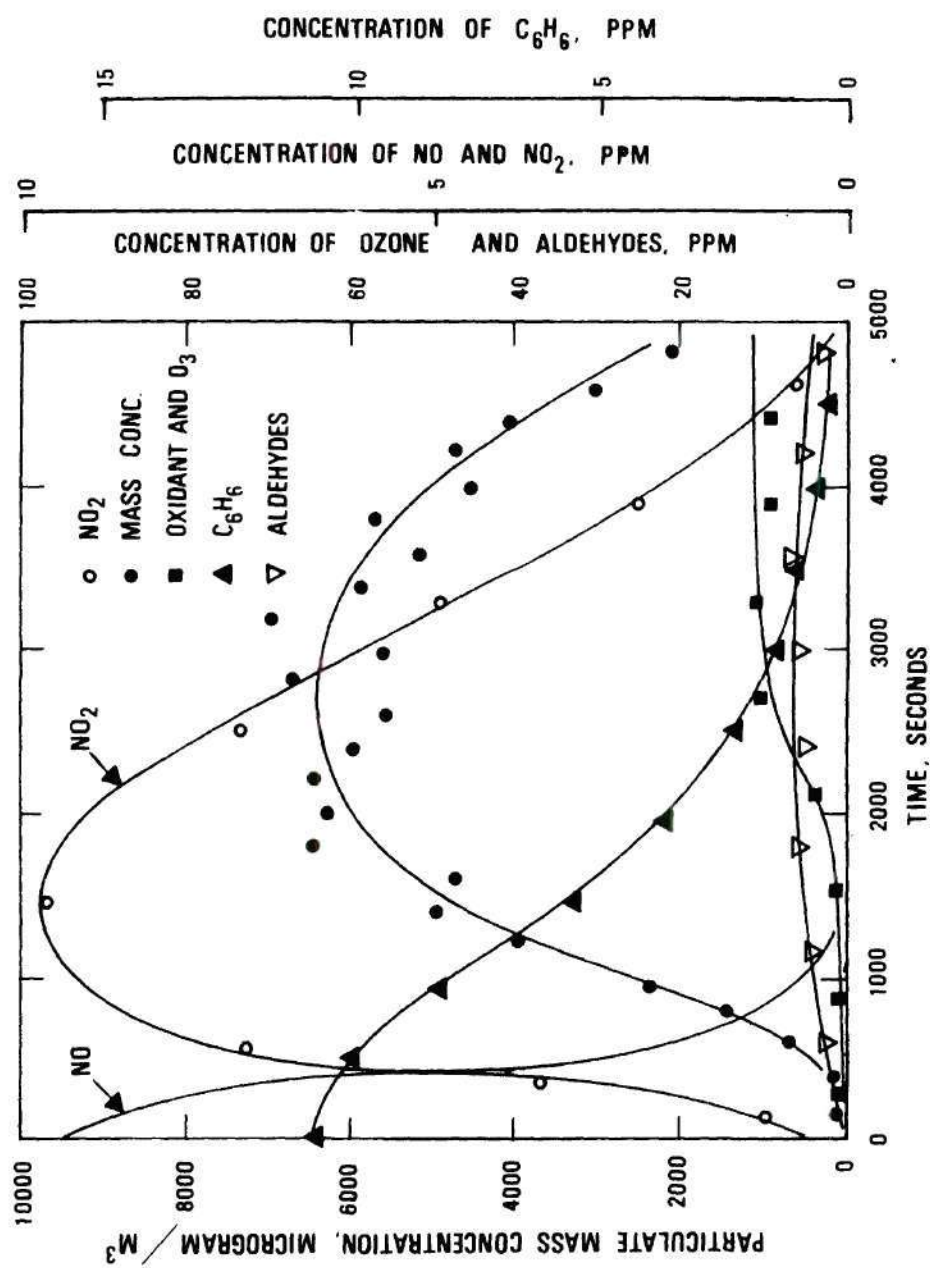


Figure 28. Concentration Changes of Reactants and Products during Ultraviolet Irradiation of Benzene-Nitric Oxide-Air Mixture.

beginning of the reaction into nitrogen dioxide, the nitrogen dioxide concentration going through a definite maximum at about 1400 seconds. This reaction most likely is the spontaneous oxidation of nitric oxide to form nitrogen dioxide according to



Nitrogen dioxide then undergoes photo-dissociation to produce normal $\text{O}(^3\text{P})$ and nitric oxide under wavelengths of 3130, 3660, and 4047 Å by the reaction



Meanwhile normal $\text{O}(^3\text{P})$ can also be formed by photo-dissociation of oxygen molecules in air as given by Equation (5.1).

Other important reactions involving atomic oxygen, ozone, and nitrogen oxides are as shown by Equation (5.2) and by



The rate of O_3 consumption may be expressed by $K(\text{NO})(\text{O}_3)$ where K is a reaction constant and (NO) and (O_3) are concentrations since the reactions of ozone with NO_2 and benzene are insignificant at this stage. At the beginning of the photochemical process, especially during the first 500 seconds, the rate of the atomic oxygen-benzene reaction is very low as shown by the benzene concentration curve in Figure 28, and the rates of reactions between atomic oxygen and nitrogen oxides are also negligible. Under such circumstances, the production rate of atomic oxygen is the combined rate of reactions (5.1) and (5.9). The photolytic yield of

atomic oxygen is constant, therefore the combined rate is more or less a constant for moderate NO_2 concentrations. This combined rate will then be equal to the rate of formation of O_3 and, in turn, equal to the rate of consumption of O_3 which is $K(\text{NO})(\text{O}_3)$. So $K(\text{NO})(\text{O}_3)$ is roughly a constant under the described conditions. As the nitric oxide concentration decreases, the ozone concentration will increase. This explains the buildup in the ozone concentration after completion of the nitric oxide conversion at about 1400 seconds. The ozone concentration reaches a peak at about 2700 seconds beyond which it levels off to a steady value of about 9 ppm. The NO_2 concentration decreases more or less constantly during the period from 1400 to 5000 seconds. As for the fate of NO_2 , it probably forms alkyl nitrates and peroxyacyl nitrates (PAN) when it reacts with alkoxy and peroxyacyl radicals as shown by the work of Stephens⁽¹²²⁾ Production of alkoxy radicals has been indicated previously, and peroxyacyl radicals are probably the intermediate products of the consecutive reactions of atomic and molecular oxygen with benzene. Kopczynski⁽⁷⁶⁾ also reported the presence of peroxyacetyl nitrate and methyl nitrate as two of the products from the photo-oxidation of a mesitylene- NO_2 mixture.

By comparison, the benzene disappearance rate was slightly lower than that of tests in the absence of nitrogen oxides; besides, a longer induction period was also observed, and the rapid consumption of benzene only started when more than 70 per cent NO had been converted into NO_2 at about 400 to 500 seconds. After this induction period, the characteristics of the benzene disappearance were similar to those of benzene without the addition of either NO or NO_2 . An aliphatic aldehyde concentration profile which reached a maximum value of about 7 ppm was observed during the 3000 to

4000 second interval. Again, the formation of aliphatic aldehydes may be explained in part by the mechanisms of reactions (5.5) and (5.6). Altshuller and Cohen⁽⁸⁾ reported that the photochemical reactions of a toluene-nitric oxide system also resulted in aliphatic aldehydes along with ozone and other peroxy compounds. They, therefore, drew the conclusion that fragmentation of the aromatic ring occurred during photo-oxidation reactions.

An aerosol profile is indicated in Figure 28. Once again, significant particulate formation began only after the fast depletion of benzene had started. A maximum concentration of about $7200 \mu\text{g}/\text{m}^3$ was reached at 2000 seconds. Compared to reaction systems without the addition of nitrogen oxides, which have a maximum of about $2600 \mu\text{g}/\text{m}^3$ at 2400 seconds, quantitative particulate formation is much enhanced by the presence and participation of nitrogen oxides. This is well illustrated in Figure 29 where particulate concentrations from different initial NO concentrations are compared. Since the benzene concentration at 2000 seconds was approximately 3.7 ppm (See Figure 28), subtracting it from the initial value of 10.8 ppm shows that about $2300 \mu\text{g}/\text{m}^3$ was consumed during the first 2000 seconds. In other words, the particulate matter must be highly oxygenated. Supposing the product to contain all of the reacted carbon atoms, a benzene molecule would combine with approximately 7 oxygen atoms plus one nitrate group to form the final particulate product. Consistently, the mass and infrared spectrometric analysis both indicate the existence of an abundance of hydroxyl and carbonyl groups, but the presence of PAN and alkyl nitrates are obscured in the infrared spectrum, probably by the strong absorption bands of oxygen-containing groups. When nitrogen dioxide

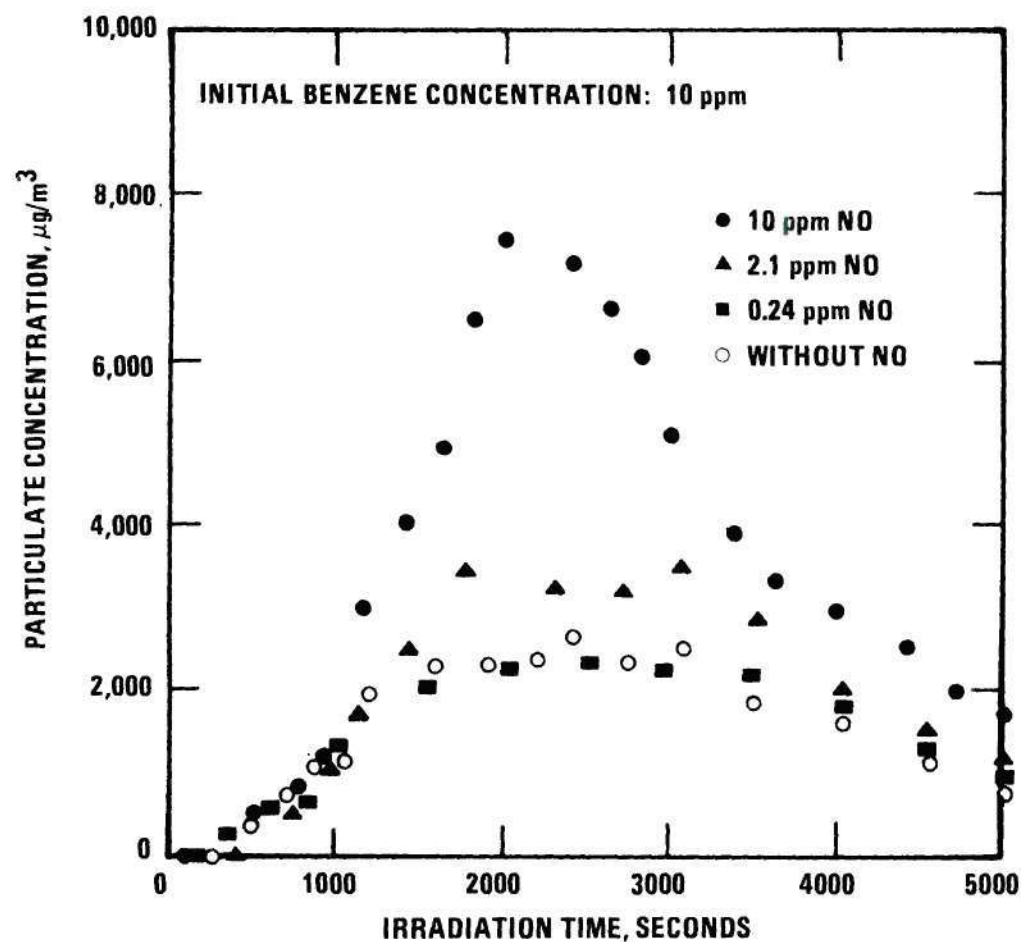


Figure 29. Yield of Particulate as a Function of Initial Nitric Oxide Concentration. (See Reference 71, P.26, Figure 10)

was added to the reaction chamber instead of nitric oxide, the induction period became shorter, and the formation of aerosol started almost immediately with the beginning of the ultraviolet irradiation. The particulate concentration reached a slightly higher maximum of about $7500 \mu\text{g}/\text{m}^3$ at 2000 seconds. This is probably explained by the attack on the benzene ring by atomic oxygen produced by the photolysis of NO_2 .

Effects of Water Vapor

In order to understand the effects of humidity on the disappearance rate of benzene and the formation of particulates, a series of tests was made by irradiating the standard mixture of 10 ppm benzene and varying amounts of water vapor in air. The results indicated that the presence of the water accelerated the depletion of benzene and greatly enhanced aerosol formation. Figure 30 shows the effect of water vapor on the disappearance rate of benzene, the half-life of benzene decreasing from 1450 seconds to 700 seconds at 1.45 per cent water vapor. Figure 31 demonstrates remarkable increases in particulate concentration, especially during the period of 1000 to 2000 seconds, when the results of the reaction mixtures at 1.03 and 0.343 per cent water vapor are compared with those of the dry mixtures. The maximum particulate concentration of $2600 \mu\text{g}/\text{m}^3$ for the dry mixture increases to $16,000 \mu\text{g}/\text{m}^3$ at 1.03 per cent water vapor content.

Goetz and Klejnot⁽⁵¹⁾ noted that aerocolloid formation from photochemical reactions of pure toluene or cumene in air increased remarkably with humidity and considered the water molecule to be a participant in the photochemical processes. An acceleration in the rate of toluene disappearance and NO_2 formation for toluene-nitric oxide-air mixtures under the irradiation of artificial sunlight was reported by Grasley and collabora-

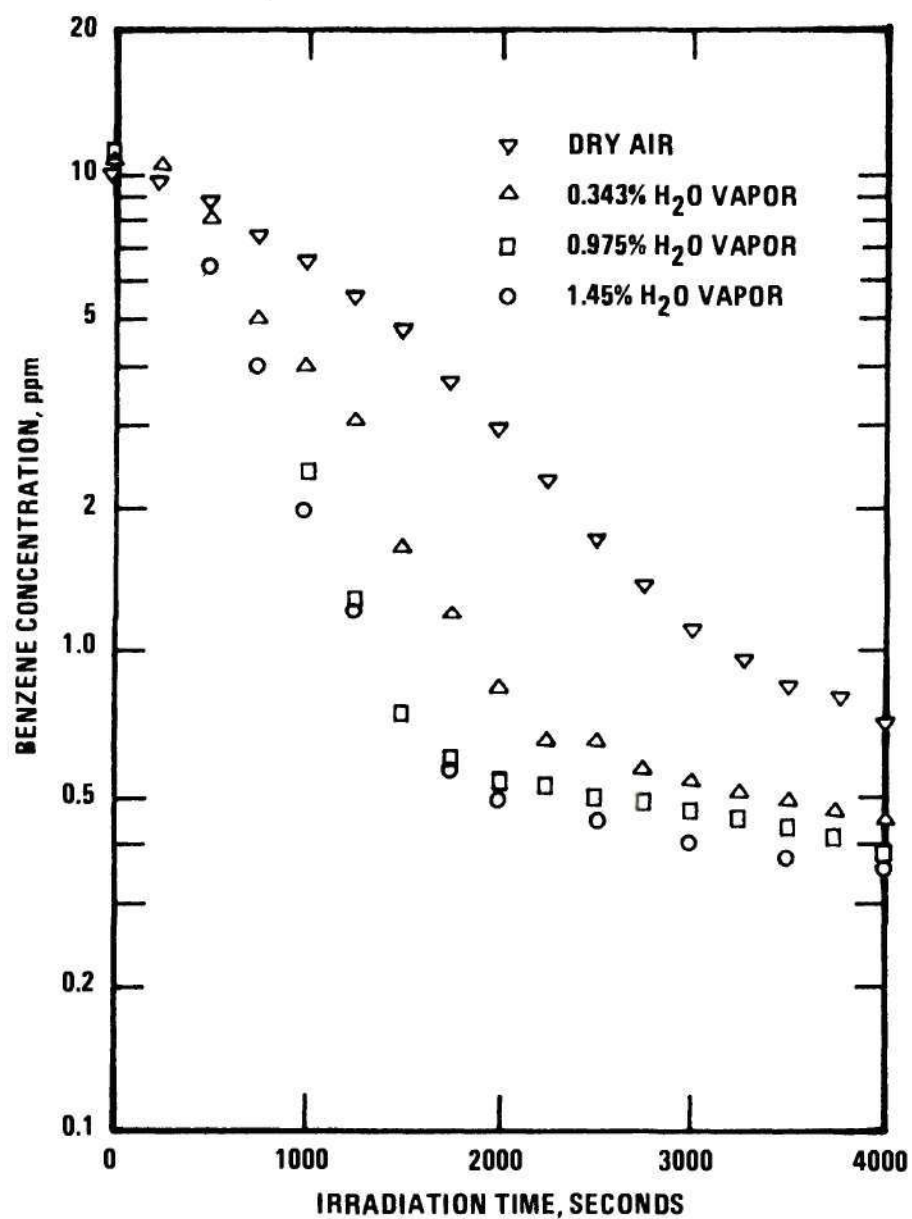
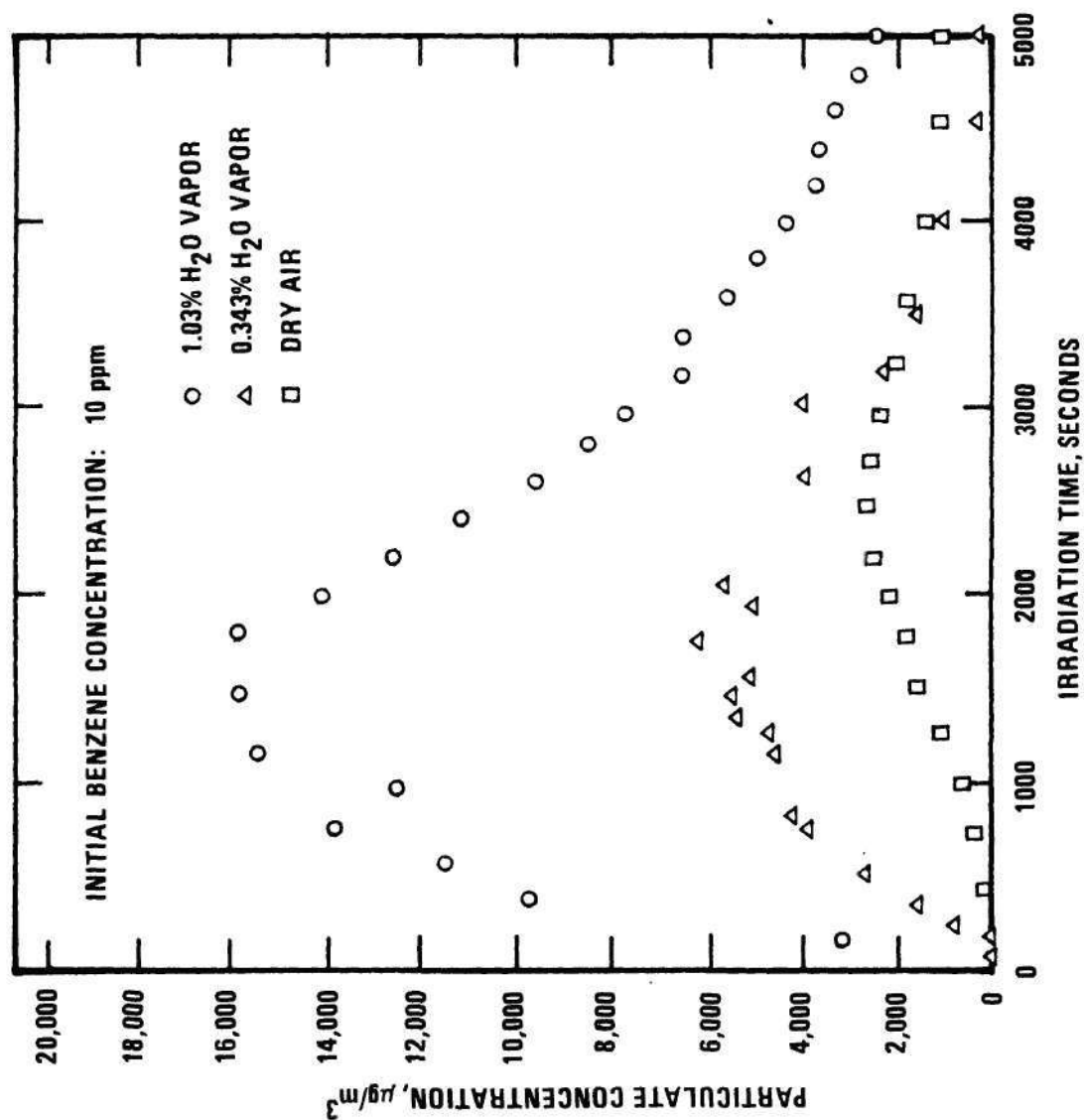


Figure 30. Disappearance Rate of Benzene as a Function of Initial Humidity.
(See Reference 71, P.29, Figure 12)



tors⁽⁵³⁾. Dimitriadis, et al.,⁽⁴⁰⁾ also discovered that the photochemical formation of NO₂, oxidant, and formaldehyde from an ethylene-nitric oxide-air mixture appears to be enhanced by the presence of water vapor.

Since photo-dissociation of water molecules under the ultraviolet radiation from a mercury lamp to form atomic hydrogen and hydroxyl radicals is not likely as indicated at the beginning of this section, a water molecule probably participates in these complex reactions by combination with one excited ¹D atomic oxygen to form two hydroxyl radicals through the reaction⁽¹⁴⁾(78)



The excited ¹D oxygen atom is produced by photolysis of O₃ as shown by reaction (5.3). Hydroxyl radicals can then react with hydrocarbon molecules to form the radical R· by way of



Reactions (5.11) and (5.12) may explain in part why the presence of water vapor favors the rapid depletion of benzene. The insignificant rate of the ozone-benzene reaction, as shown by Figure 25 and some of the preceding discussion, makes the attack of oxidizing agents on benzene molecules much more dependent on the atomic oxygen concentration. Such oxidation reaction products contain a large quantity of organic oxides and epoxides. The addition of water to these compounds certainly would lead to the incorporation of carbonyl and hydroxyl groups in their molecular structures through hydrolysis and hydroxylation, and therefore cause an increase in the particulate mass concentration.

CHAPTER VI

MICROPHYSICAL PHENOMENA AND GROWTH OF PARTICULATES

Sample Collection and Measurement of Size Distribution

Thermal precipitation was employed for the collection of particulate products for chemical and physical analysis. The latter included particle size distribution by transmission electron microscope, stereoscopic examination under the scanning electron microscope, mass spectrometric analysis, tests of solubility, thermal stability, temperature of transition, etc. Tests of thermal stability and other measurements of physical properties revealed that the x-ray induced particulates were non-volatile, insoluble, and thermally stable, therefore the use of thermal precipitators was justified since the method of collection was not likely to change the size and other chemical and physical characteristics.⁽³⁶⁾ Nevertheless, for samples collected from photochemical reaction systems, electrostatic precipitation⁽⁹³⁾ was used concurrently to facilitate comparison with the thermal precipitator sample and to detect and avoid any possible evaporation due to the temperature of the heated plate of the thermal precipitator.

A previously described⁽⁷³⁾ thermal precipitator was adapted and employed, one small modification being made. This consisted of reducing the entrance passageway in order to produce a smaller radius of deposition. The precipitation plate separation was about 0.03 cm, and the temperature difference between the heated and cooled plates was between 40 and 48°C, depending on the adjustment of the heated-plate current and the temperature of the cooling water. The resulted temperature gradient was thus between 1330

and 1600°C/cm. Another thermal precipitator described by Hendrix and Orr⁽⁵⁹⁾ was also used in same instances.

Aerosol was collected at flow rates up to 300 cc/min. The deposit pattern of the aerosol was symmetrical with respect to the center and was more or less an annular ring. Electron microscope grids were placed at randomly selected spots to collect representative samples and to avoid bias in the measurement of size distribution. By examining electron micrographs of particles deposited at different points, any size segregation effect of the precipitator was judged to be rendered insignificant. As for the effectiveness of thermal precipitation, the lower limit of particle size detected in both the x-ray and ultraviolet products was roughly 0.025 μ m. A glass substrate with a thickness of 0.005 cm was placed on the cool plate of the precipitator to collect samples for all purposes other than for electron microscope examination.

The collection method making use of electrostatics⁽⁹³⁾ involved charging the particulates by means of a corona-discharge at about 2500 volts and precipitating them onto a carbon-coated electron microscope grid placed on the end of a grounded cylinder using a Teflon holder. An electric field of 1250 to 2500 volt/cm was employed.

Enlarged electron micrographs and electron microscope negatives of particulates from both x-ray and ultraviolet light irradiation systems were employed in making particle size distributions. A light microscope calibrated by a stage micrometer with an eyepiece graticule was used in measuring images from negatives. Particle size was determined from the enlarged electron micrographs using a Zeiss Particle Size Analyzer, Model TGZ, it being a semi-automated image analysis instrument removing

some of the tediousness of particle sizing. The number of measurements per test ranged between approximately 400 and 1000. A table provided by Montgomery⁽⁹⁶⁾ was used as a guide to the number of particle measurements necessary to achieve 99 per cent certainty that the distribution of sizes was correct to within 10 per cent. The number of measurements actually made was twice that required by the table to ensure statistically reliable data.

Electron Microscopic Examination of Particulates

A transmission-type electron microscope, Model JEM-30, manufactured by Japan Electron Optics Laboratory Co., was employed. Particulate samples to be examined were either collected on carbon-coated copper grids or on specially treated iron grids. These iron grids, used mostly during preliminary studies, were held in a humid air stream at about 500°C for one or two hours until needle-like crystals, called whiskers, of iron oxide grew outward from the surface.⁽¹⁰⁰⁾ Many spherical particulates were found entrapped on the whiskers after exposure in the x-ray irradiation chamber at various positions for short times. A typical electron micrograph has already been presented as Figure 2.

For most of the work involving x-ray irradiation, thermal precipitation was used to collect particulates on carbon-coated electron microscope grids centrally located on the collecting surface. Electron micrographs of the particulates from benzene-saturated air are shown in Figures 32 and 33. Large agglomerates or chains of particulates were often found as were necks or junctions as is evident in Figure 33, suggesting that the particulates may have the properties of a very viscous liquid. Particulates from other

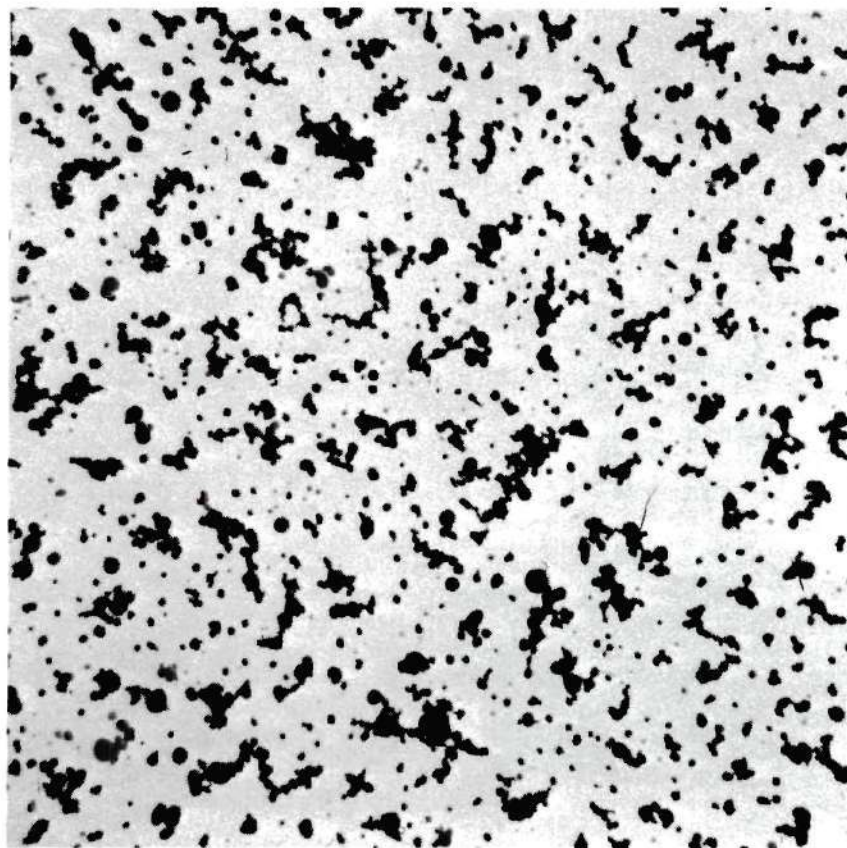


Figure 32. Electron Micrograph of Particulates Formed from X-ray Irradiation of Benzene-Saturated Air. X4,500

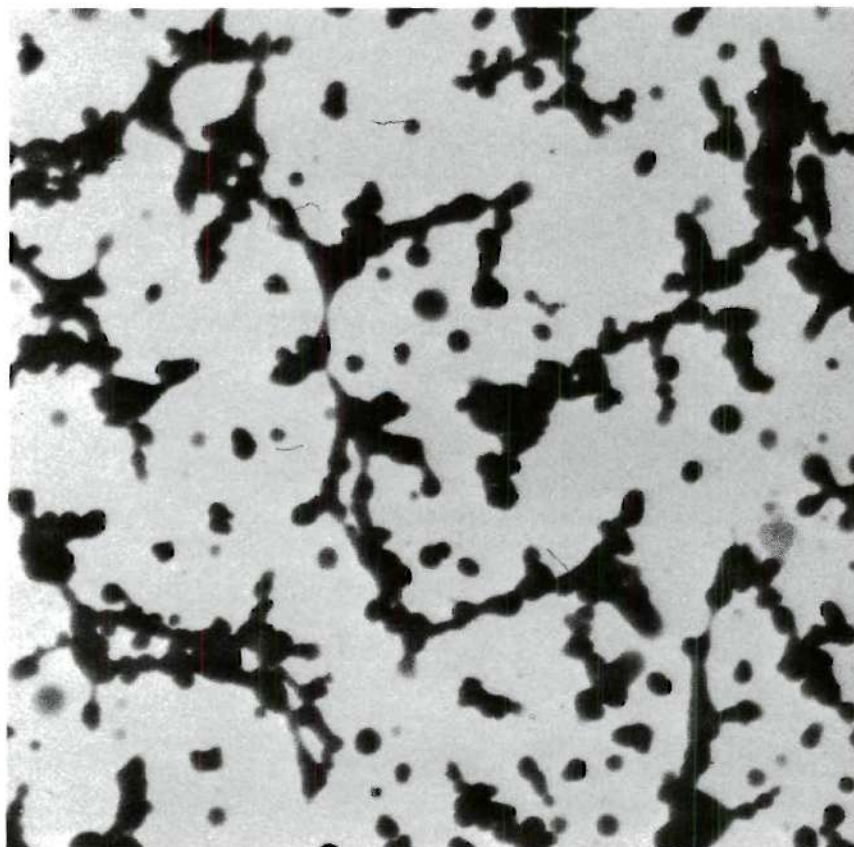


Figure 33. Electron Micrograph of Particulates Formed from X-ray Irradiation of Benzene-Saturated Air, X9,000

hydrocarbons in air generally showed very similar behavior.

Particulate matter generated by the ultraviolet irradiation of 10 ppm benzene in dry air was also examined by electron microscopy. Methods of sample collection included both thermal and electrostatic precipitation, but electrostatic precipitation was used most often. Figure 34 shows the aerosol collected electrostatically in the latter stages of a test, i.e., after 5000 to 5500 seconds. Particulates collected during the first 1000 seconds appeared transparent and were more liquid-like. They also exhibited greater deformation upon contact with carbon-coated electron microscope grids. Samples taken after the first 1000 seconds appeared to be opaque and more like the rigid spherical particulate matter shown in Figure 34.

Another electron micrograph, Figure 35, shows particulates collected during the interval from 2000 to 3000 seconds after photochemical reaction initiation with a benzene-nitric oxide-air mixture. The total yield of particulate product is two to three times that from a benzene-air system without nitric oxide. Again, the products formed near the beginning of the reaction were more or less transparent and liquid-like; they became opaque in latter stages. Linear and clumpy agglomerates were evident under the electron microscope.

For each of the reaction systems and with both x-ray and ultraviolet radiation, the particulate products were examined by scanning electron microscopy using the Cambridge Stereoscan, Mark IIA. Stereoscopic electron micrographs were made at an angle of 45° , usually with a platinum coating of approximately 200 \AA thickness. Figure 36 shows particulates from x-ray irradiation of benzene-saturated air. This particular sample was not platinum coated. Both single particulates and aggregates are evident on the

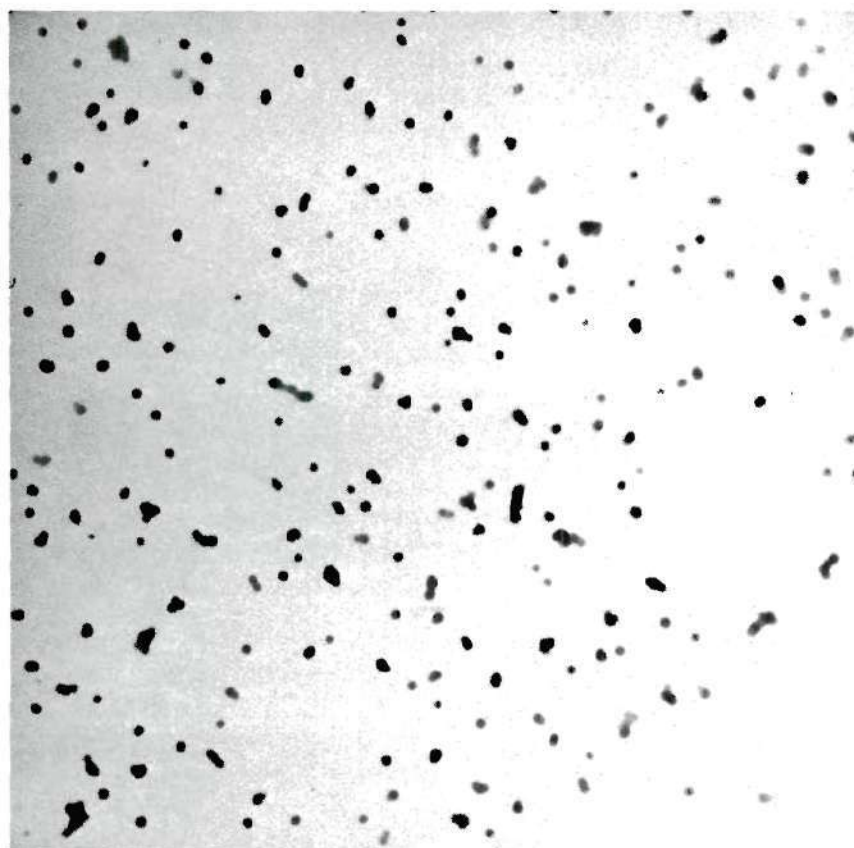


Figure 34. Electron Micrograph of Particulates Formed from Ultraviolet Light Irradiation of 10 ppm Benzene in Air. X6,900

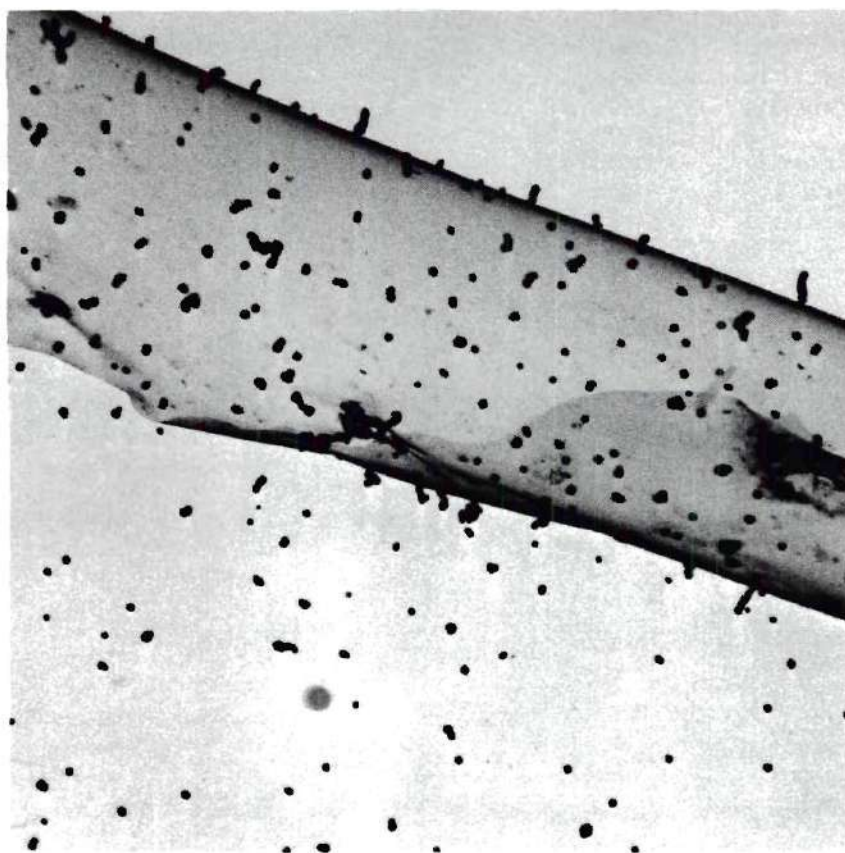


Figure 35. Electron Micrograph of Particulates Formed from Ultraviolet Light Irradiation of 10 ppm Benzene and 10 ppm Nitric Oxide in Air.X5,270

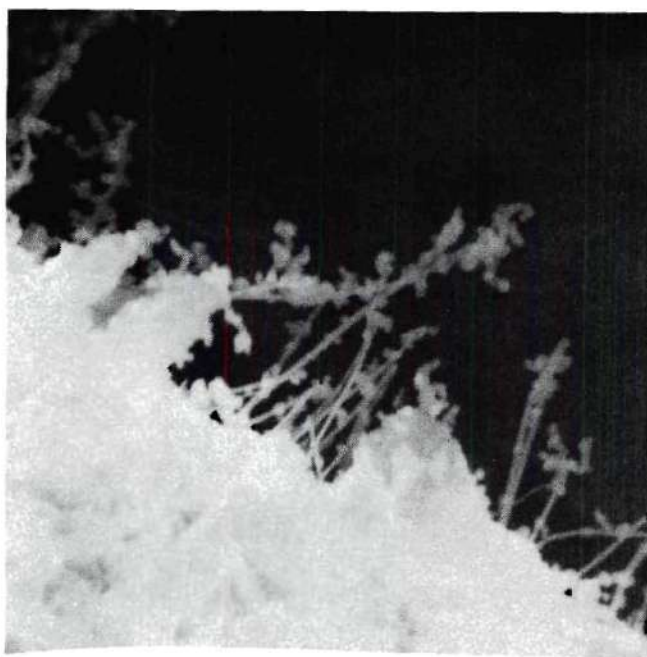


Figure 36. Scanning Electron Micrograph of Whiskers and the Attached Particulates Formed from X-ray Irradiation of Benzene-Saturated Air.X9,350

iron oxide whiskers. Figure 37 shows product from the x-ray irradiation of the air containing both benzene and water vapor. These particles were collected on a Pyrex glass substrate with a thermal precipitator. The larger spheres are up to 1 μm in diameter. Figure 38 shows particulates from the x-ray irradiation of an acetylene-air mixture prepared by similar procedures. Photochemical aerosol particulates formed from the oxidation reaction of benzene in air during the irradiation period between 5500 and 6000 seconds are shown by Figure 39. Some few agglomerates are evident.

Particulates were also collected on Nuclepore filters manufactured by the General Electric Co. and having a pore size of approximately 0.5 μm . These samples were collected during irradiation times between 2000 and 6000 seconds. After platinum coating, scanning electron micrographs were obtained as shown in Figures 40, 41, and 42. Particulates generated by the photo-induced reaction of benzene-nitric oxide-air are shown in Figure 40. Particulates formed with toluene, Figure 41, must be liquid-like, as they appear to be hemispherical on the filter. The o-xylene product, Figure 42, contains some relatively large particulates together with small ones. The small spheres might have been formed during a late stage of the reaction; on the other hand, the liquid-like droplets probably formed at an early stage.

Physical Properties of Particulates

X-ray Irradiation Products

Observations were also made using an ordinary light microscope⁽²⁰⁾⁽⁸⁸⁾ Particulates formed from an acetylene-air system always appeared white when

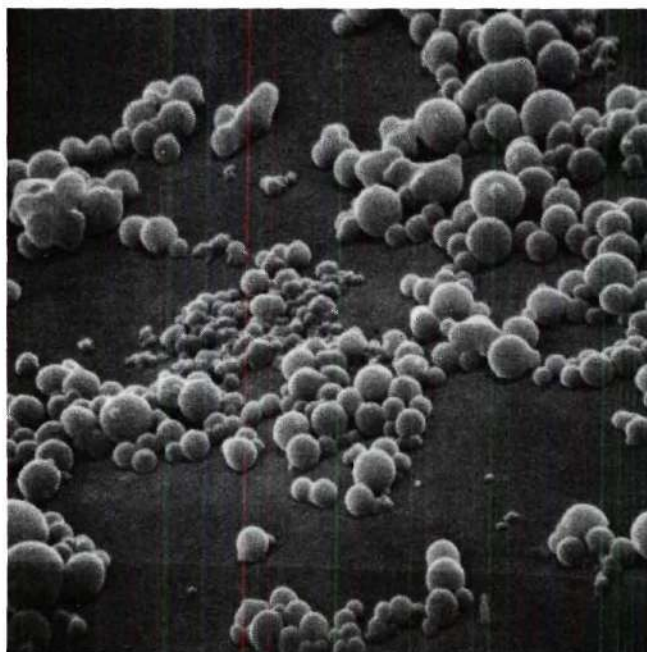


Figure 37. Scanning Electron Micrograph of Particulates Formed from X-ray Irradiation of Air Containing Partially Saturated Benzene and Water Vapor. X9,350



Figure 38. Scanning Electron Micrograph of Particulates Formed from X-ray Irradiation of Acetylene-Air Mixture.
X9,350

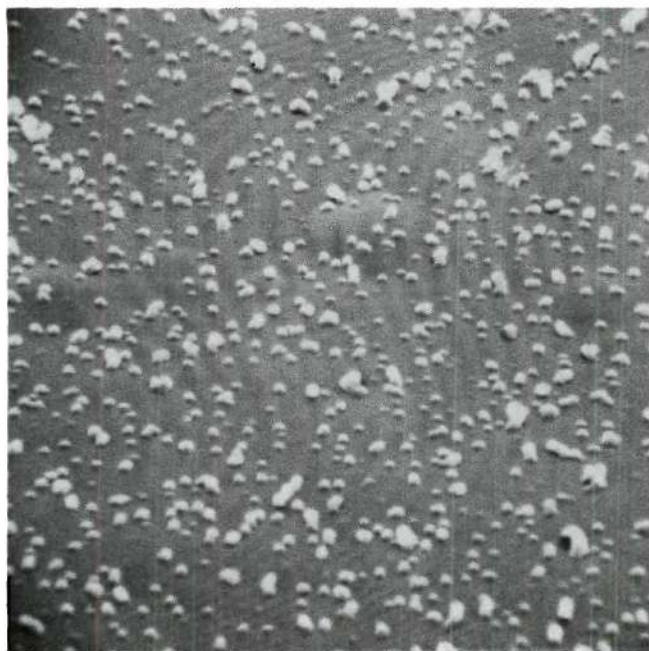


Figure 39. Scanning Electron Micrograph of Particulates Formed from Ultraviolet Irradiation of Air Containing 10 ppm Benzene. X4,760

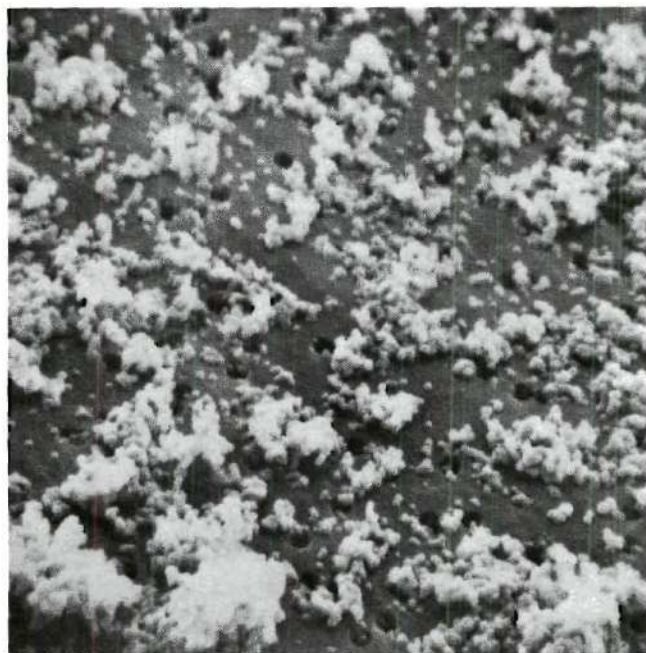


Figure 40. Scanning Electron Micrograph of Nuclepore Filter and the Attached Particulates Formed from Ultra-violet Irradiation of Air Containing Both Benzene and Nitric Oxide at 10 ppm. X4,760

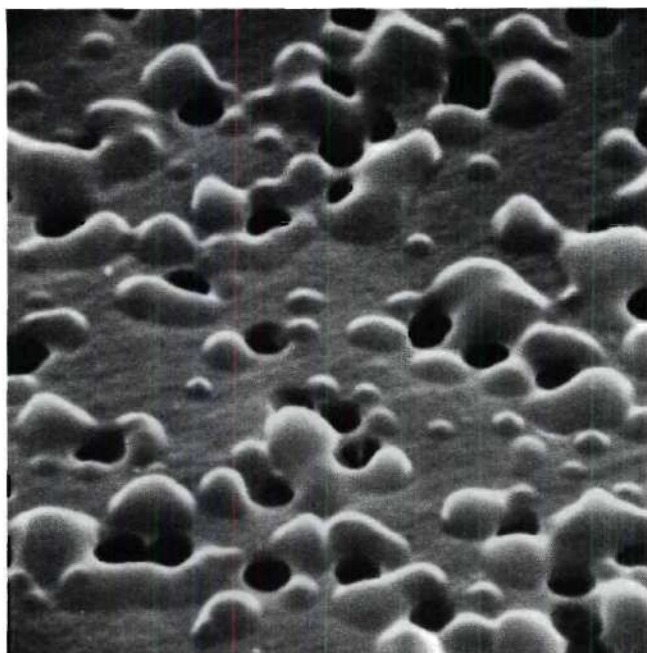


Figure 41. Scanning Electron Micrograph of Nucleopore Filter and Particulates Formed from Ultraviolet Irradiation of Air Containing 10 ppm Toluene.X8,930

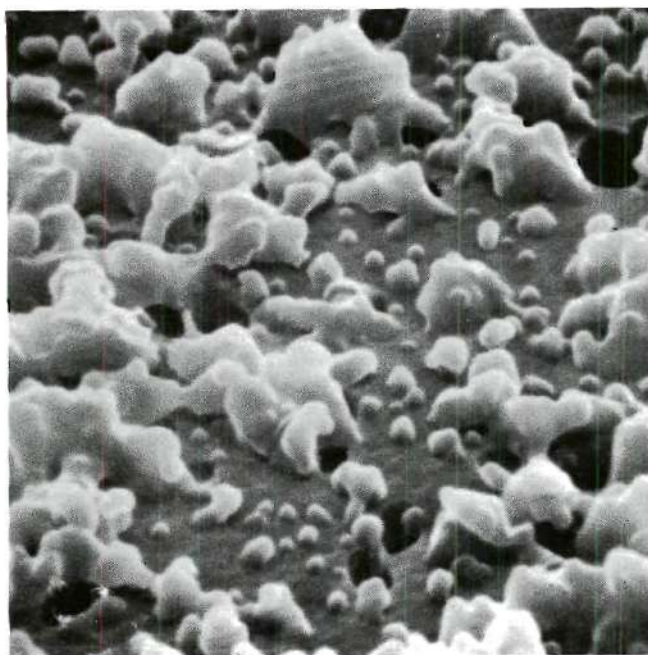


Figure 42. Scanning Electron Micrograph of Nuclepore Filter and Particulates Formed from Ultraviolet Irradiation of Air Containing 10 ppm Xylene.X8,930

collected as a thin layer on a glass substrate, but the color changed to yellow and even brown as thick layers developed. The product from cyclohexene-air mixtures showed only a light yellow color. The specific gravity of masses of particulates produced from a benzene-air system were measured to be between 1.51 and 1.58. Benzene, n-decane, n-butanol, and carbon tetrachloride were used in attempts to dissolve the particulates, but the samples remained unchanged in size and appearance for at least 2 days. In addition, they showed neither a melting point nor a temperature of transition when heated gradually to 400°C in a scanning differential calorimeter.

The particulates were essentially non-volatile at room temperature, even remaining after exposure to the high vacuum of the electron microscope for 50 hours. Electron micrographs of the particulates formed from a benzene-air mixture and collected on iron oxide whiskers before and after the exposure to a vacuum for 50 hours are presented in Figures 43 and 44. The crystals themselves were somewhat deformed, but the particulates apparently remain unchanged. Particulates were also heated while exposed to ambient air. Electron micrographs showing before and after heating are presented in Figure 45. From these, a decrease in particulate size with some deformation is apparent. Most of the particulates are still present, however, after heating at 250°C for 4 hours. The largest particulate was still evident after 30 hours at this temperature. A microscope hot stage was used for these tests; its temperature was maintained and controlled electrically.

A thick layer of particulates formed from a benzene-air mixture was collected on a glass substrate of known weight. The decrease in weight of

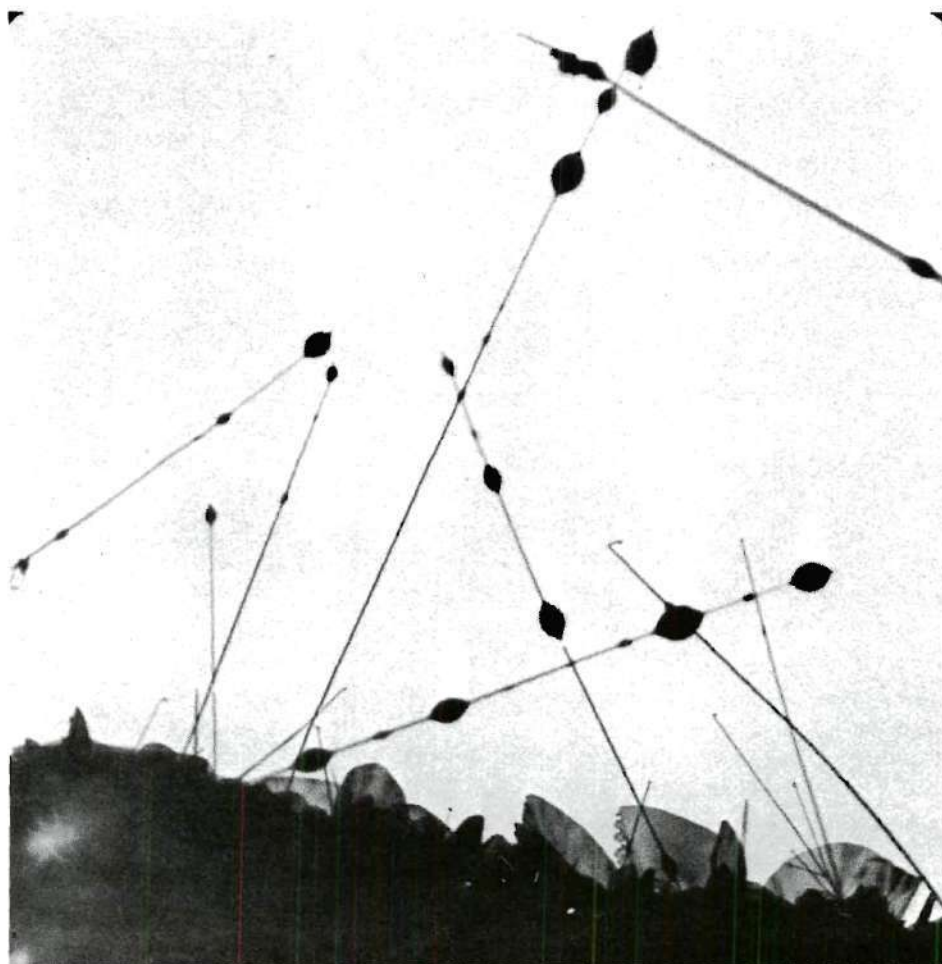


Figure 43. Electron Micrograph of Whiskers and Particulates
Formed from X-ray Irradiation of Benzene-Air Mixture
before Exposure to Vacuum. X8,350

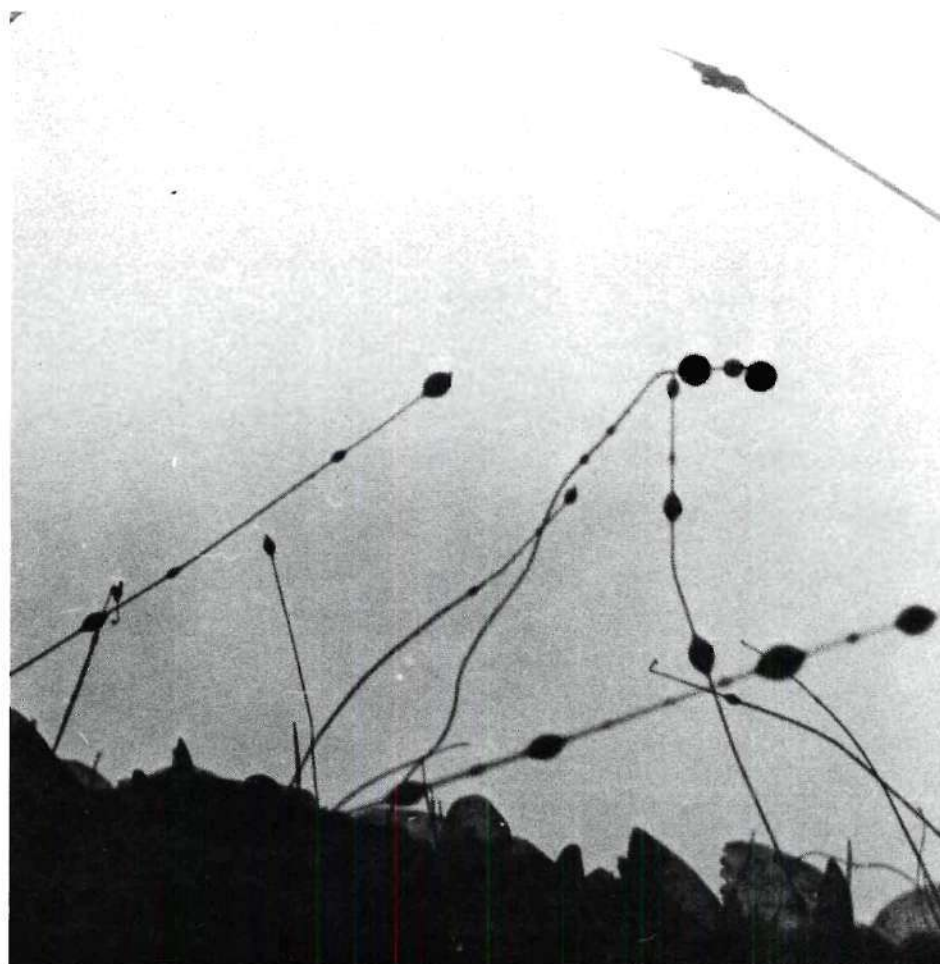


Figure 44. Electron Micrograph of Whiskers and Particulates Formed from X-ray Irradiation of Benzene-Air Mixture Mixture after Exposure to Vacuum for Two Days. X8,350

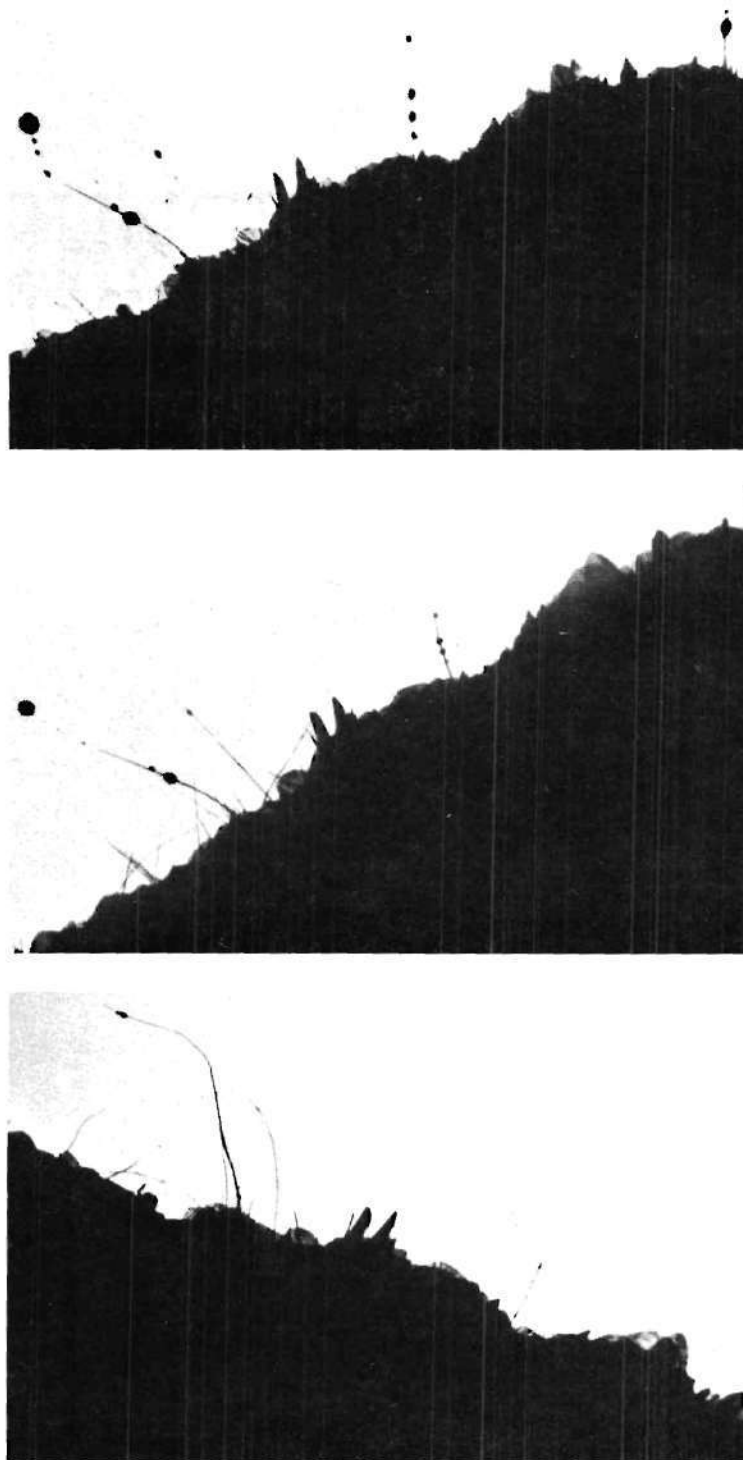


Figure 45. Particulates Formed from X-ray Irradiation of Benzene-Air Mixture before (Upper Photo), after 4 Hours (Middle Photo), and after 30 Hours (Bottom Photo) at 250°C, X5,000 (See Reference 71, P.58, Figure 32)

the particulates following heating was obtained by periodically weighing the glass substrate. These results are given in Figure 46. The reduction in weight appeared to cease after about 2 hours at four different temperature levels. Similar weight measurements were also made on particulates formed from a benzene-air mixture before and after additional x-ray irradiation, however no significant weight change was detected. The particulate substances also appeared by microscopic examination to be unchanged.

Ultraviolet Irradiation Products

Particulates generated from benzene-air mixtures with and without the addition of nitrogen oxides appeared as a light yellow resinous powder. When a sample was placed in a capillary tube and heated in a melting point apparatus, it showed no melting point but began to darken at 90°C and charred at 200°C. For other samples formed from benzene-air mixtures, thin layer chromatograms were made using Eastman Kodak 6061 silica gel chromatographic paper. Acetone was used as the solvent and development was with I_2 . At least three unknown components were detected; one eluted fast and the other two very slowly.(125) Other organic solvents were tested, but the particulates were only slightly soluble in methyl acetate and n-propanol and insoluble in chloroform, benzene, and amyl acetate.

Particulates produced from benzene-nitric oxide-air mixtures were partially soluble in ethyl alcohol and slightly soluble in acetone. These particulates did not show a reduction in size when exposed to a high vacuum environment for periods of up to 48 hrs. This indicates that particulates formed photochemically also consist of non-volatile components.

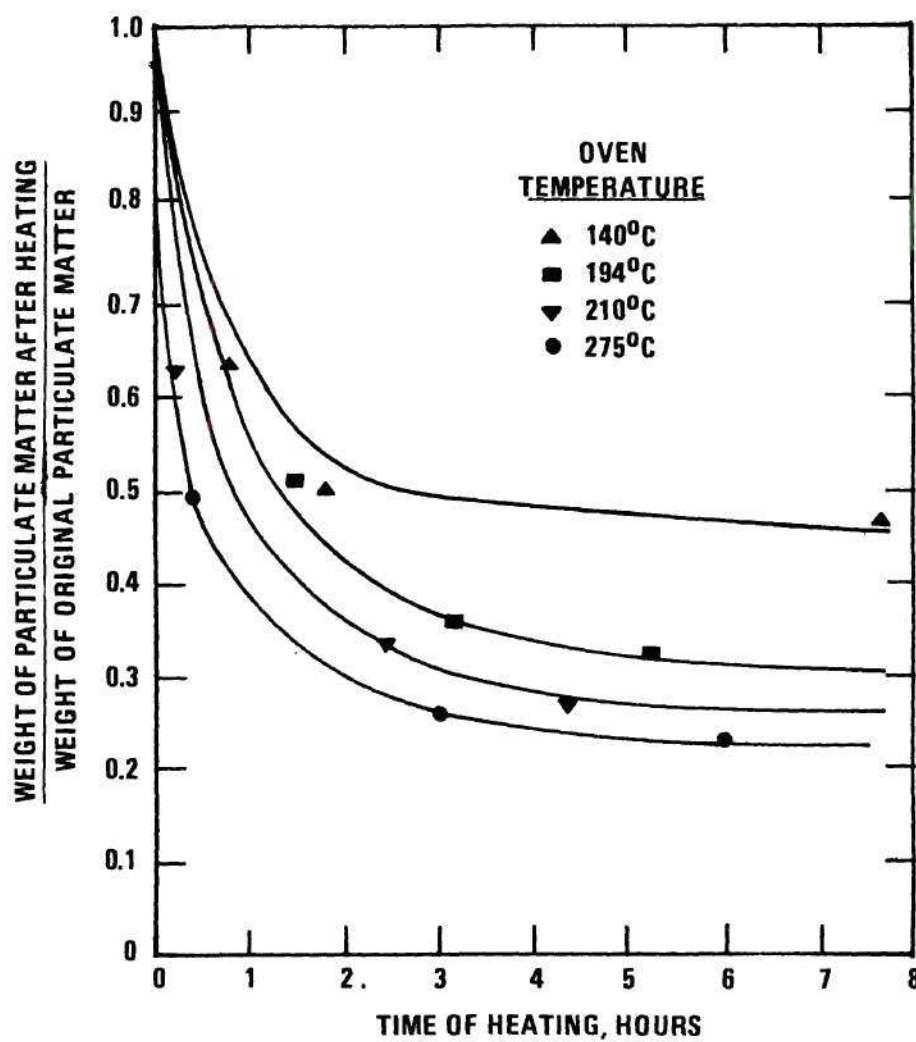


Figure 46. Reduction in Weight of Particulates as a Function of Heating Time and Oven Temperature.
(See Reference 71, P.59, Figure 33)

Growth of Particulates

X-ray Irradiation Products

Particulates, once deposited, were found to grow on iron oxide whiskers if the x-ray irradiation were continued and organic vapors were present. Grids carrying the whiskers were located along the axis of the cylindrical irradiation chamber just before the outlet. Later upon examining the grids by electron microscopy, larger particulates were found at the locations nearer the x-ray tube, hence at higher x-ray intensity. Particulate growth was also observed to continue in the presence of gases leaving the irradiation chamber. Size distributions of particulates from air containing initially 10 per cent acetylene at progressively increasing times, designated aging time, beyond four minutes of x-ray irradiation are shown in Figure 47. Growth of the particulates was also indicated, as shown in Figure 48, by the increase of median diameters as a function of aging time. These data suggest the growth rate slowed after 10 to 20 minutes and reached an equilibrium state after about 50 minutes.

The distributions of Figure 49 reveal the dependence of ultimate particulate growth on hydrocarbon concentration. The distributions appear to widen as hydrocarbon concentration increases. This behavior is consistent with the principle of activation in radiation chemistry which states that the extent of chemical reaction is proportional to the number of ion pairs produced in the reaction medium by ionizing radiation. Figure 50 shows the effect of water vapor on the growth of particulates. Even though the mass concentration begins to decrease at about 5 per cent relative humidity as given in Figure 23, particulates formed at higher humidity are larger on the average.

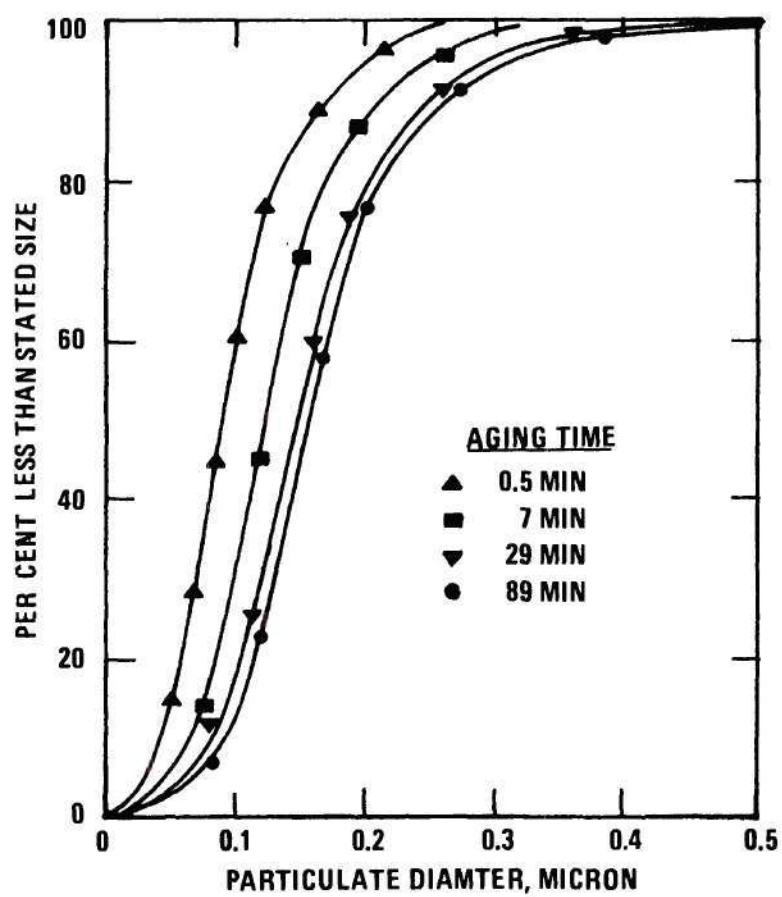


Figure 47. Size Distributions of X-ray Induced Particulates as Functions of Aging Time.
(See Reference 71, P.52, Figure 27)

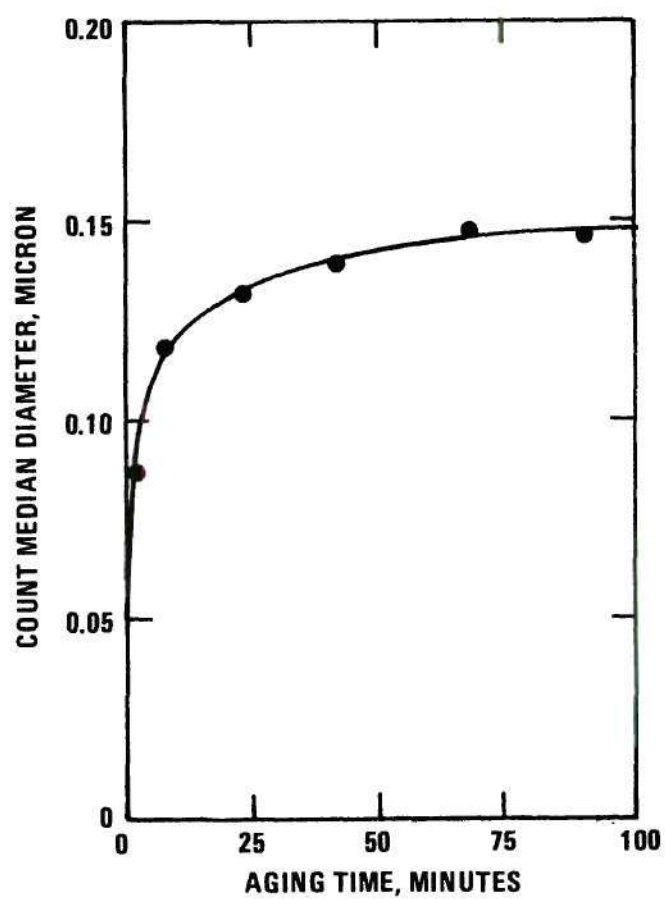


Figure 48. Median Diameters of X-ray Induced Particulates as Function of Aging Time.
(See Reference 71, P.53, Figure 28)

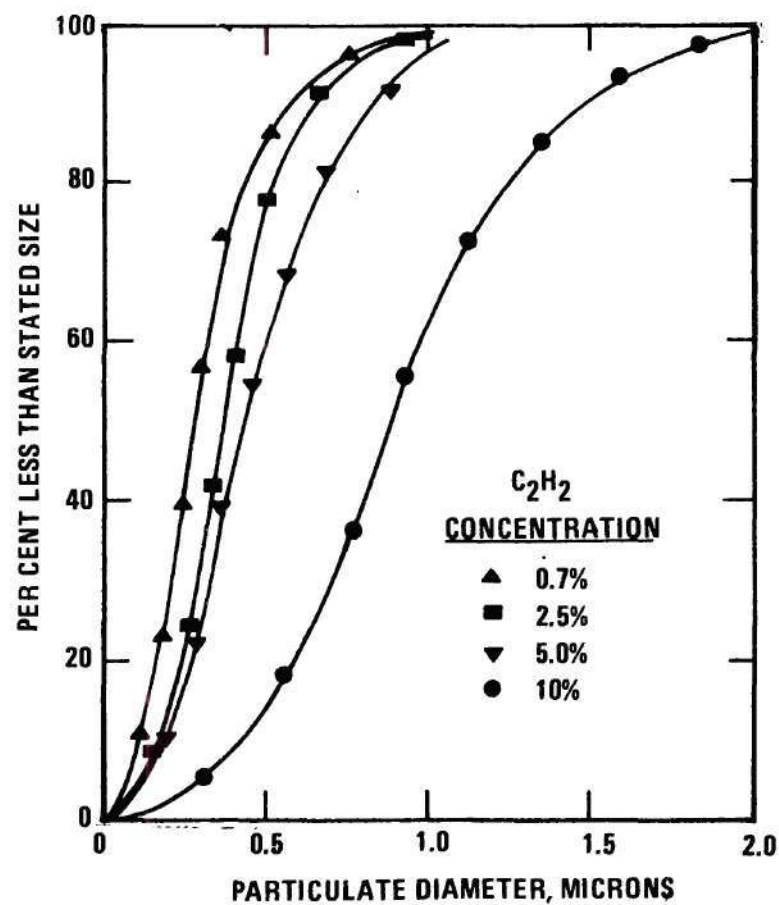


Figure 49. Size Distributions of X-ray Induced Particulates as Functions of Acetylene Concentrations (See Reference 71, p. 48, Figure 24).

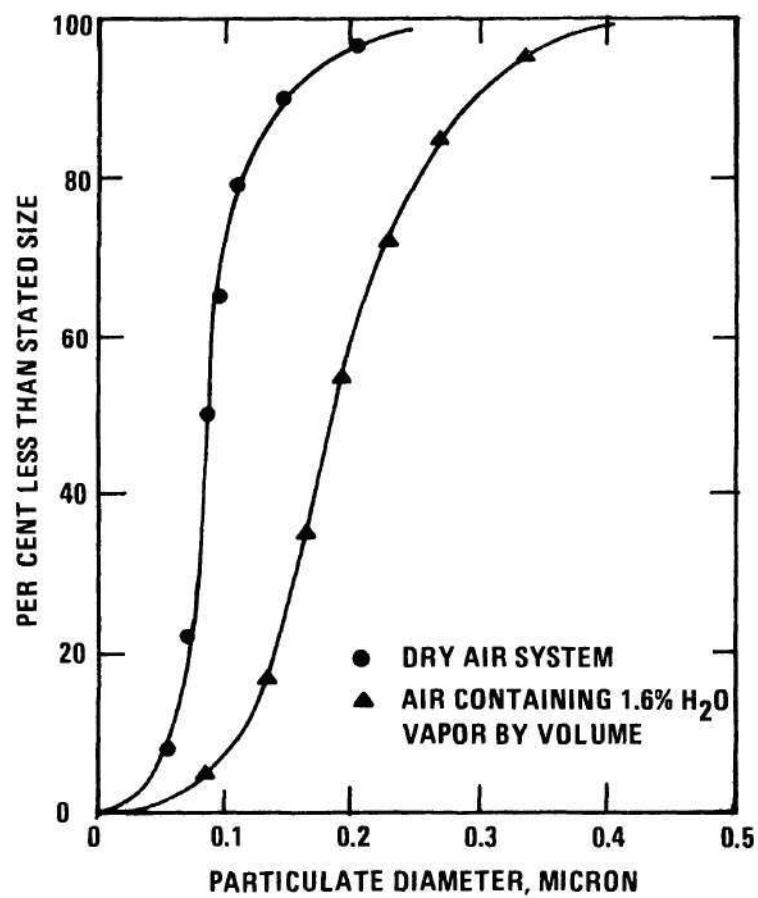


Figure 50. Comparison Between Size Distributions of X-ray Induced Particulates Formed in Dry and Humidified Air Containing 10 per cent Acetylene (See Reference 71, p. 55, Figure 30).

Watson and Kaufman⁽¹³³⁾ reported particle size distribution data from α -ray induced cuprene aerosols. Diameters ranged from about 3000 to 10,000 Å in the oxidized sample, and from about 1000 to 13,000 Å in the unoxidized sample. These sizes are in general agreement with those of this study although they were produced differently. The particle sizes reported here are presented in the form of either frequency or cumulative distributions. They also show a fairly straight line when plotted as logarithmic-probability graphs.

Ultraviolet Irradiation Products

Particulate growth began after induction periods, one of about 200 seconds for benzene-air mixtures and one ranging between 120 and 300 seconds for benzene-air mixtures with the addition of nitric oxide or water vapor. This is revealed by the trends of aerosol mass concentration on previous figures. In addition, the number of nonvolatile particulates also increased as shown by aerosol deposition on electron microscope grids. However, size distributions of nonvolatile particulates measured after different irradiation periods suggest little change in particulate growth. As shown on Figure 51, only the larger sizes seem to be altered as reaction proceeds. One explanation could be that the particulates were more fluid during the early stage of the reaction and flattened on contact with the carbon film of the electron microscope grid and thus distorted the size measurements. It could also be due to a photosensitized cleavage of aromatic rings and further oxidation of unreacted double bonds in the presence of high concentrations of atomic oxygen and ozone. Presumably low molecular weight, volatile compounds such as formaldehyde and carbon monoxide were formed but evaporated.

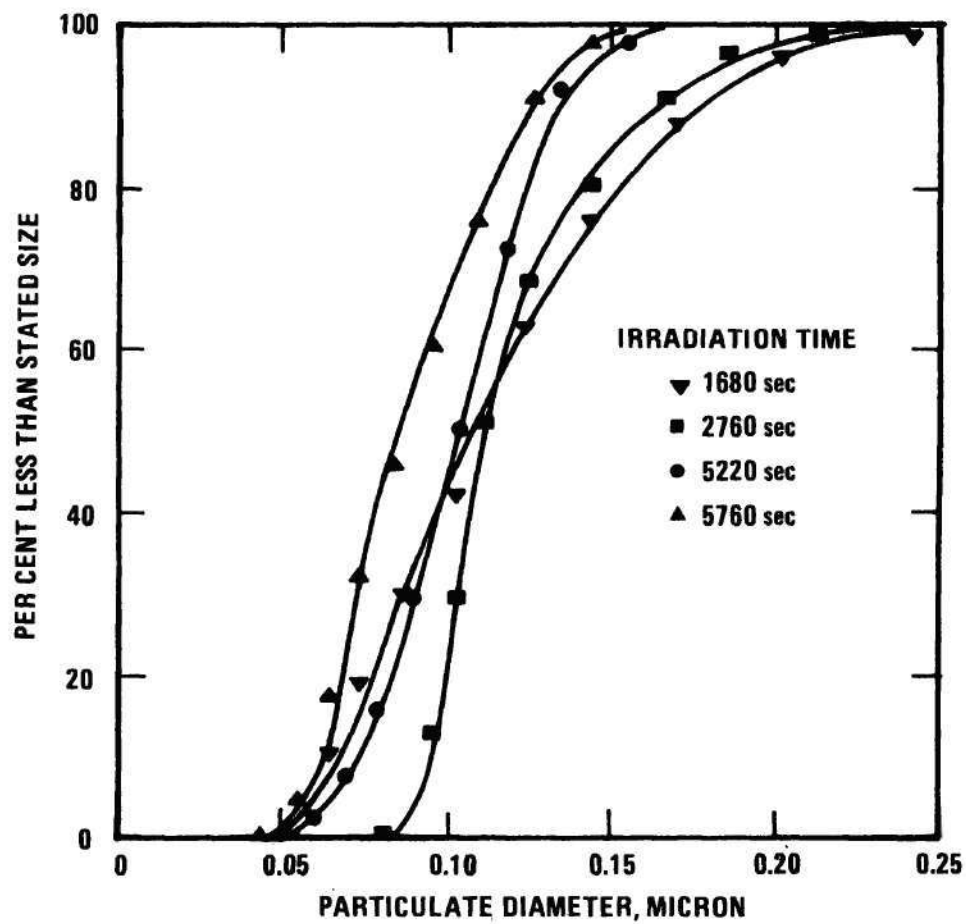


Figure 51. Size Distributions of Nonvolatile Photochemical Particulates Sampled During Different Irradiation Periods from Air Containing 10 Parts Per Million Benzene.

Particulate size distributions as shown by Figure 52 were also obtained during three irradiation periods for benzene-nitric oxide-air mixtures. The size distributions again were very similar, although the mass concentration increased significantly in the period between 30 and 60 minutes and decreased afterward as shown on Figure 28. Size measurements were made on the basis of individual particulates, and agglomerates were not considered. As shown by the electron micrographs of particulates sampled in the late stages of photochemical reactions (Figures 34, 35, 39 and 40) coagulation was observed frequently. Another investigator⁽⁶⁵⁾ also reported as a function of time the size distribution of photochemical aerosols produced using ambient atmospheric air and natural solar radiation. That work suggested that the particulate growth process was governed by diffusion controlled vapor deposition and by coagulation, a result not contrary to those reported here for humidified systems.

Nucleation Phenomena

Three phenomena bearing on nucleation are significant here. First, multicomponent systems were involved. As mentioned in the preceding two chapters, many oxygenated compounds, especially aldehydic ones, were detected in the gas phase. The second feature was the presence of very reactive species such as free radicals. The last was the presence of gaseous ions.⁽¹³⁰⁾ A thermodynamic model, the Volmer-Becker-Doering theory⁽¹³⁸⁾ for instance, probably could only be applied conceptually to this case because of its extreme complexity. Commenting on the nucleation of photochemical smog, Hidy and coworkers⁽⁶²⁾ have stated as follows:

"An interesting question must be raised in evaluating the heterogeneous nucleation mechanism. There is very little information available on the hydrocarbon products produced in photochemical

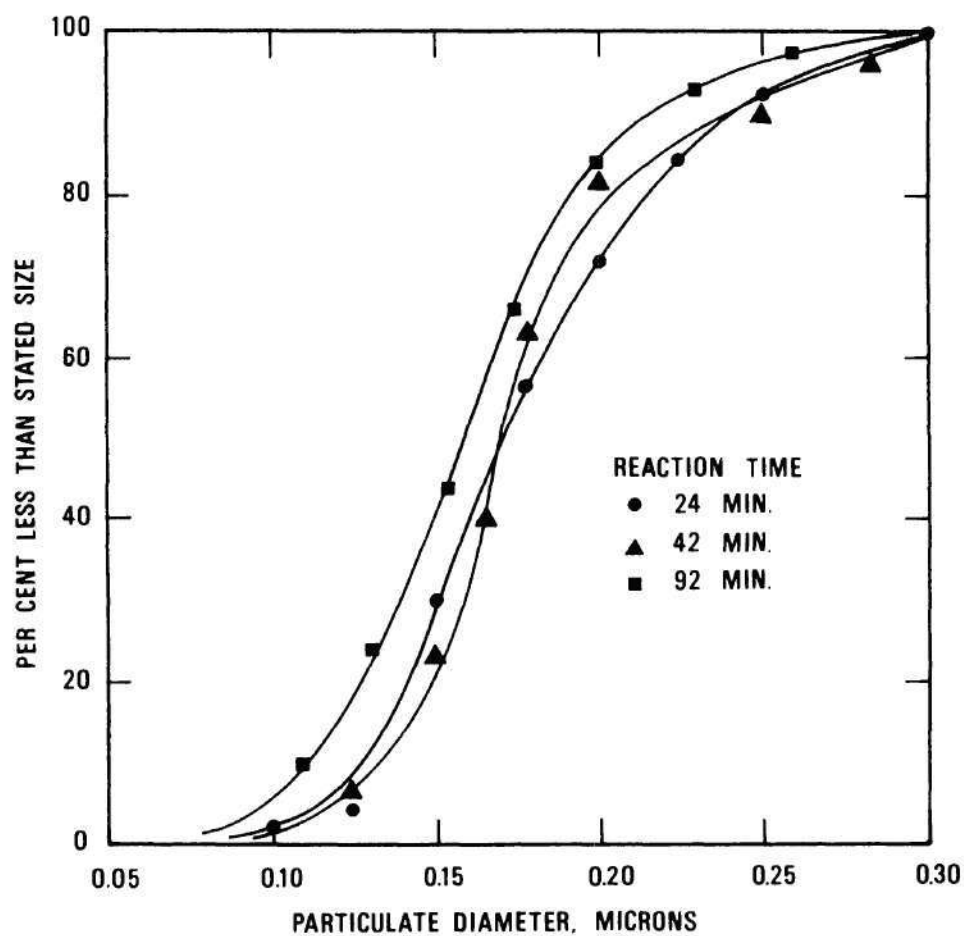


Figure 52. Size Distributions of Nonvolatile Photochemical Particulates with Addition of Nitric Oxide Sampled during Different Irradiation Periods.

smog, but Leighton's view and more recent evaluations suggest that the reactive hydrocarbons undergo oxidation reactions in the gas phase in preference to polymerization. This question of chemical mechanisms is a crucial one and must be answered at least partially by controlled laboratory studies before the photochemical aerosol behavior can be understood."

The Onset of Particulate Formation

Although particulates were the most abundant product from ultraviolet irradiations, measurements showed that these appeared only after an induction period of 140 to 210 seconds for both "dry" and humidified benzene-air mixtures. Figure 53 indicates the beginning of particulate formation for three systems. Induction times for benzene-air mixtures without water vapor were very close to the ones for mixtures with 0.24 ppm nitric oxide.

By comparison, the appearance of particulates in systems with a relative humidity of 25.2 per cent began at about 140 seconds or about 30 seconds earlier than ones with a relative humidity of 8.8 per cent. The latter system had a higher rate of aerosol mass production during early stages, but ultimately ended with a lower mass concentration after 1000 to 3000 seconds. In general, shorter times are required for the onset of particulate formation in reaction systems containing water vapor.

Significant production of particulates from photochemical reactions of benzene-nitric oxide-air mixtures started only after more than half of the NO had been converted into NO_2 . This is consistent with other reports⁽¹³⁾⁽¹³⁶⁾ that the formation of both nuclei and aerosol did not occur rapidly until the NO_2 concentration peaked and a very low NO concentration had been reached. Since many photochemical smog studies indicate the production and accumulation of reactive intermediates such as alkyl and alkoxy radicals after most of the NO has been oxidized into NO_2 , particulates may well be products from reactions among highly reactive species.

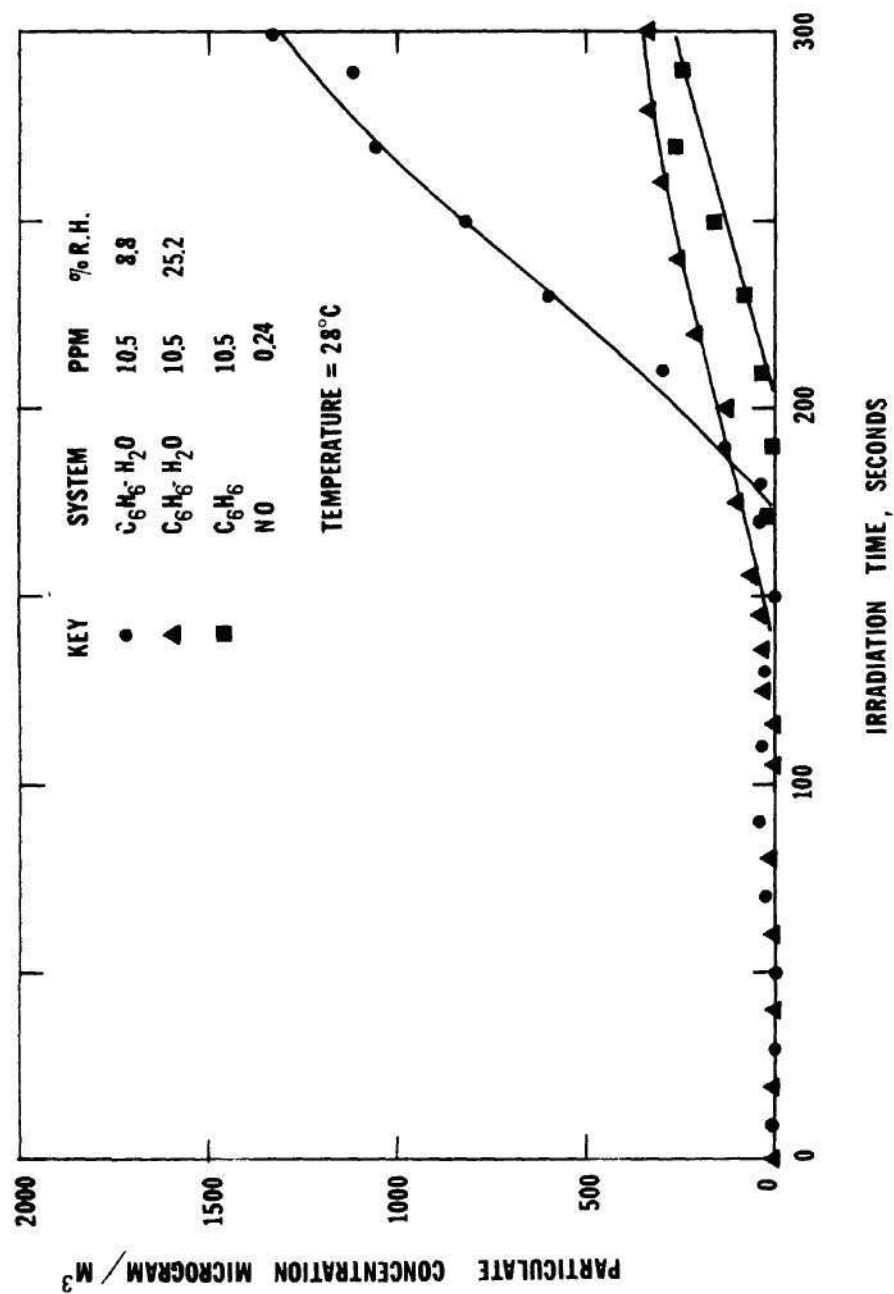


Figure 53. The Onset of Formation of Photochemical Particulates.

As described in preceding chapters, no apparent induction period, or a very short one at least, was observed for benzene-nitric oxide-air mixtures irradiated with ultraviolet light. Therefore, short induction periods and early formation of particulates is favored by increasing nitric oxide concentrations.

Formation of Nuclei and the Characteristics of Nucleation

A cloud chamber or nuclei counting facility was not available to this effort for the measurement of nuclei concentration. For purposes of illustrating the formation of nuclei, part of the research of Altshuller, *et al.*,⁽¹³⁾ is reproduced in Figure 54. Nuclei in amounts of 10^3 - 10^5 per cubic centimeter were measured for trans-2-butene-NO mixtures after most of the NO had been converted into NO₂. However, aerosols with particle sizes large enough to make feasible light scattering measurements or to permit mass or weight detection were not produced. Nuclei in the same number range were also detected during the ultraviolet irradiation of 1,3,5 trimethyl benzene-NO and toluene-NO mixtures. Large amounts of aerosol were detected from these two systems. The simultaneous onset of aerosol production and the decrease in nuclei concentration in Figure 54 is worthy of note.

Nucleation in its phenomenological aspects is illustrated by a plot of nuclei concentration during an irradiation period is shown by Figure 55. Nuclei are considered formed after a "waiting", or induction period, when their size has grown to exceed that of a critical embryo. In the cases here, there exist both reactive species and gaseous ions, so the mechanism is undoubtedly more complex than when nucleation is from an single or binary vapor in an inert gaseous atmosphere. Evolution of nuclei probably involves reactions of these highly reactive species. Nucleation either starts at

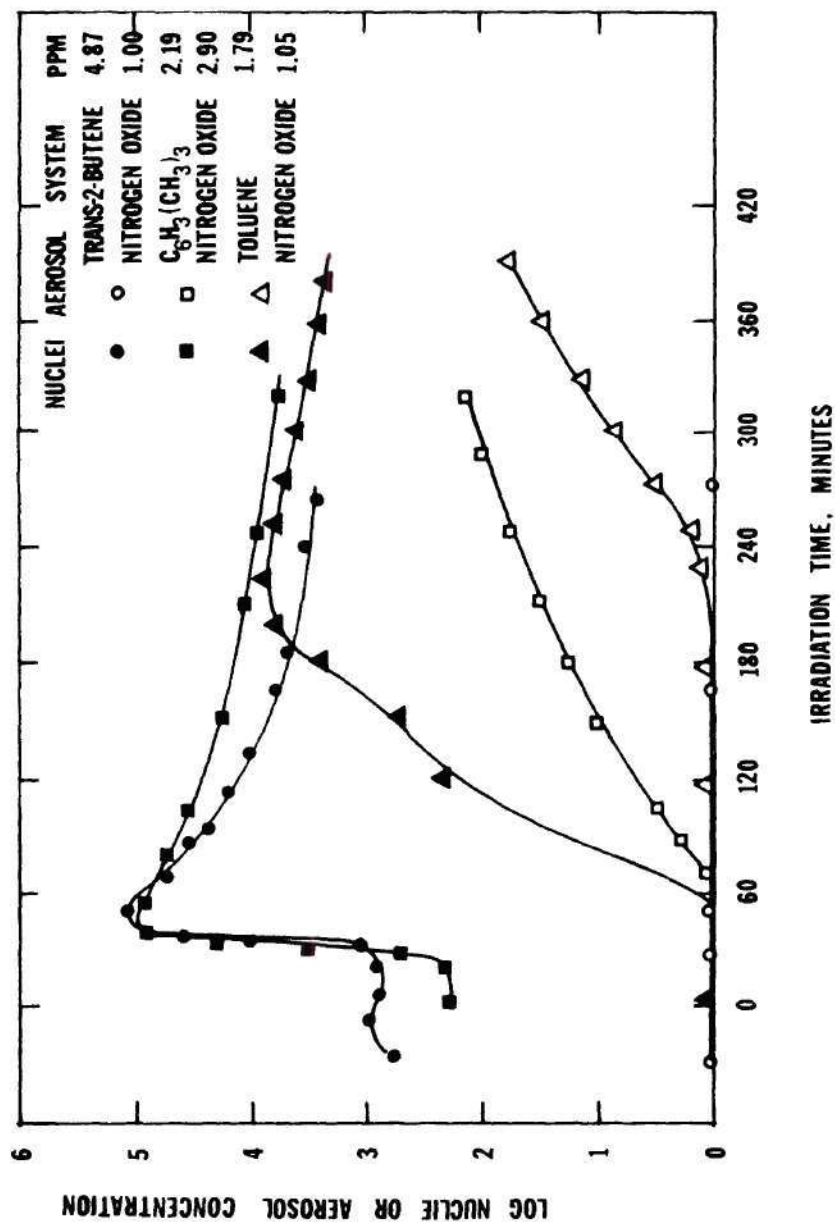


Figure 54. Concentration Profile of Condensation Nuclei and Aerosols During Ultraviolet Irradiation of Trans-2-butene-Nitric Oxide-Air, Toluene-Nitric Oxide-Air, and 1,3,5-trimethylbenzene-Nitric Oxide-Air Mixtures (See Reference 13, p.88 Figure 2).

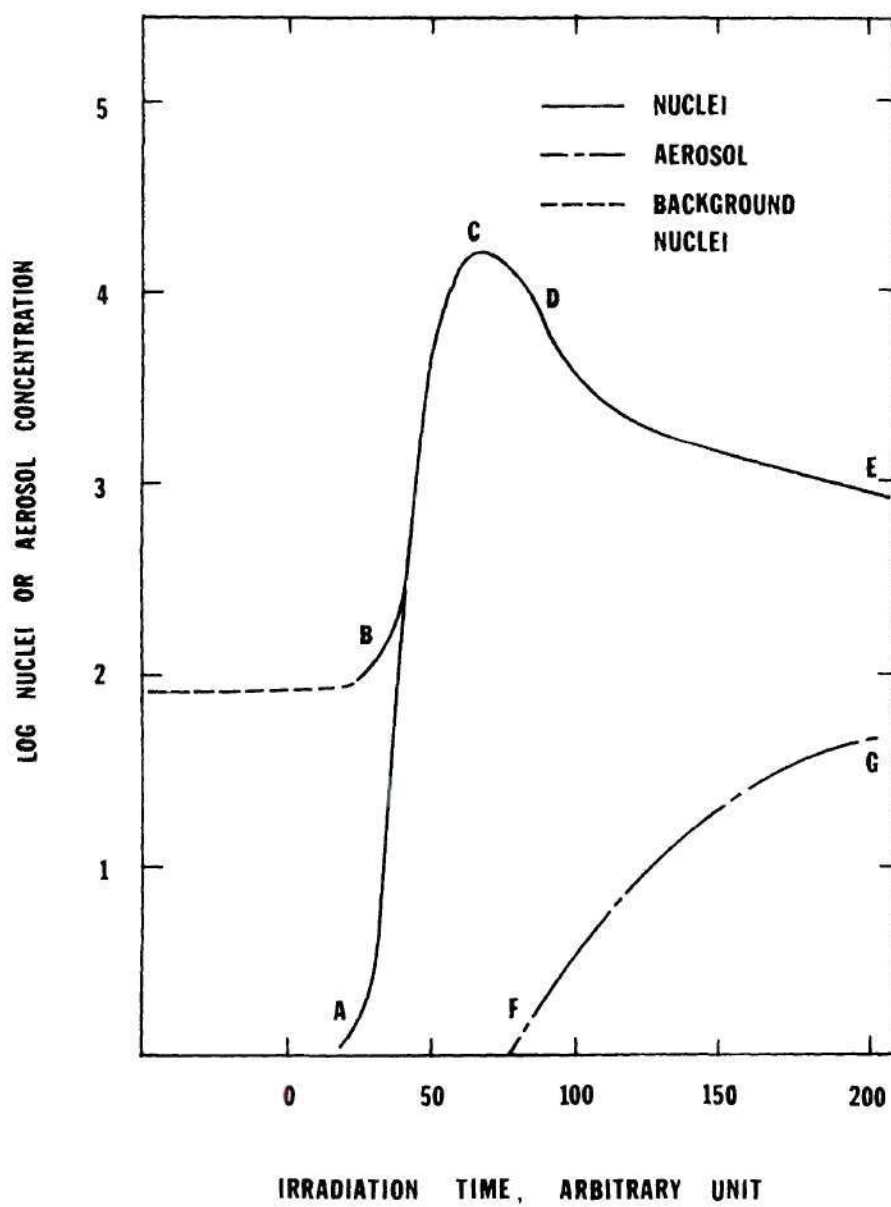


Figure 55. Characteristics of Nucleation.

point A when the gas is particle- or nuclei-free and at point B when there are background nuclei. In either event, production of nuclei continues to a peak at point C. The slope of the line AC is quite steep for some photochemical induced nuclei formations⁽⁶⁵⁾ and the same is probably also true for radiolytic systems.⁽¹⁹⁾ Point C probably corresponds to the starting point of fast hydrocarbon depletion, where, due to the high concentration of reactive intermediates or supersaturated products, the formation of aerosol competes with that of nuclei. This effect and also the coagulation of nuclei cause a decrease in nuclei number to point D. As irradiation proceeds, the concentration of aerosol increases rapidly from point F to point G, while that of nuclei reduces to point E.

Nucleation and Growth by Condensation

Volatile particulates were formed by the condensation of supersaturated gaseous products in some cases.⁽²⁴⁾ More of these aerosol particulates probably formed in very earlier stages of photochemical reaction. They were important products and likely predominant ones in humidified photochemical reaction systems such as those of cyclohexene-air and α -pinene-air. The condensation of supersaturated vapors on nuclei to form aerosols is supported by certain experimental findings. First, the evaporation of some particulates was observed under ambient conditions or vacuum, and second, evaporation and degradation of particulates were also noticed under further ultraviolet light irradiation (see Figure 31). This indicates that some products were not polymeric substances but probably consisted of vapors of condensable aldehydes, ketones, and other oxygenated compounds having low vapor pressures. Under attack by oxidizing agents such as ozone and atomic oxygen, these would undergo oxidation to form both gaseous and

nonvolatile products. That volatile aerosols became less prevalent as irradiation continued was noted in conjunction with electron microscopic examinations. This could be explained by an oxidation reaction or by the addition of reactive species through the gas-aerosol interface to form "oxygen saturated" polymeric substances.

Volmer, Becker, and Döring⁽¹³⁸⁾ developed the classical theory of homogeneous nucleation. In the absence of nuclei, an embryo droplet of radius r , containing N molecules, and having surface tension γ is formed by random collision of monomeric vapor molecules at supersaturation ratio S . The free energy change corresponding the formation of this embryo is

$$\Delta G = 4\pi r^2 \gamma - V k T \ln S \quad (6.1)$$

where
$$V = \frac{4}{3} \pi r^3 M \quad (6.2)$$

Maximizing Equation (6.1) with respect to r gives the size of the critical embryo, r^*

$$r^* = \frac{2\gamma}{M k T \ln S} \quad (6.3)$$

where M is the number of molecules per cubic centimeter of liquid. An embryo grows into a droplet when it attains a size greater than r^* , and the free energy increase corresponding to $r = r^*$ is

$$\Delta G^* = \frac{16\pi\gamma^3}{3(MkT\ln S)^2} \quad (6.4)$$

For condensation on an inert particle, i.e., heterogeneous nucleation, G^* only differs from Equation (6.4) by the factor $(2 + \cos\theta)(1 - \cos\theta)^2/4$ which is smaller than unity. The contact angle is given by the symbol θ .

The metastable equilibrium concentration of critical nuclei in terms of the Van't Hoff reaction isotherm is then

$$N_i^* = N_1 \exp(-\Delta G^*/kT) \quad (6.5)$$

where N_i^* is the concentration of clusters containing i molecules, and N_1 is the monomer concentration equal to p/kT . The nucleation rate is expressed⁽²²⁾ by

$$I = \frac{dN_i^*}{dt} = K_N N_1 \exp(-\Delta G^*/kT) \quad (6.6)$$

where K_N is a factor expressing the chance of collision with and capture by a monomer of a critical nuclei. The application of the above equations to the systems here is still far from reality because of the inadequacy of physical data and the difficulties of identification of products.

Nucleation in photochemical systems probably starts with the forming of nuclei from chemical interactions and combinations of reactive radicals and unsaturated hydrocarbon molecules or from products which possess low saturated vapor pressures. Possible products include high molecular weight phenyl ketones, or quinones; fluorenones; and polyenic dialdehydes. Once nuclei are formed other chemical species with lower saturation ratios will add to them through heterogeneous nucleation.

Gas-Particulate Interaction and Polymerization⁽²⁹⁾

Microphysical measurements and mass spectrometric analyses on all x-ray induced particulates and most of the ultraviolet light induced particulates from dry-air systems described here revealed them to have extremely low vapor pressures and to be polymeric substances with chain lengths of at least 10 carbon atoms. This indicates particulate nucleation and growth

is more likely chemical in nature than a result of condensation. In all photochemical reaction systems, the production of particulates reached a maximum coincident with the most rapid depletion of hydrocarbon and when about 90 per cent of the hydrocarbon had been consumed. Processes which account for the disappearance of hydrocarbons are classified as follows:

(1) The hydrocarbon molecules first form free radicals and excited species, the process being described in Chapter V. Chemical interaction and combination of free radicals, excited molecules, and other reactive species then form small nuclei. (2) This is followed by heterogeneous photochemical reactions, presumably largely oxidation ones, on the nuclei and already formed particulates. The mechanism is probably a kind of polymerization, the products being formed and becoming attached to the surface of existing particulates due to the forces of chemical affinity. Such interfacial reactions and the effects of nucleating agents were investigated by Goetz and Pueschel,⁽⁵²⁾ with results supporting the idea that particulate formation is due to chemical reactions at the surfaces of airborne particles and nuclei and that the physical properties of the nucleating agents control the rates of formation of the particulates. (3) Finally, high molecular weight aldehydic substances are formed, leading to volatile and unstable aerosols by condensation. Gaseous products such as CO, CO₂, and low molecular weight aldehydes constitute the remaining species.

CHAPTER VII

CONCLUSIONS AND RECOMMENDATIONS

Conclusions

Chemical Composition

Infrared and mass spectrometric analysis provide most of the information on the chemical composition of the particulate products. The infrared spectra showed very strong carbonyl absorption bands at 1710-1730 cm^{-1} , hydroxyl absorption bands at 3100-3500 cm^{-1} , and some weak aliphatic and aromatic absorption bands. The mass spectra revealed ion fragment patterns for aldehydes, ketones, quinones, and carboxylic acids and indicated that some components can have molecular weights of 200 or higher and consist of 10 or more carbon atoms. These particulate products are thus undoubtedly polymeric substances.

From the x-ray irradiation of benzene vapor in nitrogen rather than in air, it was found that infrared absorption bands characteristic of carbonyl and hydroxyl groups diminished while aromatic bands remained. This reaction was inhibited under ultraviolet irradiation. The importance of radiation induced oxidation was thus revealed.

X-ray Induced Oxidation Processes

X-rays ionize air and hydrocarbon molecules which leads to the formation of a variety of ionized atoms and molecules, free radicals, and excited species. The interaction between these reactive ions and atoms such as O^+ , N^+ , N_2^+ , N , and O causes the formation of ozone and nitric oxide during irradiation. Oxidizing agents such as atomic, molecular, and ionized

oxygen and ozone react with hydrocarbon molecules and free radicals to create oxygen-containing intermediates which enter further complex recombination reactions, forming the high molecular weight particulate products. Gaseous aldehydes are produced from the acetylene-air system. The yield of particulates was found to increase with increasing hydrocarbon concentration, irradiation time, and x-ray intensity. A rapid increase in the yield of particulates was found when very small amounts of water vapor were added to the air, the maximum yield occurring at about 5 per cent relative humidity.

Photochemical Oxidation Processes

Photochemical first-order reaction rate constants for cyclohexene, benzene, toluene, and o-xylene separately in air were determined at the 10 ppm level by a photochemical smog chamber method to be 1.9×10^{-3} , 1.0×10^{-3} , 1.5×10^{-3} , and $2.0 \times 10^{-3} \text{ sec}^{-1}$, respectively. Oxygen is required for these reaction systems as indicated by the inhibition of aerosol formation and the absence of hydrocarbon disappearance when nitrogen is used instead of air. At low concentrations of oxygen in nitrogen the quantitative production of aerosol is roughly proportional to the oxygen content. Production of ozone was found to occur mostly by a combination of molecular and atomic oxygen, the latter being formed by photolysis of oxygen at 2000-2424 Å. Benzene undergoes very slow reaction with ozone, but rapid disappearance of benzene was found in the presence of ultraviolet light due to fast reactions with atomic oxygen and other free radical intermediates. In general, hydrocarbon molecules react with atomic oxygen and ozone to form oxygen-containing radicals such as alkoxyl and peroxyalkyl that recombine and add to hydrocarbon molecules through a series of complex reactions. Final products included large amounts of aliphatic aldehydes and highly oxygenated particulates consisting of 63 to 81 per cent of the reacted carbon atoms.

When nitric oxide was present, it was found that particulate formation, which appears only to begin after half the nitric oxide has been converted into nitrogen dioxide, is much enhanced by the presence and participation of nitrogen oxides. The maximum particle concentration was 2.4 times that from systems without nitrogen oxides. The highly oxygenated products consist of approximately 7 oxygen atoms and one nitrogen-containing group for each reacted benzene molecule. The presence of water vapor greatly accelerates benzene disappearance and enhances aerosol formation by a factor of about five, although infrared spectra show little or no change in chemical composition.

Microphysical Processes and Properties

The particulates are relatively insoluble, nonvolatile, and thermally stable. Their average size and mass concentration increase with increasing irradiation time, aging time, and hydrocarbon concentration. X-ray induced particles show size distributions of the logarithmic normal type. The presence of nitrogen dioxide and water vapor promote the early onset of particulate formation. The more volatile particulates form by condensation on nuclei from supersaturated gaseous products. some nonvolatile polymeric particulates form on nuclei by chemical reaction, i.e., through interaction and combination of free radicals, hydrocarbon molecules, and other reactive intermediates on nuclei and already-formed particulate surfaces.

Recommendations

Two series of experiments which should prove beneficial in understanding the basic physical processes are :

1. Determine experimentally the coagulation rates and rate constants for both radiochemically and photochemically produced particulates. Preliminary studies conducted in conjunction with this investigation on the coagulation of photochemical aerosols from a benzene-air system indicated that the observed coagulation constants were in fair agreement with theoretical ones calculated from Smoluchowski's equation.⁽⁴⁸⁾⁽⁹⁷⁾ The extension of this calculation to the coagulation of chemically induced particles certainly would be of value in understanding the physical processes of photochemical smog.

2. Measure condensation nuclei concentrations and the rate of nuclei formation as functions of irradiation time, hydrocarbon concentration, humidity, and nitrogen and sulfur oxide content. The onset of nuclei formation from radiation induced reactions and their evolution and growth to fine particulates might be followed with a condensation nuclei counter. The method might be used also for nuclei formation by radical-radical combinations and radical-hydrocarbon interactions. Specific radicals can be produced by the photolysis of selected ketones and aldehydes after they have been identified in the reaction systems. For example, photolysis of acrolein may lead to the formation of ultrafine polymeric particles, and a condensation nuclei counter could serve as a detector for the onset and presence of such nuclei.

Two analytical methods are suggested for a more complete determination of particulate and gaseous products and possibly a more complete derivation of the reaction mechanisms.

1. Determine the chemical composition of particulates as a function of irradiation time, particle size, initial concentration of nitrogen oxides

and sulfur oxides, etc. by elemental analysis. Since the chemical constituents of photochemical aerosols are known in only a few cases, the employment of microanalytical chemical techniques would be helpful in resolving the atomic percentages of C, H, O, and N, thereby yielding some very useful data on reaction mechanisms.

2. Utilize a high resolution mass spectrometer coupled directly to the reaction chamber for the mass spectral analysis of both particulate and gaseous products from photochemical reaction systems. Certain other modifications may be possible. An absolute filter or similar device might be employed to separate the gaseous products from the particulate ones. Since the yield of gaseous products is very low, a cold trap at liquid nitrogen temperature could collect this product in a concentrated form. Finally, a combination of mass spectral analysis and a radioisotope tracer technique might be found advantageous in deducing reaction mechanisms.

APPENDIX A

GAS ANALYTICAL METHODS

Gas Chromatography and Hydrocarbon Analyzer

At the beginning of this study when the x-ray irradiation experiments were performed, Perkin-Elmer, Models 800 and 900, and a Hewlett-Packard, Model 776, gas chromatographs with flame ionization detectors⁽¹¹⁾⁽⁹²⁾ were employed to measure and calibrate the concentrations of the hydrocarbon components in the gas samples. The hydrocarbons, mainly aromatic hydrocarbons, were analyzed on copper columns containing packings of apiezon or tricresyl phosphate materials. The operating temperature was between 80° to 130°C. The carrier gas was dry nitrogen. Quantitative calibrations were made by either generating known quantities of hydrocarbons from a diffusion cell or by preparing a vapor mixture of the single compound and air in a large glass bottle.

When the experiments involving samples of hydrocarbons in the parts per million range required an improved response to detect possible aldehydic products, the Hewlett-Packard Model 776 chromatograph was modified with a 42 cc, U-shape gas sampler. Another column was constructed from a 10 ft. long, 1/4 in. O.D. glass tube containing 15 per cent carbowax on Teflon beads. The chromatograms taken while photochemical reactions were in progress showed methane to be the predominant constituent of the background along with the benzene. Some small and unidentified peaks having short retention times between the values for those of acetaldehyde and

propionaldehyde were also observed. Further investigation was limited by the sensitivity of the gas chromatograph even though aldehydic compounds were indicated to be the reaction products by spectrophotometry.

In later stages of this work, a flame ionization hydrocarbon analyzer, Beckman Model 400, was purchased which detected hydrocarbon concentrations down to 0.01 ppm. This equipment used zero-grade air and zero-grade hydrogen as oxidant and fuel, respectively, and was calibrated with Matheson calibration gas containing 8 ppm propane in zero-grade air. Both the gas chromatograph and the hydrocarbon analyzer were employed to detect the concentration of hydrocarbons, especially the concentration of benzene during the course of a photochemical reaction. The readings of the hydrocarbon analyzer were compared with the output of the gas chromatograph; the values were fairly close to one another.

Analysis of Aliphatic Aldehydes⁽¹⁾

The sample was drawn at 200 cc/min through a rotary vane or a fritted scrubber. The absorption solution was distilled water with the addition of 0.01 per cent Kodak Photo-Flo 200 as wetting agent. To 5 cc of the absorption solution, 5 cc of reagent A and 2 cc of reagent B were added. Reagent A was a 2.0 mole methylamine hydrochloride and 0.20 mole sodium pyrophosphate aqueous solution. Reagent B was a 0.01 mole o-amino-benzaldehyde aqueous solution. The absorbance at 440 mμ was then measured.

The production of o-aminobenzaldehyde⁽¹¹⁹⁾ was carried out as follows: 5 grams of o-nitrobenzaldehyde, 100 cc distilled water, and 100 grams ferrous sulfate heptahydrate were brought to a boil, then 50 cc of ammonium hydroxide was added. Later the mixture was distilled. The distillate was

chilled in an ice bath to crystallize the o-aminobenzaldehyde product. The crystal product was finally separated by filtration and stored at -20°C .

Analysis of Nitrogen Dioxide⁽¹¹¹⁾⁽¹¹²⁾

The colorimetric analyzer used here was a WACO air analyzer, Model 300 A. The absorption solution contained 0.05 per cent N-(1-naphthyl)-ethylenediamine dihydrochloride and sulfanilamide. First, the analyzer and a Sargent recorder were turned on and warmed for 30 minutes. Then the flow rate of the gas stream was adjusted. The gaseous sample passed through a rotary vane scrubber where nitrogen dioxide was supposed to be completely absorbed by the solution. Afterwards, the absorption solution flowed through the colorimeter, the light extinction being measured against fresh reagent and indicated by the recorder. Calibration was made by comparison with samples of nitrogen dioxide of known concentration.

Analysis of Ozone and Oxidants⁽³⁵⁾⁽³⁸⁾

Ozone and oxidant determinations by iodometry were performed in accord with the following procedures: the gas sample was passed at 200 cc/min through a rotary vane scrubber containing 10 cc of an aqueous solution of 0.1 gram KI and 0.04 gram NaOH. To eliminate the disturbing influence of NO_2 , about 3 cc of acetic acid (1:5) was pipetted into the solution until a pH value of 3.8 was reached. Then the volume of solution was adjusted to 25 cc with distilled water and the absorbance, or extinction, at 352 m μ was measured by either a Beckman DU or Model B spectrophotometer. The calibration curve for the determination was plotted using the reagent after adding standard KIO_3 solution to the absorption solution and acidifying with acetic acid.

APPENDIX B

MATERIALS AND CHEMICALS

The air used in this study was either zero-grade or dry-grade as supplied in cylinders by the Matheson Company. The hydrocarbon content of the zero-grade air was actually less than 1.0 ppm CH_4 hydrocarbon. The dry-grade air was further treated by passage through a filter made by the Gould Company which consisted of molecular sieve, silica gel, and activated charcoal. This generally reduced the hydrocarbon content to less than 1.0 ppm with a maximum value of 2.0 ppm. The hydrocarbon content was mainly light hydrocarbons. Methane and smaller amount of ethane were the major constituents as shown by gas chromatographic analysis. Air and all gaseous mixtures were filtered through a membrane filter, the G.S. type made by the Millipore Corp., before entering the x-ray and UV light irradiation chambers.

The nitrogen used in the photolysis of NO_2 was also zero grade, containing less than 0.5 ppm CH_4 hydrocarbon and less than 4 ppm oxygen. The nitrogen and hydrogen employed as the carrier gas and fuel for the gas chromatographs were both dry grade and obtained in cylinders from Air Products and Chemicals, Inc. Zero-grade air, hydrogen, and the 8 ppm propane calibration mixture were supplied by the Matheson Company. They were used with the flame ionization hydrocarbon analyzer.

Nitric oxide of 98.5 per cent purity and the nitrogen dioxide of 99.5 per cent purity were obtained from the Matheson Company. For the tests in which very low concentration of nitric oxide were needed, the

volume of nitric oxide was extracted from a mixture having 490 ppm NO in nitrogen and supplied by Air Products and Chemicals, Inc.

The acetylene employed was a purified grade having a minimum purity of 99.6 per cent and supplied by the Matheson Company. The cyclohexene was pure grade with 99.5 per cent purity; it was supplied by the Phillips Petroleum Company.

Research-grade benzene, toluene, and ortho-xylene having 99.99 per cent purity and containing toluene, benzene, and para-xylene, respectively, as the most abundant impurities were obtained from the Phillips Petroleum Company. The Eastman Kodak Company supplied the α -pinene.

Chemicals used in preparation of working and standard solutions for the acid-potassium iodide method for determining ozone were potassium iodide, potassium iodate, sodium hydroxide, and glacial acetic acid; all were reagent grade and were supplied by the Fisher Scientific Company.

Two reagents employed in the analysis of aliphatic aldehydes were methylamine hydrochloride, reagent grade, supplied by the Fisher Scientific Company, and sodium pyrophosphate, "Baker Analyzed" reagent grade, supplied by the J. T. Baker Chemical Company. The third reagent, o-aminobenzaldehyde was prepared by a modified method of Smith and Opie.⁽¹¹⁹⁾ The chemicals used in this synthesis were o-nitrobenzaldehyde of 95-99 per cent purity supplied by K & K Laboratories, Inc.; ammonia hydroxide, reagent grade, by the Fisher Scientific Company; and ferrous sulfate heptahydrate, reagent grade, by the J. T. Baker Chemical Company. Propionaldehyde, obtained from the Eastman Kodak Company, was used as the aldehyde standard; it was further purified by distillation in a packed column.

The concentration of NO₂ was determined with a Saltzman reagent which

contained N-1 (Naphthyl) ethylenediamine hydrochloride supplied by the Fisher Scientific Company. Another absorption solution consisted of sulfanilamide obtained from the Eastman Kodak Company and hydrochloric acid, "Baker Analyzed" reagent grade, obtained from the J. T. Baker Chemical Company.

APPENDIX C

NOMENCLATURE

A	Cross-sectional area
C	transient concentration
C ₀	original concentration
c	velocity of light
D _A	diffusivity of component A in Air
E	energy of a quantum of radiation
G	Gibbs free energy
h	Planck's constant
I	nucleation rate
K	rate constant of chemical reaction
K _a	rate of light absorption
K _d	first-order rate constant for NO ₂ photolysis
K _N	factor of chance of collision and capture of a monomer by critical nuclei
k	Boltzmann constant
L	length of diffusion path
M	number of molecules per cubic centimeter of liquid
N _i	concentration of clusters containing i molecules
r	radius of particulate
r*	radius of critical embryo
P	total pressure or atmospheric pressure

P_A	vapor pressure of component A
Q	flow rate
R	alkyl or aryl radicals
R_{GAS}	gas law constant
S	supersaturation ratio
t	time
T	temperature
W	mass transfer rate by volume

Greek Letters

γ	surface tension
θ	contact angle
λ	wavelength
ν	frequency
ϕ	primary quantum yield

BIBLIOGRAPHY

1. Albrecht, A. M., W. I. Scher, Jr., and H. J. Vogel, "Determination of Aliphatic Aldehydes by Spectrophotometry," Anal. Chem., 34, 398-400 (1962).
2. Alley, F. C., and L. A. Ripperton, "The Effect of Temperature on Photochemical Oxidant Production in a Bench Reaction System," J. Air Poll. Control Assoc., 11, 581-584 (1961).
3. Alley, F. C., G. B. Martin, and W. H. Ponder, "Apparent Rate Constants and Activation Energies for the Photochemical Decomposition of Various Olefins," J. Air Poll. Control Assoc., 15, 348-350 (1965).
4. Altshuller, A. P., "An Evaluation of Techniques for the Determination of the Photochemical Reactivity of Organic Emissions," J. Air Poll. Control Assoc., 16, 257-260 (1965).
5. Altshuller, A. P., "Reactivity of Organic Substances in Atmospheric Photo-oxidation Reactions," Intl. J. Air Wat. Poll., 10, 713-733 (1966).
6. Altshuller, A. P., and J. J. Bufalini, "Photochemical Aspects of Air Pollution: A Review," Photochem. and Photobio., 4, 97-146 (1965).
7. Altshuller, A. P., and I. R. Cohen, "Atmospheric Photo-oxidation of the Ethylene-Nitric Oxide System," Intl. J. Air Wat. Poll., 8, 611-632 (1964).
8. Altshuller, A. P., and I. R. Cohen, "Structural Effects on the Rate of Nitrogen Dioxide Formation in the Photo-oxidation of Organic Compound-Nitric Oxide Mixtures in Air," Intl. J. Air Wat. Poll., 1, 787-797 (1963).
9. Altshuller, A. P., I. R. Cohen, and T. C. Purcell, "Photo-oxidation of Hydrocarbons in the Presence of Aliphatic Aldehydes," Science, 156, 937-939 (1967).
10. Altshuller, A. P., I. R. Cohen, S. F. Sleva and S. L. Kopozynski, "Air Pollution Photo-oxidation of Aromatic Hydrocarbons," Science, 138, 442-443 (1962).
11. Altshuller, A. P., and C. A. Clemons, "Gas Chromatographic Analysis of Aromatic Hydrocarbons at Atmospheric Concentrations Using Flame Ionization Detection," Anal. Chem., 34, 466-471 (1962).

12. Altshuller, A. P., and P. W. Leach, "Reactivity of Aromatic Hydrocarbons in Irradiated Automobile Exhaust," Intl. J. Air Wat. Poll., 8, 37-42 (1964).
13. Altshuller, A. P., D. L. Klosterman, P. W. Leach, I. J. Hindaw, and J. E. Sigsby, Jr., "Products and Biological Effects from Irradiation of Nitrogen Oxides with Hydrocarbons or Aldehydes under Dynamic Conditions," Intl. J. Air Wat. Poll., 10, 81-98 (1966).
14. Avramenko, L. I. and R. V. Kolesnikova, "Mechanisms and Rate Constants of Elementary Gas Phase Reactions Involving Hydroxyl and Oxygen Atoms," Advances in Photochemistry, edited by Noyes, W. A., Jr., G. S. Hammond, and J. N. Pitts, Jr., Vol. 2, pp 25-62, Interscience, New York (1964).
15. Avramenko, L. I., R. V. Kolesnikova, G. I. Savinova, "The Reaction Constants for the Reactions of Oxygen Atom with Cyclohexene and C_6H_6 ," Ser. Khim. Izv. Akad Naak SSSR 1, 28-35 (1965).
16. Barlage, W. B., Jr. and F. C. Alley, "Sampling and Mass Spectrometer Analysis of Reaction Products from the Photochemical Decomposition of Various Olefins," J. Air Poll. Control Assoc., 15, 235-238 (1965).
17. Beynon, J. H., R. A. Saunders and A. E. Williams, The Mass Spectra of Organic Molecules, Elsevier, Amsterdam (1968).
18. Beynon, J. H., and A. E. Williams, "Mass Spectra of Various Quinones and Polycyclic Ketones," Applied Spectroscopy, 14, 156-160 (1960).
19. Billard, F., J. Bricard, J. Madelaine, and N. Clerc, "The Formation and Evolution of Radiolysis Particles," Proc. of the 7th Intl. Conf. on Condensation and Ice Nuclei, 169-172, Academia, Prague (1969).
20. Billings, C. E., and L. Silverman, "Aerosol Sampling for Electron Microscopy," J. Air Poll. Control Assoc., 12, 586-590 (1962).
21. Boocock, G., and R. J. Cvetanovic, "The Reaction of Oxygen Atom with Benzene," Can. J. Chem., 39, 2436-43 (1961).
22. Bricard, J., M. Cabane, G. Madelaine, and D. Vigla "Formation and Properties of Neutral Ultrafine Particles and Small Ions Conditioned by Gaseous Impurities of the Air," Aerosol and Atmospheric Chemistry Edited by Hidy, G. M., pp 271-284, Academic Press, New York (1972)..
23. Bricard, J., J. Madelaine, and D. Vigla, "Aerosols Generated Through the Action of Ultraviolet and Solar Radiation," Proc. of the 7th Intl. Conf. on Condensation and Ice Nuclei, 173-177, Academia, Prague (1969).

24. Brock, J. R., "Condensation Growth of Atmospheric Aerosols," Aerosol and Atmospheric Chemistry, edited by Hidy, G. M., pp 149-153, Academic Press, New York (1972).
25. Brocklehurst, B., and K. R. Jennings, "Reactions of Nitrogen Atoms in the Gas Phase," Progress in Reaction Kinetics, edited by Porter, G., 4, pp 1-36, Pergamon Press, New York (1967).
26. Budzikiewicz, H., C. Djerassi, and D. H. Williams, Mass Spectrometry of Organic Compounds, Holden-Day, San Francisco (1967).
27. Bufalini, J. J., and A. P. Altshuller, "Oxidation of Nitric Oxide in the Presence of Ultraviolet Light and Hydrocarbons," Environ. Sci. & Tech., 3, 469-472 (1969).
28. Bufalini, J. J., and A. P. Altshuller, "The Effect of Temperature on Photochemical Smog Reactions," Intl. J. Air Wat. Poll., 7, 769-711 (1963).
29. Cadle, R. D., "Formation and Chemical Reaction of Atmospheric Particles," Aerosol and Atmospheric Chemistry, Edited by Hidy, G. M., pp 141-147, Academic Press, New York (1972).
30. Cadle, R. D., Particles in the Atmosphere and Space, Reinhold, New York (1966).
31. Cadle, R. D., and C. Schade., "Kinetics of the Gas Phase Reaction Between Acetylene and Ozone," J. Chem. Phys. 21, 163 (1953).
32. Calvert, J. G., and J. N. Pitts, Photochemistry, Wiley, New York (1966).
33. Charlesby, A., Atomic Radiation and Polymers 195, Pergamon Press, New York, (1960).
34. Chien, J. C. W., "The Photooxidation of Hydrocarbons," Hercules Chem., 53, 19-23 (1966).
35. Cohen, R. I., T. C. Purcell, and A. P. Altshuller, "Analysis of the Oxidant in Photooxidation Reactions," Environ. Sci. & Tech. 1, 247-252 (1967).
36. Coughlin, R. W., "Physiochemical Aspects of Sampling Particulates," presented to AIChE 65th Annual Meeting, New York (1972).
37. Davis, A. S. and R. B. Cundall, "Primary Processes in the Gas-Phase Photochemistry of Carbonyl Compounds," Progress in Reaction Kinetics, edited by Porter, G., 4, pp 149-214, Pergamon Press (1967).

38. Deutsch, S., "Acid Potassium Iodide Method for Determining Atmospheric Oxidants," J. Air Poll. Control Assoc. 18, 78-83 (1968).
39. Dimitriadis, B., "Methodology in Air Pollution Studies Using Irradiation Chambers," J. Air Poll. Control Assoc. 17, 460-466 (1967).
40. Dimitriadis, B., "Effects of Hydrocarbons and Nitrogen Oxides on Photochemical Smog Formation," Environ. Sci. & Tech., 6, 253-260 (1972).
41. Dmitriev, M. T., "Some Physical and Chemical Processes in Air Caused by Ionizing Radiation," translated by Wade, C. M., Atmospheric and Oceanic Physics Series, 1, 302-312 (1965).
42. Doyle, G. C., "Design of a Facility (Smog Chamber) for Studying Photochemical Reaction under Simulated Tropospheric Conditions," Environ. Sci. & Tech., 4, 907-916 (1970).
43. Doyle, G. J., and Renzetti, N. A., "The Formation of Aerosols by Irradiation of Diluted Auto Exhaust," J. Air Poll. Control Assoc., 8, 23-32 (1958).
44. Eastman, R. H. and R. M. Silverstein, "Anomalies in the Vapor Phase Ozonolysis of Cyclohexene," J. Am. Chem. Soc., 75, 1493-1494 (1953).
45. Ellis, C. F., "Sunlight Photo-oxidation of Isobutylene and Butene-1 with NO_2 in Low- and High-Oxygen Concentrations," Atmos. Environ., 5, 83-88 (1971).
46. Foote, J. K., M. H. Mallon, and J. N. Pitts, Jr., "The Vapor Phase Photolysis of Benzene at 1849 Å," J. Am. Chem. Soc., 88, 3698-3701 (1966).
47. Friedlander, S. K., and J. H. Seinfeld, "A Dynamic Model of Photochemical Smog," Environ. Sci. & Tech. 3, 1175-1181 (1969).
48. Fuchs, N. A., The Mechanics of Aerosols, Pergammon Press, Oxford, (1964).
49. Glasson, W. A. and C. S. Tuesday, "Hydrocarbon Reactivities in the Atmospheric Photo-oxidation of Nitric Oxide," Environ. Sci. & Tech., 4, 916-924 (1970).
50. Glasson, W. A., and C. S. Tuesday, "Reactivity Relationships of Hydrocarbon Mixtures in Atmospheric Photo-oxidation," Environ. Sci. & Tech., 5, 151-154 (1971).
51. Goetz, A., and O. J. Klejnot, "Formation and Degradation of Aerosols by Ultraviolet Radiation," Environ. Sci. & Tech., 6, 143-151 (1972).

52. Goetz, A., and R. Pueschel, "Basic Mechanisms of Photochemical Aerosol Formation," Atmos. Environ., 1, 287-306 (1967).
53. Grasley, M. H., B. R. Appel, I. G. Burstain, J. L. Laity, and H. F. Richards, "The Relationship of Smog Chamber Methodology to Hydrocarbon Reactivity in Polluted Air," Am. Chem. Soc. Div. Org. Coatings Plast. Chem. Paper, 29, 422-426 (1969).
54. Grigoryan, G. L., A. A. Mantashyan, A. B. Nalbandyan, "Photooxidation of Benzene in the Gas Phase," Armiansk, Khim. Zh. 19, 140-149 (1966).
55. Haagen-Smith, A. J., "Chemistry and Physiology of Los Angeles Smog," Ind. Eng. Chem., 44, 1342 (1952).
56. Haagen-Smith, A. J., "The Effect of Light on Air Pollution," Report No. 15, Proc. Conf. on Chemical Reactions in Urban Atmospheres, Air Pollution Foundation, San Marino, Calif. (1956).
57. Hannah, R. W., J. L. Dwyer, "Infrared Analysis of Suspended Particulates with Millipore Filters and Attenuated Total Reflection," Anal. Chem., 36, 2341-2344 (1964).
58. Heicklen, J. and N. Cohen, "The Role of Nitric Oxide in Photochemistry," Advances in Photochemistry, edited by Noyes, W. A., Jr., G. S. Hammond, and J. N. Pitts, Jr., Vol. 5, pp 157-328, Interscience, New York (1968).
59. Hendrix, W. P., and C. Orr, Jr., "Thermal Precipitator," Rev. Sci. Instruments, 35, 1373-1374 (1964).
60. Henri, V. P., C. R. Maxwell, W. C. White, and D. C. Peterson, "The Chemical Effects of α -particles Upon Some C₆-Hydrocarbons in the Vapor State," J. Phys. Chem., 56, 153-155 (1952).
61. Hersch, P. A., "Controlled Addition of Experimental Pollutants to Air," J. Air Poll. Control Assoc., 19, 164-172 (1969).
62. Hidy, G. M., P. K. Mueller, Tokiwa and S. Twiss, "Aerometric Factors Affecting the Evolution of the Pasadena Aerosol," Aerosols and Atmospheric Chemistry, edited by Hidy, G. M., pp 219-236, Academic Press, New York (1972).
63. Hoare, D. E., and G. S. Pearson, "Gaseous Photooxidation Reaction," Advances in Photochemistry, edited by Noyes, W. A., Jr., G. S. Hammond, and J. N. Pitts, Jr., Vol. 3, pp 83-156, Interscience, New York, (1964).
64. Holmes, H. H., and F. Daniels, "The Photolysis of Nitrogen Oxides: N₂O₅, N₂O₄ and NO₂," J. Am. Chem. Soc., 56, 630-637 (1934).

65. Husar, R. B., "On the Formation of Photochemical Aerosol," Presented to International Workshop on Nucleation Theory and Its Applications, Clark College, Atlanta (1972).
66. Johnston, H. S. and F. Cramarossa, "Highly Complex Photochemical Mechanisms," Advances in Photochemistry edited by Noyes, W. A., Jr., G. S. Hammond, and J. N. Pitts, Jr. Vol. 4, pp 1-24, Interscience, New York (1968).
67. Jones, A. R., "On the Radiation-Induced Gas-phase Polymerization of Acetylene and Benzene," J. Chem. Phys., 32, 953-954 (1960).
68. Jones, J. H. R., and R. J. Cvetanovic, "Reaction of Oxygen Atoms with Toluene," Can. J. Chem., 39, 2444-2451 (1961).
69. Junge, C. E., Air Chemistry and Radioactivity, pp 111, Academic Press, New York (1963).
70. Kaufman, F., "Reactions of Oxygen Atoms," Progress in Reaction Kinetics, edited by Porter, G., 1, 1-40, Pergamon Press (1961).
71. Keng, E. Y. H., R. R. C. Chu, J. A. Knight, Jr., and C. Orr, Jr., Formation of Nonvolatile Particulates from Organic Vapors, Final Technical Report, Project B-358, Engineering Experiment Station, Georgia Institute of Technology (1972).
72. Keng, E. Y. H., R. R. C. Chu, J. A. Knight, Jr., and C. Orr, Jr., "Aerosols Produced by X-rays," J. Coll. Int. Sci., 39, 94-101 (1972).
73. Keng, E. Y. H., and C. Orr, Jr., "Thermal Precipitation and Particle Conductivity," J. Coll. Int. Sci., 22, 107-116 (1966).
74. Knight, J. A., Jr., Radiation Chemistry of Organic Substances, Final Report, Project A-323, Engineering Experiment Station, Georgia Institute of Technology, (1959).
75. Knight, J. A., Jr., Personal Communication (1972).
76. Kopczynski, S. L., "Photooxidation of Alkylbenzene-Nitrogen Dioxide Mixtures in Air," Intl. J. Air Wat. Poll., 8, 107-120 (1964).
77. Laity, T. L., "A Smog Chamber Study Comparing Blacklight Fluorescent Lamps with Natural Sunlight," Environ. Sci. & Tech., 5, 1218-1220 (1971).
78. Leighton, P. A., "Photochemical Reactions in the Contaminated Atmospheres: A Survey," Chemical Reactions in the Lower and Upper Atmosphere, edited by Cadle, R. C., pp 1-14, Interscience, New York (1961).

79. Leighton, P. A., Photochemistry: Vol. IX Photochemistry of Air Pollution, Academic Press, New York (1961).
80. Leithe, W., The Analysis of Air Pollutants, Ann Arbor-Humphrey Science Publisher, Ann Arbor (1970).
81. Lind, S. C., Radiation Chemistry of Gases, Reinhold, New York (1961).
82. Lind, S. C. and D. C. Bardwell, "The Chemical Action of Gaseous Ions Produced by Alpha Particles, IX. Saturated Hydrocarbons," J. Am. Chem. Soc., 48, 2335-2350 (1926).
83. Lind, S. C., D. C. Bardwell, and J. H. Perry, "The Chemical Action of Gaseous Ions Produced by Alpha Particles. VII Unsaturated Carbon Compounds," J. Am. Chem. Soc., 48 1556-1575 (1926).
84. Lipeles, M., and N. Malmuth, "Analytical Studies of Simplified Photochemical Smog Kinetics," Environ. Sci. & Tech., 6, 360-365 (1972).
85. Liu, B. Y. H., K. T. Whitey, and H. H. S. Yu, "Electrostatic Aerosol Sampler for Light and Electron Microscopy," Rev. Sci. Instruments 38, 100-102 (1967).
86. Mayo, F. R., "Free-Radical Autooxidation of Hydrocarbons," Accounts of Chemical Research, 1, 193-201 (1968).
87. McAndrews, J. I., T. H. Anderson, and S. B. Martin, Radical Yields in Irradiated Aromatics, U. S. Naval Radiological Defense Laboratory Report, USNRDL-TR-718 (1964).
88. McCrone, W. C., and M. A. Salzenstein, "The Microscopic Identification of Atmospheric Particulates," J. Air Poll. Control Assoc., 12, 195-197 (1962).
89. McNesby, J. R., and Okabe, H., "Vacuum Ultraviolet Photochemistry," Advances in Photochemistry, edited by Noyes, W. A., G. S. Hammond, and J. N. Pitts, Jr., Vol. 3, pp 157-240 (1964).
90. Meyerson, S., "Mass Spectra, Radiolysis, and Photolysis of Phenyl Alkyl Ketones," J. Phys. Chem. 68, 968-969 (1964).
91. Mohnen, V. A., and J. P. Lodge, Jr., "General Review and Survey of Gas-to-Particle Conversions," Proc. of the 7th Intl. Conf. on Condensation and Ice Nuclei, pp 69-91, Academic, Prague (1969).
92. Morris, R. A., and R. L. Chapman, "Flame Ionization Hydrocarbon Analyzer," J. Air Poll. Control Assoc., 11, 467-469 (1961).

93. Morrow, P. E., and T. T. Mercer "A Point to Plane Electrostatic Precipitor for Particle Size Sampling" J. Am. Ind. Hyg. Assoc., 25, 8-14 (1964)
94. Noyes, W. A., Jr., and P. A. Leighton, The Photochemistry of Gases, Reinhold, New York (1941).
95. Olin, J. G., and G. J. Sem, "Piezoelectric Microbalance for Monitoring the Mass Concentration of Suspended Particles," Atmos. Environ., 5, 653-688 (1971).
96. Orr, C., Jr., "Particle Size Measurement," to be published in Treatise on Analytical Chemistry, edited by Koltheff, I. M., and P. J. Elving, Interscience, New York.
97. Orr, C., Jr., Particulate Technology, Macmillan, New York, (1966).
98. Palmer, R. C., "The Effects of Low Energy X-rays on Organic Gasses and on Organic Gas-Noble Gas Mixtures," Ph.D. Thesis, Vanderbilt University, (1958).
99. Palmer, R. C., D. C. Bardwell, and M.D. Peterson, "Acceleration of X-ray Energized Chemical Reactions of Organic Gases by Energy Transfer from Noble Gases," J. Chem. Phys. 28, 167 (1958).
100. Pfefferkorn, G., "Electron Microscope Investigation of Metal Oxidation" English Translation, Zeitschrift für Metallkunde, 46, 204-207 (1955).
101. Pfefferkorn, G., "Electronenmikroskopischer Nachweis Katalytischer Oberflächenreaktionen," Phys. Verh., 8, 239 (1957).
102. Pfefferkorn, G., "The Photochemical Formation of Non-volatile Droplets from Organic Vapors in Air," Staub-Reinhalt der Luft, 27, 29-31 (1967).
103. Pinchas, S., "Infrared Absorption of the Aldehydic C-H Group," Anal. Chem., 27, 2-6 (1955).
104. Pinner, S. H., "Cationic Polymerizations Induced by High Energy Radiation," Chap. 17, The Chemistry of Cationic Polymerization, edited by Plesch, P. H., Pergamon Press, New York, (1963).
105. Pitts, J. N., Jr., J. K. Foote and J. K. S. Wan, "Some Correlations Between Spectroscopic and Photochemical Processes," Photochem. and Photobio., 4, 323-333 (1965).
106. Prager, M. J., E. R. Stephens, and W. E. Scott, "Aerosol Formation from Gaseous Air Pollutants," Ind. & Eng. Chem., 52, 521-524 (1960).
107. Reid, K. F., Properties and Reactions of bonds in Organic Molecules, American Elsevier, New York, (1968).

108. Renzetti, N. A., and G. J. Doyle, "The Chemical Nature of the Partulates from Irradiated Automobile Exhaust," J. Air Poll. Control Assoc., 8, 293-296 (1959).
109. Renzetti, N. A., and G. J. Doyle, "Photochemical Aerosol Formation in Sulfur Dioxide-Hydrocarbon Systems," Intl. J. Air Poll., 2, 327-345 (1960).
110. Rose, A. H., Jr., R. C. Stahman, M. W. Korth, "Dynamic Irradiation Chamber Tests of Automotive Exhaust, Part 1 and Part 2," J. Air Poll. Control Assoc., 12, 468-473, 522-523 (1962).
111. Saltzman, B. E., "Colorimetric Microdetermination of Nitrogen Dioxide in the Atmosphere," Anal. Chem., 26, 1949-1955 (1954).
112. Saltzman, B. E., "Modified Nitrogen Dioxide Reagent for Recording Air Analyzer," Anal. Chem., 32, 135-136 (1960).
113. Saltzman, B. E., "Kinetic Studies of Formation of Atmospheric Oxidants," Ind. Eng. Chem., 50, 677-681 (1958).
114. Sawicki, E., and T. R. Hauser, "Infrared Spectral Detection of Carboxylic Acids and Aldehydes in Air-Borne Particulates," Anal. Chem., 31, 523-527 (1959).
115. Scars, W. C., and W. W. Parkinson, Jr., "Post-irradiation Oxidation in Rubber and Plastics," J. Polymer Science, 21, 325-326 (1956).
116. Shindo, K. and S. Lipsky, "Photochemistry of Benzene Vapor at 1849 Å," J. of Chem. Phys., 45, 2292-2297 (1966).
117. Silverstein, R. M., and G. C. Bassler, Spectrometric Identification of Organic Compounds, Wiley, New York (1963).
118. Sloan, H. J., "Infrared Differential Technique Employing Membrane Filters," Anal. Chem., 35, 1556-1558 (1963).
119. Smith, L. I., and J. W. Opie, "O-Aminobenzaldehyde," Organic Syntheses, 28, 11-13 (1948).
120. Stafford, R. W., J. F. Shay, and R. J. Francel, "Identification of Dicarboxylic Acids in Polymeric Esters," Anal. Chem., 26, 656-661 (1954).
121. Stephens, E. R., and M. A. Price "Comparison of Synthetic and Smog Aerosols," Aerosol and Atmospheric Chemistry, edited by Hidy, G. M., pp 167-181, Academic Press, New York (1972).
122. Stephens, E. R., "The Photochemical Olefin-Nitrogen Oxides Reaction," Chemical Reactions in the Lower and Upper Atmosphere, edited by Cadle, R. C., pp 51-69 Interscience, New York (1961).

123. Stephens, E. R., "Reactions of Oxygen Atoms and Ozone in Air Pollution," Intl. J. Air Wat. Poll., 10, 649-663 (1966).
124. Stephens, E. R., and M. A. Price, "Atmospheric Photochemical Reactions in a Tube Flow Reactor," Atmos. Environ., 3, 573-582 (1969).
125. Tedder, D. W., Personal Communication, (1971).
126. Thomas, P. T., and J. L. Dwyer, "Collection of Gas Chromatographic Effluents for Infrared Spectral Analysis," J. Chromatog., 13, 366-371 (1964).
127. Tuesday, C. S., "The Atmospheric Photooxidation of Trans-2-butene and Nitric Oxide," Chemical Reaction in the Lower and Upper Atmosphere, edited by Cadle, R. C., pp 15-49, Interscience, New York (1961).
128. Turner, George, Personal Communication (1973).
129. Tyndall, J., "On the Blue Color of the Sky, the Polarization of Skylight, and on the Polarization of Light by Cloudy Matter Generally," Phil. Mag. 37, No 250, 384-394 (1869).
130. Vohra, K. G., M. C. Subba Ramu and K. N. Vasudevan, "Behavior of Aerosols Formed by Clustering of Molecules around Gaseous Ions," Atmos. Environ., 3, 99-105 (1969).
131. Vohra, K. G., and P. V. N. Nair, "Recent Thinking on the Chemical Formation of Aerosols in the Air by Gas Phase Reactions," Aerosol Science, 1, 127-133 (1970).
132. Volman, D. H., "Photochemical Gas Phase Reactions in the Hydrogen-Oxygen System," Advances in Photochemistry, edited by Noyes, W. A., Jr., G. S. Hammond, and J. N. Pitts, Jr., Vol. 1, pp 43-82, Interscience, New York, (1963).
133. Watson, J. H. L. and K. Kaufman, "Electron Microscope Examination of the Microphysical Properties of the Polymer Cuprene," J. Appl. Phys., 17, 996-1005 (1946).
134. Wei, K., J. C. Mani, J. N. Pitts, "The Formation of Polyenic Dialdehydes in the Photooxidation of Pure Liquid Benzene," J. Am. Chem. Soc. 89, 4225-4227 (1967).
135. Wilson, J. E., and W. A. Noyes, Jr., "Photochemical Studies, XXXIV. The Photochemical Decomposition of Benzene," J. Am. Chem. Soc., 63, 3025-3028 (1941).
136. Wilson, W. E., Jr. and A. Levy, "A Study of Sulfur Dioxide in Photochemical Smog I. Effect of SO₂ and Water Vapor Concentration in the 1-Butene/NO_x/SO₂ Systems," J. Air Poll. Control Assoc., 20, 385-390 (1970).

137. Yamate, N., "Studies on Photochemical Products of Aromatic Hydrocarbon-Nitrogen Dioxide Mixtures in Air," J. Japan Soc. Air Poll., 6, 51 (1971).
138. Zettlemoyer, A. C., Nucleation, M. Dekker, New York (1969).

VITA

Richard Ruonn-Ching Chu was born in Chungking, China, on November 10, 1941. In 1949 he and his family moved to Taipei, Taiwan. He attended elementary school at the Mandarin Experimental School in Taipei. In the Summer of 1954, he enrolled in the junior high class at Provincial Chien-Kuo High School in Taipei. In 1957, he was promoted to the senior high class without being required to take an examination. He chose scientific electives and English during these last two years of high school. In 1961, he passed the College Entrance Examination and enrolled at the National Taiwan University, Taipei, where he majored in Chemical Engineering. Subsequently, he received a Bachelor of Science degree in Engineering with the equivalent of a B average. He applied to several graduate schools in the United States in 1966, and was offered scholarships by Clarkson College of Technology, Tufts University, and Georgia Tech. He enrolled in the School of Chemical Engineering at Georgia Tech in September, 1966, and was awarded a research assistantship under the supervision of Dr. G. L. Bridger in the field of phosphate fertilizer processing. He completed the Master of Science program in Chemical Engineering in the spring of 1968. The following year he became associated with a PHS-sponsored air pollution research project which led into this Ph.D. research effort under the supervision of Dr. Clyde Orr, Jr. At present he is employed by the Bechtel Power Corporation, Gaithersburg, Maryland.

.